CRITICAL EVALUATION OF TORSIONAL PROVISION IN IS-1893: 2002

A thesis

Submitted by

Bijily B
(210CE2021)

In partial fulfillment of the requirements
for the award of the degree of

Master of Technology
In
Civil Engineering
(Structural Engineering)

Department of Civil Engineering
National Institute of Technology Rourkela
Orissa -769008, India
May 2012

CRITICAL EVALUATION OF TORSIONAL PROVISION IN IS-1893: 2002

A thesis
Submitted by

Bijily B
(210CE2021)

In partial fulfillment of the requirements
for the award of the degree of

Master of Technology
In
Civil Engineering
(Structural Engineering)

Under The Guidance of
Dr. PradipSarkar

Department of Civil Engineering
National Institute of Technology Rourkela
Orissa -769008, India
May 2012

NATIONAL INSTITUTE OF TECHNOLOGY
ROURKELA, ORISSA -769008, INDIA

This is to certify that the thesis entitled, "**CRITICAL EVALUATION OF TORSIONAL PROVISION IN IS-1893: 2002**" submitted by **Bijily B** in partial fulfillment of the requirement for the award of **Master of Technology** degree in **Civil Engineering** with specialization in **Structural Engineering** at the National Institute of Technology, Rourkela is an authentic work carried out by her under my supervision and guidance. To the best of my knowledge, the matter embodied in the thesis has not been submitted to any other University/Institute for the award of any degree or diploma.

Research Guide

Place: Rourkela
Date: 26/05/2012

Dr. Pradip Sarkar
Associate Professor
Department of Civil Engineering
NIT Rourkela

ACKNOWLEDGEMENTS

First and foremost, praise and thanks goes to my God for the blessing that has bestowed upon me in all my endeavors.

I am deeply indebted to **Dr. Pradip Sarkar,** my advisor and guide, for the motivation, guidance, tutelage and patience throughout the research work. I appreciate his broad range of expertise and attention to detail, as well as the constant encouragement he has given me over the years. There is no need to mention that a big part of this thesis is the result of joint work with him, without which the completion of the work would have been impossible.

I am grateful to **Prof. N Roy**, Head, Department of Civil Engineering for his valuable suggestions during the synopsis meeting and for the unyielding support over the year.

I am expressing my gratitude to **Dr. Robin. Davis. P,** faculty in Civil engineering department, for his sincere help.

I am expressing my gratitude to **Dr. M R Barik** and **Dr. K C Biswal**, faculties in Civil Engineering Department.

My parents and my brothers, they played a great roll in my carrier and their love and support has been a major stabilizing force till this moment.

I should express my sincere thanks to my friends **Mr. Baburaj M, Ms. Snehash Patel, Ms. Suji P, Ms. Dhanya V V, Ms. Chithra R, Ms. Neethu Krishna, Mr. Mallikarjun**

B, Mr. Kirtikanta Sahoo, and Mr. Avadhoo Bhosla and to all my classmates for their moral support and advices.

So many people have contributed to my thesis, to my education, and to my life, and it is with great pleasure to take the opportunity to thank them. I apologize, if I have forgotten anyone.

Bijily B

ABSTRACT

KEYWORDS: *Asymmetric, pushover analysis, plastic hinge, torsion, reinforced concrete, non-linear dynamic analysis, time history analysis, and spectral consistent ground motion*

For a building to be symmetric it must have, at each floor level, coincident centers of mass and stiffness that lie on common vertical axis. In practice, this condition is rarely encountered and most buildings are unsymmetrical to varying degrees, due to asymmetry in plan, elevation, distribution of vertical members or mass distribution on the floors. Although considerable research on response of asymmetric structures under seismic excitation has been reported in the literature, the performance of asymmetric structures designed in accordance with the Indian code has not been studied adequately. Frequent occurrences of devastating earthquakes in India clearly call for the need of evaluation of Indian buildings for seismic safety.

The earthquake resistant code in India, IS: 1893 (Part1), has been revised in 2002 to include provisions for asymmetric buildings. An attempt has been made in the present study to investigate the gap in the seismic design of asymmetric RC structures in the Indian context. Three reinforced concrete moment-resisting frame buildings with different types of asymmetry are designed based on prevailing Indian codes as test examples. Nonlinear static (pushover) and dynamic (time-history) analyses are performed on these structures and a comparison is made of displacements, inter-storey drift ratio, ductility and hinge pattern of the frames to show the changes in their behaviour due to torsion which is recognized as a principal cause of severe damage in eccentric multi-storey buildings during earthquakes.

Nonlinear dynamic analysis (time history analysis) is done for ten recorded ground motion and five generated ground motion consistent to IS-1893: 2002 (Part1) response spectrum.

Results obtained from this study show that the plan asymmetry in the building makes it non-ductile even after design with code provision. The maximum base shear demands for the three building variant are almost same. This is because the fundamental periods of all the three building are almost identical. It is found that there is a considerable amount of variation in the maximum roof displacement responses of the three building variants subjected to generated earthquake ground motion. The maximum roof displacement responses for symmetric building variants are found to be lesser compared to the two asymmetric buildings for all the cases studied here. However the average maximum roof displacement responses for two asymmetric buildings are found to be approximately same.

Base moment demand obtained from nonlinear dynamic analyses is found to be almost same for both of the two asymmetric buildings for all the cases studied here. Also, in most of the cases base shear – roof displacement and base moment – roof rotation hysteresis curves are found to be similar for both the asymmetric buildings with small translational/rotation shift.

It is found that the yielding for both the asymmetric building occurs at the same time step of the dynamic analyses after following the same elastic eccentricity even though ASYM2 (designed with code provision) has a greater strength compared to ASYM1 (designed without code provision).

Considering that all the building structures will undergo inelastic deformation under an expected earthquake it is meaningless to relate the design criterion to the elastic centre of rigidity. Design criterion given in IS 1893:2002 (Part-1) with regard to plan asymmetry

seems to be not very efficient. Code criterion for plan asymmetry recommends increasing the strength distribution in the building but it does not look for changing the stiffness distribution of the building. Change in the stiffness distribution to reduce eccentricity can be a useful for such buildings.

TABLE OF CONTENTS

Title **Page No.**

ACKNOWLEDGEMENTS i
ABSTRACT iii
TABLE OF CONTENTS vi
LIST OF TABLES xi
LIST OF FIGURES xii
ABBREVIATIONS xvii
NOTATIONS xix

CHAPTER 1 INTRODUCTION

1.1. Overview 1
1.2. Literature Review 3
1.3. Objective 8
1.4. Scope of Study 9
1.5. Methodology 9
1.6. Organization of Thesis 10

CHAPTER 2 PREVAILING CODE PROVISIONS

2.1. Overview 12
2.2. Strength Design of Members 13
2.3. Indian standards IS-1893:2002 14
2.4. International Building CodeIBC 2003 15
2.5. FEMA 450:2003(NEHRP) 16
2.6. New Zealand Code NZS 4203:1992 16

Title **Page No**

2.7. Euro Code prEN1988-1:2003 17

2.8. Canada Code NBCC 1995 18

2.9. Summary 18

CHAPTER 3 STRUCTURAL MODELLING

3.1. Introduction 19

3.2. Computational Model 19

3.2.1. Material Properties 20

3.2.2. Structural Elements 20

3.3. Building Geometry 21

3.4. Modelling of Flexural Plastic Hinges 24

3.4.1. Stress-Strain Characteristics for Concrete 25

3.4.2. Stress-Strain Characteristics for Reinforcing Steel 27

3.4.3. Moment-Curvature Relationship 28

3.4.4. Modelling of Moment-Curvature in RC Sections 31

3.4.5. Moment-Rotation Parameters 32

3.5. Nonlinear Time History Analysis 36

3.5.1. Natural Record of Earthquake Ground Motion 38

3.5.2. Spectral consistent earthquake data 39

3.6. Summary 40

CHAPTER 4 NONLINEAR STATIC ANALYSIS: PUSHOVER ANALYSIS

4.1. Introduction 41

4.2. Modal Analysis 41

4.3. Pushover Analysis 42

4.4. Summary 46

Title **Page No**

CHAPTER 5 NONLINEAR DYNAMIC ANALYSIS

5.1. Introduction 47

5.2. Base shear versus roof displacement 47

5.2.1. Results obtained from Natural Ground Motion Data 48

5.2.2. Results obtained from Generated Ground Motion Data 54

5.3. Base moment versus roof rotation 58

5.3.1. Results obtained from Natural Ground Motion Data 59

5.3.2. Results obtained from Generated Ground Motion Data 64

5.4. Variation of eccentricity during nonlinear analysis 67

5.5. Summary 75

CHAPTER 6 SUMMARY AND CONCLUSIONS

6.1 General 76

6.2 Summary 76

6.3 Conclusions and recommendations 78

6.4 Scope for Future Work 80

ANNEXURE -A EARTHQUAKE RESISTANT DESIGN

A.1. Introduction 82

A.2. Load combination 83

A.3. Linear analysis methods 84

A.3.1. Equivalent static method 84

A.3.1.1.Centre of mass 84

A.3.1.2.Effect of torsion 85

A.3.1.3.Seismic weight 85

A.3.1.4.Lumped mass 85

A.3.1.5.Calculation of lateral forces 86

Title **Page No**

A.4. Response spectrum analysis 88

A.4.1. Calculation of Modal Response..... 90

A.4.2. Modal combination 90

A.4.3. Modal Mass 91

A.4.4. Modal Participation factor..... 91

A.4.5. Design Lateral Force in Each Mode 91

A.4.6. Shear Force in Each Mode 92

A.4.6.1.Storey Shear Force due to All Modes Considered..... 92

A.4.6.2.Lateral Force at Each Storey due to All Modes Considered 92

A.5. Dynamic Analysis..... 92

A.5.1. Determination of Structural Properties 93

ANNEXURE -B PUSHOVER ANALYSIS

B.1. Introduction 96

B.1.1. Pushover Analysis Procedure..... 98

B.1.2. Lateral Load Profile 99

B.1.3. Target Displacement 102

B.1.3.1.Displacement Coefficient Method (FEMA 356) 103

B.1.3.2.Capacity Spectrum Method (ATC 40) 104

ANNEXURE –C TIME HISTORY ANALYS

C.1. Time History Data 108

C.2. Additional results from time history analysis..... 114

C.2.1. Roof Displacement Response during Nonlinear Dynamic Analysis 114

C.2.2. Roof Rotation Response during Nonlinear Dynamic Analysis..... 121

Title **Page No**

ANNEXURE –D SPECTRAL IDENTICAL DATA

D.1. Input Window 129

D.2. Plot time history 133

D.3. Analysis of generated ground motion 134

D.4. Target Response Spectrum 135

REFERENCES 137

LIST OF TABLES

Title **Page No**

Table 2.1: Design Eccentricity for different International code clause..... 13

Table 3.1: Longitudinal reinforcement details of column sections..... 23

Table 3.2: Longitudinal reinforcement details of beam sections..... 23

Table 3.3: Characteristics of the selected ground motion 37

Table 4.1: Modal properties of the selected buildings for first three modes 42

Table 5.1: Maximum response of the building subjected to natural ground motion . 53

Table 5.2: Maximum response of the building subjected to generated ground motion 58

LIST OF FIGURES

Title **Page No**

Fig. 1.1:Generation of torsional moment in asymmetric structures during seismic excitation. 2

Fig. 1.2:Different types of uni-directionally asymmetric idealized structural systems used in Dutta, 2001. 8

Fig. 2.1: Figure explaining δmax and δavg in asymmetric building 14

Fig. 3.1: Use of end offsets at beam-column joint 21

Fig. 3.2(a): Typical floor plan showing columns 22

Fig. 3.2(b):Typical floor plan showing beams 22

Fig. 3.3: The coordinate system used to define the flexural and shear hinges 24

Fig. 3.4: Typical stress-strain curve for M-20 grade concrete (Panagiotakos and Fardis, 2001) 27

Fig. 3.5: Stress-strain relationship for reinforcement – IS 456 (2000) 28

Fig. 3.6: Curvature in an initially straight beam section (Pillai and Menon, 2006) 29

Fig. 3.7: (a) cantilever beam, (b) Bending moment distribution, and (c) Curvature distribution (Park and Paulay 1975) 33

Fig. 3.8: Idealised moment-rotation curve of RC elements 35

Fig 3.9: SAP window showing the nonlinear time history load case 38

Fig.3.10: Acceleration spectra for the artificial accelerograms (5% damping) 40

Fig. 4.1: Comparison of capacity curves of the three buildings 43

Fig. 4.2: Base moment versus roof rotation relation for the asymmetric buildings 43

Fig. 4.3: Variation in the static eccentricity in different nonlinear steps 44

Fig. 4.4: Hinge distribution at collapse for two XY frames of ASYM1 45

Fig. 4.5: Hinge distribution at collapse for two XY frames of ASYM2 46

Fig. 5.1: Base shear-versus-roof displacement data for Imperial Valley Eq. (1940) 48

Fig. 5.2: Base shear-versus-roof displacement data for Loma Prieta – Oakland (1989) 49

Title **Page No**

Fig. 5.3: Base shear-versus-roof displacement data for Loma Prieta - Corralitos (1989) 49

Fig. 5.4: Base shear-versus-roof displacement data for Northridge – Santa Monica (1994) 50

Fig. 5.5: Base shear-versus-roof displacement data for Northridge – Sylmar (1994) 50

Fig. 5.6: Base shear-versus-roof displacement data for Northridge Century City (1994) 51

Fig. 5.7: Base shear-versus-roof displacement data for Landers – Lucerne Valley (1992) 51

Fig. 5.8: Base shear-versus-roof displacement data for Sierra Madre – Altadena (1991) 52

Fig. 5.9: Base shear-versus-roof displacement data for Imperial Valley Eq. (1979) 52

Fig. 5.10: Base shear-versus-roof displacement data for Morgan Hill – Gilroy4 (1984) 53

Fig. 5.11: Base shear-versus-roof displacement data for Data-A 55

Fig. 5.12: Base shear-versus-roof displacement data for Data-B 55

Fig. 5.13: Base shear-versus-roof displacement data for Data-C 56

Fig. 5.14: Base shear-versus-roof displacement data for Data-D 56

Fig. 5.15: Base shear-versus-roof displacement data for Data-E 57

Fig. 5.16: Base moment-versus-roof rotation data for Loma Prieta – Oakland (1989) 59

Fig. 5.17: Base moment-versus-roof rotation data for Loma Prieta - Corralitos (1989) 59

Fig. 5.18: Base moment-versus-roof rotation data for Northridge – Santa Monica (1994) 60

Fig. 5.19: Base moment-versus-roof rotation data for Northridge – Sylmar (1994) 60

Fig. 5.20: Base moment-versus-roof rotation data for Northridge Century City (1994) 61

Fig. 5.21: Base moment-versus-roof rotation data for Landers – Lucerne Valley (1992) 61

Fig. 5.22: Base moment-versus-roof rotation data for Sierra Madre – Altadena (1991) 62

Title **Page No**

Fig. 5.23: Base moment-versus-roof rotation data for Imperial Valley Eq. (1979) 62

Fig. 5.24: Base moment-versus-roof rotation data for Morgan Hill – Gilroy4 (1984)63

Fig. 5.25: Base moment-versus-roof rotation data for Data-A 64

Fig. 5.26: Base moment-versus-roof rotation data for Data-B 65

Fig. 5.27: Base moment-versus-roof rotation data for Data-C 65

Fig. 5.28: Base moment-versus-roof rotation data for Data-D 66

Fig. 5.29: Base moment-versus-roof rotation data for Data-E 66

Fig. 5.30: Eccentricity-versus-time data for Loma Prieta – Oakland (1989) 67

Fig. 5.31: Eccentricity -versus-time data for Loma Prieta - Corralitos (1989) 68

Fig. 5.32: Eccentricity-versus-time data for Northridge – Santa Monica (1994) 68

Fig. 5.33: Eccentricity-versus-time data for Northridge – Sylmar (1994) 69

Fig. 5.34: Eccentricity-versus-time data for Northridge Century City (1994) 69

Fig. 5.35: Eccentricity-versus-time data for Landers – Lucerne Valley (1992) 70

Fig. 5.36: Eccentricity-versus-time data for Sierra Madre – Altadena (1991) 70

Fig. 5.37: Eccentricity-versus-rime data for Imperial Valley Eq. (1979) 71

Fig. 5.38: Eccentricity-versus-time data for Morgan Hill – Gilroy4 (1984) 71

Fig. 5.39: Eccentricity-versus-time data for Data-A 72

Fig. 5.40: Eccentricity-versus-time data for Data-B 72

Fig. 5.41: Eccentricity-versus-time data for Data-C 73

Fig. 5.42: Eccentricity-versus-time data for Data-D 73

Fig. 5.43: Eccentricity-versus-time data for Data-E 74

Fig. A.1: Response spectra for 5 percent damping (IS 1893: 2002) 87

Fig. A.2: Building model under seismic load 88

Fig.B.1: Schematic representation of pushover analysis procedure 99

Fig. B.2: Lateral load pattern for pushover analysis as per FEMA 356

(Considering uniform mass distribution) 102

Title **Page No**

Fig. B.3: Schematic representation of Displacement Coefficient Method (FEMA 356) 103

Fig. B.4: Schematic representation of Capacity Spectrum Method (ATC 40) 105

Fig.B.5: Effective damping in Capacity Spectrum Method (ATC 40) 106

Fig. C.1: Natural ground motions used for nonlinear analysis 108

Fig. C.2: Artificially generated Spectral consistent earthquake motion 111

Fig. C.3: Roof Displacement-versus-time data for Loma Prieta – Oakland (1989) 114

Fig. C.4: Roof Displacement-versus-time data for Loma Prieta - Corralitos (1989)115

Fig. C.5: Roof Displacement versus-time data for Northridge – Santa Monica (1994) 115

Fig.C.6: Roof Displacement-versus-time data for Northridge – Sylmar (1994) 116

Fig. C.7: Roof Displacement-versus-time data for Northridge Century City (1994)116

Fig.C.8: Roof Displacement-versus-time data for Landers – Lucerne Valley (1992) 117

Fig. C.9: Roof Displacement-versus-time data for Sierra Madre – Altadena (1991)117

Fig.C.10: Roof Displacement-versus-rime data for Imperial Valley Eq. (1979) 118

Fig. C.11: Roof Displacement-versus-time data for Morgan Hill – Gilroy4 (1984) 118

Fig.C.12: Roof Displacement-versus-time data for Data-A 119

Fig. C.13: Roof Displacement-versus-time data for Data-B 119

Fig.C.14: Roof Displacement-versus-time data for Data-C 120

Fig. C.15: Roof Displacement-versus-time data for Data-D 120

Fig.C.16: Roof Displacement-versus-time data for Data-E 121

Fig.C.17: Roof Rotation-versus-time data for Loma Prieta – Oakland (1989) 121

Fig.C.18: Roof Rotation-versus-time data for Loma Prieta - Corralitos (1989) 122

Fig.C.19: Roof Rotation-versus-time data for Northridge – Santa Monica (1994) 122

Fig.C.20: Roof Rotation-versus-time data for Northridge – Sylmar (1994) 123

Fig. C.21: Roof rotation-versus-time data for Northridge Century City (1994) 123

Title **Page No**

Fig.C.22: Roof Rotation-versus-time data for Landers – Lucerne Valley (1992) 124

Fig.C.23: Roof Rotation-versus-time data for Sierra Madre – Altadena (1991) 124

Fig. C.24: Roof Rotation-versus-rime data for Imperial Valley Eq. (1979) 125

Fig.C.25: Roof Rotation-versus-time data for Morgan Hill – Gilroy4 (1984) 125

Fig.C.26: Roof Rotation-versus-time data for Data-A 126

Fig. C.27: Roof Rotation-versus-time data for Data-B 126

Fig.C.28: Roof Rotation-versus-time data for Data-C 127

Fig.C.29: Roof Rotation-versus-time data for Data-D 127

Fig.C.30: Roof Rotation-versus-time data for Data-E 128

Fig. D.1: Input Window in SIMQKE commercial software 129

Fig. D.2: Spectral consistent time history ground motion generated 134

Fig. D.3: Window in SIMQKE software where Target Response Spectrum data is entering 136

ABBREVIATIONS

ADRS	Acceleration Displacement Response Spectrum
ASYM1	First asymmetric variant
ASYM2	Second asymmetric variant
CM	Center of mass
CQC	Complete Quadratic Combination
CR	Center of rigidity
CS	Center of stiffness
CSM	Capacity Spectrum Method
DBE	Design Basis Earthquake
DCM	Displacement Coefficient Method
DL	Dead load
ECR	Elastic center of resistance
EL	Earthquake load
FEMA	Federal emergency management agency
g	Acceleration due to gravity
HHT	Hiber-Hughes-Taylor
IBC	International Building Codes
IS	Indian Standards
LL	Live load
MCE	Maximum Considered Earthquake
MDOF	Multi degree of freedom system
MPA	Modal push over analysis

NBCC	National Building Codes of Canada
NZS	New Zealand Standards
PGA	Peak ground acceleration
prEN	Euro code
R	Response factor
RC	Reinforced Concrete
SDOF	Single degree of freedom
SRSS	Square Root of Sum of Squares
SYM	Symmetric building variant
T	Time period
UY	Cumulative mass distribution

NOTATIONS

English

a_i	Distance of element i from CS
A_h	Design horizontal seismic coefficient.
A_k	Design horizontal acceleration spectrum
A_x	Design eccentricity coefficients
b	Plan dimension perpendicular to the force direction
d_b	Diameter of the longitudinal bar
D	Depth of the beam
dx	Element length of member
e	Eccentricity of centre of mass from elastic centre of resistance
e_{fc}, e_{sc} , e_d	Design eccentricity
E_c	Short term modulus of elasticity
EI	Flexural rigidity
E	Modulus of elasticity
f_{ck}	Characteristic compressive strength of concrete cube
f_{cc}'	Peak strength of concrete.
f_{co}'	Unconfined compressive strength
f_y	Yield stress of the longitudinal reinforcement
f_{yh}	Grade of the stirrup reinforcement
F_i	Lateral force at each story
$F(t)_I$	A vector of inertia forces acting on the node masses
$F(t)_D$	A vector of viscous damping or energy dissipation forces
$F(t)_S$	A vector of inertia force carried by the structure

$F(t)$	A vector of externally applied loads
h_i	Height of floor I measured from base
I	Moment of area of section
k	Adjustment factor
k_i	Confinement effectiveness coefficient
k_e	Lateral stiffness of element i
l_p	Equivalent length of plastic hinge
l_s	Mass radius of gyration of the floor
l	Length of element
L, B	Plan dimension
L_{max}	Large plan dimension of the building
L_{min}	Smaller plan dimension of the building
M	Applied moment
n	Number of stories in the building is the number of levels at which the masses are located
N	Number of modes to be considered
p_{ni}	Mode participation factor
Q_i	Design lateral force at floor i
Q_{ik}	Design lateral force in floor i mode k
$q_n(t)$	Modal coordinate
r	Number of modes being considered
r_x	Torsional radius (square root of torsional to the lateral stiffness ratio in the force direction)
R	Radius of curvature

S	Static seismic shear of code designed building
S_i	Lateral shear in element i
S_a/g	Average response acceleration coefficient
SR_A, SR_v	Spectral reduction factors
$S(\omega)_n$	Pseudo acceleration spectrum
T	Time period
T_a	Approximate time period
T_{eq}	Equivalent period
T_i	Initial period
$u(\omega)_{max}$	Maximum peak response
V_B	Base shear
V_i	Peak story force
V_0	The design base shear
W	Seismic weight of the building
W_i	Seismic weight of floor i
Z	Zone factor

<u>Greek</u>

α, β	Dynamic amplification factor
α	Post yield stiffness ratio
γ	Coefficient for accidental eccentricity
β_{eq}	Equivalent damping ratio
ω	Frequency
ω_i, ω_j	Circular frequency in i^{th} and j^{th} mode respectively
ω_n	n^{th} mode natural frequency

δ_{max}	Maximum displacement of a building floor
δ_{avg}	Average displacements of two extreme points of a building floor
δ_t	Target displacement
τ	Modal damping ratio
λ	Plan aspect ratio of the building ($= L_{max}/L_{min}$)
λ_i, λ_j	Response quantity in mode i and j respectively
μ	Displacement ductility ratio
Ω_R	Uncoupled torsional to lateral frequency
ρ_{ij}	Cross-modal coefficient
ρ_s	Volumetric ratio of confining steel
ξ_n	Damping ratio
ϵ_c	Compressive strain
$\epsilon_{cu}\ \epsilon_{cc}$	Critical compressive strains
ϵ_{co}	Unconfined compressive strain
ϵ_{sm}	Steel strain at maximum tensile stress.
ϵ_1, ϵ_2	Extreme fibre strains
ϕ_{ik}	Mode shape coefficient at floor i in k mode
$\phi_{n,roof}$	n^{th} mode shape at roof level
φ	Curvature
φ_u	Ultimate curvature
φ_y	Yield curvature
θ	Rotation
θ_p	Plastic rotation

θ_u	Ultimate rotation
θ_y	Yield rotation
$\{u\}$	Floor displacements relative to the ground
$[m]$	Mass matrices of the system
$[c]$	Classical damping of the system
$[k]$	Later stiffness matrices of the system
$\{\phi_n\}$	n^{th} mode of structure

CHAPTER 1

INTRODUCTION

1.1. OVERVIEW

Starting from the very beginning of civilization, mankind has faced several threat of extinction due to invasion of severe natural disasters. Earthquake is the most disastrous among them due to its huge power of devastation and total unpredictability. Unlike other natural catastrophes, earthquakes themselves do not kill people, rather the colossal loss of human lives and properties occur due to the destruction of man-made structures. Building structures are one of such creations of mankind, which collapse during severe earthquakes, and cause direct loss of human lives. Numerous research works have been directed worldwide in last few decades to investigate the cause of failure of different types of buildings under severe seismic excitations. Massive destruction of high-rise as well as low-rise buildings in recent devastating earthquake of Gujarat on 26th January, 2001 proves that also in developing counties like ours, such investigation is the need of the hour.

Seismic damage surveys and analyses conducted on modes of failure of building structures during past severe earthquakes concluded that most vulnerable building structures are those, which are asymmetric in nature. Hence, seismic behaviour of asymmetric building structures has become a topic of worldwide active research since about last two decades. Numerous investigations have been conducted on elastic and inelastic seismic behaviour of asymmetric systems to find out the cause of seismic vulnerability of such structures. A comprehensive list of such investigations in this field is available in the literature (e.g., Rutenberg, 1992;

Chandler *et. al.*, 1996). However, these previous investigations generally considered a simplified idealised model that may not correctly represent the actual characteristics of the three dimensional real buildings.

Asymmetric building structures are almost unavoidable in modern construction due to various types of functional and architectural requirements. The lateral-torsional coupling due to eccentricity between centre of mass (CM) and centre of rigidity (CR) in asymmetric building structures generates torsional vibration even under purely translational ground shaking. During seismic shaking of the structural systems, inertia force acts through the centre of mass while the resistive force acts through the centre of rigidity as shown in Fig. 1.1. Due to this non-concurrency of lines of action of the inertia force and the resistive force a time varying twisting moment is generated which causes torsional vibration of the structure in addition to the lateral vibration.

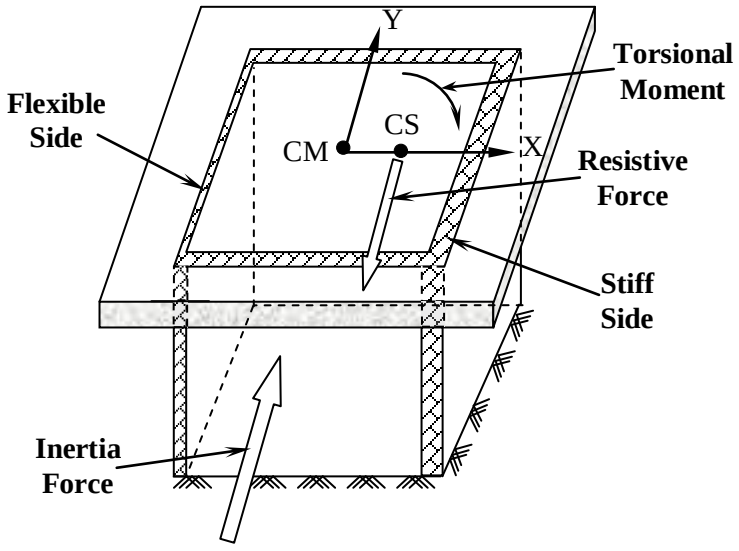

Fig. 1.1: Generation of torsional moment in asymmetric structures during seismic excitation

Most seismic codes require an equivalent static load method for the design of asymmetric building against earthquake forces. Design eccentricities include a

multiplier on the static eccentricity to account for possible dynamic amplification of the torsion. Also, the design eccentricities often include an allowance for accidental torsion that is supposed to be induced by the rotational component of ground motion, by possible deviation of the ECR (elastic centre of resistance) and centre of mass (CM) from their calculated positions or by unfavourable distribution of live loads.

The design eccentricity formulae given in most of the building codes can be written in the following form:

$$e_{fc} = \alpha e + \beta b \qquad (1a)$$

$$e_{sc} = \gamma e - \beta b \qquad (1b)$$

The torsion design provisions of Indian Standard (IS-1893:2002 (Part1)) specify the use of design eccentricity expressions Eq. 1a and Eq. 1b with α=1.5, β=0.05 and γ=1.Eqs. 1a and 1b result four possible design centre of mass (DCM) location in each floor of the building. To satisfy the design code one has to analyse a building multiple time considering all possible combination of DCM locations. This is time consuming and cumbersome exercise and generally not followed correctly in the design office. To address this problem it is important to know how different a code-designed asymmetric building behaves from a similar building designed without considering the code provision. This is the principal motivation for the present study.

1.2. LITERATURE REVIEW

A detailed literature review is carried out on seismic behaviour of asymmetric building. It is found that research on this topic started way back in 1958. Housner and Outinen (1958) reported large discrepancies between dynamic and static responses of

asymmetric structural systems. Reason for this discrepancy is the lateral-torsional coupling due to modification of eccentricity of inertia force resulting from rotatory inertia of the floor mass.Hart*et. al.* (1975) pointed out that torsional motion of buildings as a result of the 9th February 1971 San Fernando earthquake was substantial and for many cases it has been attributed to building asymmetry.

Irvine and Kountouris (1980) analysed an idealized asymmetric structural system with two lateral load-resisting elements to estimate the peak ductility demand of the asymmetric system and to compare the same with that of similar but symmetric system.

Models adoptedby Kan and Chopra (1981a),Kan and Chopra (1981b) and Sadek*et. al.*(1992) is equivalent single element model for approximate dynamic analysis of asymmetric structures under seismic excitations. Use of this type of model simplifies the process of analysis by considering a single lateral load-resisting element located at the centre of stiffness (CS) of the idealized system. The element is assumed to have dynamic as well as yielding properties equivalent to the original structures with many resisting elements. However, adoption of this model may limit the applicability of results for asymmetric structures with a specified range of variation of structural parameters.

Surveys and analyses following the 19th September 1985 Mexico earthquakeconducted byChandler, 1986; Rosenblueth and Meli, 1986and it is concluded that approximately 50% of the failures were either directly or indirectly attributed to asymmetry.

Tso and Ying (1990); Rutenberg*et. al.*(1992); Tso and Ying(1992); Tso and Zhu (1992); Duan and Chandler(1993); Chandler and Duan(1997) used idealized

asymmetric structural systems with three lateral load-resisting elements in the direction of excitation under uni-directional simulated ground excitation.

On the contraryChopra and Goel (1991), Chandler and Hutchinson (1992),Correnza*et. al*. (1994),Goel and Chopra (1994), andDuan and Chandler (1997) these have included transverse lateral load-resisting structural elements in considered idealized structural systems to establish the closeness of them with prototype structures. But these studies used ground motion input to the idealized system in one direction only. Transverse structural elements, in almost all of the above-mentioned study, were located only near the edge of the idealized asymmetric systems.

Sadek*et. al*.(1992)concluded that the equivalent single element model of approximate dynamic analysis is not at all suitable to estimate response of highly inelastic stiff structures with plan asymmetry. Moreover, these investigations mainly focused on assessment of maximum displacement and rotation of asymmetric systems during seismic excitations.

Rutenberg (1992)pointed out that the research works considering single element models could not yield the ductility demand parameter properly, because they have considered distribution of strength in same proportion as their elastic stiffness distribution. Considering these drawbacks of the equivalent single element model, many investigations in this field adopted a generalized type of structural model which had a rigid deck supported by different numbers of lateral load-resisting elements representing frames or walls having strength and stiffness in their planes only.

De Stefano *et. al*,(1993) noticed considerable variation in different investigations about strength and stiffness distribution as well as position of lateral load-resisting elements in idealized asymmetric systems. Most of these idealized building systems

were devoid of any structural elements in direction perpendicular to the direction of seismic excitation. These transverse structural elements if present can reduce the effect of torsion. Hence, consideration of transverse structural elements may lead to overestimation of seismic torsional responses of asymmetric building systems. However, it is to be mention that inclusion of transverse structural elements may not be significant in some case when linear properties of structural elements are kept intact, i.e., when elastic response is the matter of interest.

De La Llera and Chopra (1994)suggest that structural elements in transverse direction should be excluded when uni-directional seismic excitation is used. Riddell and Santa-Maria (1999) presented inelastic seismic response of asymmetric-plan structures under bi-directional ground motion has considered lateral load-resisting elements in both directions but located only near the edge of the structural system. This is again not a true representation of the regular building structures, which generally have their lateral load-resisting elements uniformly distributed over the plan.

Chandler *et. al*. (1996) shows that presence or absence of transverse elements in the response studies makes some difference as they affect torsional strength of the systems, which was not considered by many researchers.

The idealized systems considered by Goel (1997) and Tso and Smith (1999) consist of rigid deck supported by the three lateral load-resisting structural elements in each of the two orthogonal principal directions. Moreover, one of those recent investigations (Goel, 1997) did not consider any restriction about the position of the lateral load-resisting elements to avoid lack of generality.

Significant asymmetry in the plan of the structure can result from uneven distribution of mass, which may occur due to modifications/additions after the building is

constructed, and this was a major factor as per Goel (2001) that contributed to the failure of at least one building in the 26th January 2001 Gujarat earthquake.

A preliminary investigation (Dutta, 2001) in the area of seismic torsional behaviour of reinforced concrete asymmetric structures, considered three different types of idealized systems, representative of three different types of real life building structures. Each type of idealized structural system as shown in Fig.1.2 consists of a rigid deck slab supported on different numbers of lateral load-resisting elements.

In the first type of idealized system, mentioned as two-element system, the rigid deck slab is supported on two lateral load-resisting elements (as shown in Fig. 1.2(a)). This type of idealized structural system represents a class of buildings, which have shear wall type structural elements near two opposite edges. These structures (e.g., airport hanger type buildings), generally, have much stronger lateral stiffness in one principal direction compared to the other one.

The second type of idealized structural system represents auditorium type buildings in which almost all of the lateral stiffness is normally distributed over the four edges. The rigid deck slab in this case, is considered to be supported on four lateral load-resisting elements located near the four edges of the idealized structural system (as shown in Fig. 1.2(b)). This idealized structural system is entitled as four element system in the investigation (Dutta, 2001) for convenience of understanding.

To represent the situation of most common buildings structures (e.g., residential building or office buildings) in which lateral stiffness remain more or less equally distributed over the entire plan area, the third type of idealized structural system may be considered. In this case, the rigid deck slab is supported by three lateral load-resisting elements (as shown in Fig. 1.2(c)) in each of the two principal directions.

The lateral stiffness of central lateral load-resisting element in each of the principal direction is assumed to be half of the total lateral stiffness in that particular direction. The rest of the same is equally distributed among two lateral load-resisting elements located near the edge. This type of idealized structural system is termed as six-element system in the earlier literature (Dutta, 2001).

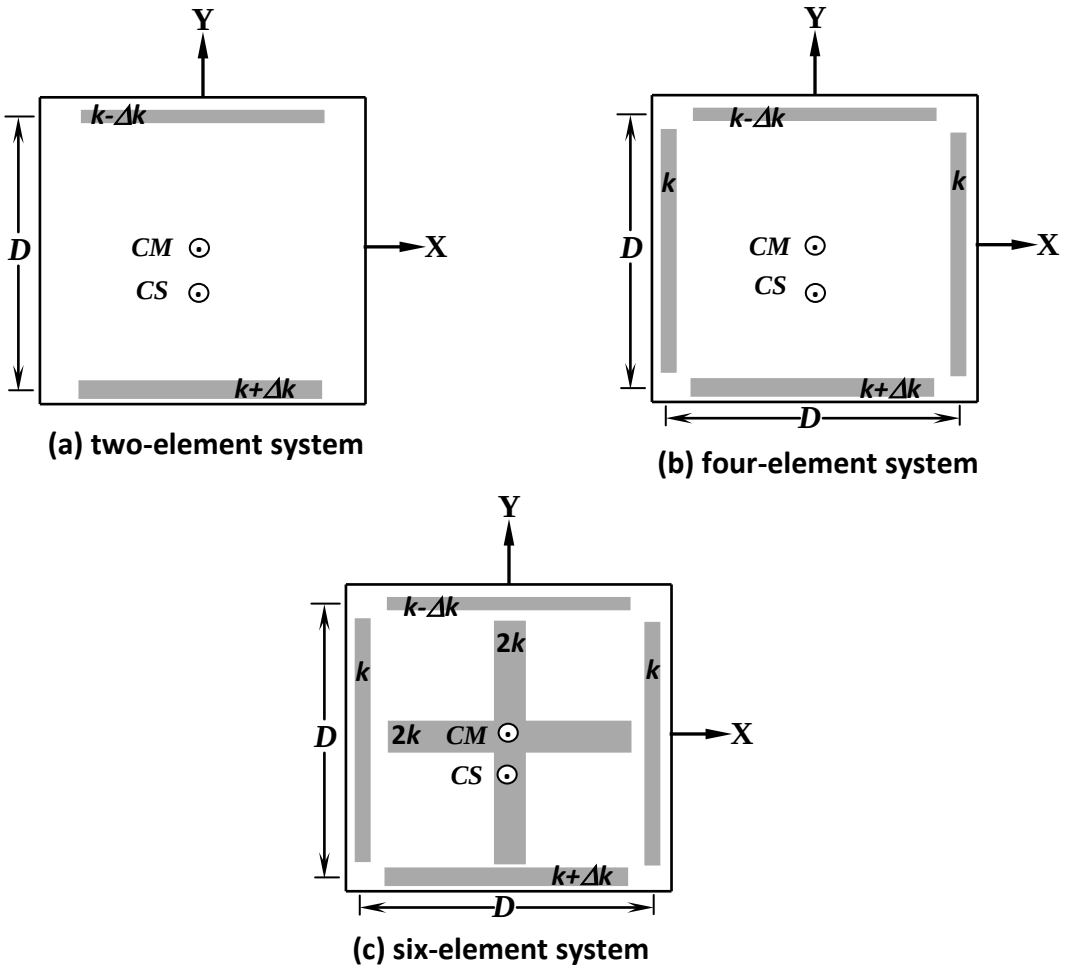

Fig.1.2: Different types of uni-directionally asymmetric idealized structural systems used in Dutta, 2001.

1.3. OBJECTIVE

With this background and the literature review presented here and codal provision given later, the salient objectives of the present study have been identified as follows:

- To compare the behaviour of asymmetric building designed with or without considering IS 1893:2002 (Part1) code provisions on torsional irregularity.
- To propose improvement over IS 1893:2002 (Part1) code provisions on torsional irregularity for design of asymmetric building.

1.4. SCOPE OF THE STUDY

i) The present study is based on a case study of a four storeyed RC framed building. Only mass eccentricity is considered in the present study. Stiffness eccentricity of building is kept outside the scope of the present work.

ii) The present study considers mass eccentricity in one direction only although eccentricity in both the horizontal orthogonal directions in asymmetric building is more general. Also, the building models are analysed against uni-directional loading.

iii) Nonlinear modelling considers point plastic flexural hinges only. This can be justified as flexural failure precedes the shear failure for all code designed buildings.

iv) Column ends are assumed to be fixed at the supports. Soil-structure interaction is ignored for the present study.

1.5. METHODOLOGY

The methodology worked out to achieve the above-mentioned objectives is as follows:

i. Review the existing literature andinternational design code provisions for designing asymmetric building

ii. Select asymmetric building models designed considering and without considering code provisions

iii. Analysis (nonlinear static and dynamic) of the selected building models and a similar regular building model for comparison.

iv. Observations of results and discussions

1.6. ORGANIZATION OF THESIS

This introductory chapterpresents the background and motivation behind this study followed by a brief report on the literature survey. The objectives and scope of the proposed research work are identified in this chapter.

Chapter 2 reviews Euro code (prEN 1998-1:2003), International Building Codes (IBC-2003), New Zealand Standards (NZS-4203: 1992) and National Building Codes of Canada (NBCC-1995) with regard to the torsional provision and compare IS-1893: 2002 clauses with these international standards.

Chapter 3 presents computational modelling of selected buildings using SAP 14. The building details also explained in this chapter. The analytical models used in the present study for representing the actual behaviour of different structural components in the building frame are explained in this chapter. It also describes in detail the modelling of point plastic hinges used in the present study, algorithm for generating hinge properties and the assumptions considered. Spectral identical data generation is presented in that chapter which is used for nonlinear dynamic analysis.

Chapter 4 presents the results obtained from nonlinear static (pushover) analyses of the selected building models along with the discussions on these results.

Chapter 5 presents and discusses the results obtained from nonlinear dynamic (time history) analysis based natural and generated ground motions.

Finally, in Chapter 6, the summary and conclusions are presented. The scope for future work is also discussed.

CHAPTER 2

REVIEW OF CODE PROVISIONS

2.1. OVERVIEW

The earthquake resistant code in India, IS: 1893 (Part1), has been revised in 2002 to include provisions for asymmetric buildings. This chapter presents a review of leading international building codes such as Euro code (prEN 1998-1:2003), International Building Codes (IBC-2003), New Zealand Standards (NZS-4203: 1992) and National Building Codes of Canada (NBCC-1995) with regard to the torsional provision and how IS-1893: 2002 clauses compare with these international standards. Most seismic codes require linear static or dynamic load method for the design of asymmetric building against earthquake forces.

Static Eccentricity (e) is defined in the design code as the distance between centre of mass (CM) and centre of rigidity (CR). Design eccentricities (e_{fc}, e_{sc}) include a multiplier on the static eccentricity to account for possible dynamic amplification of the torsion. Also, the design eccentricities often include an allowance for accidental torsion that is supposed to be induced by the rotational component of ground motion, by possible deviation of the ECR (elastic center of resistance) and centre of mass (CM) from their calculated positions or by unfavourable distribution of live loads.

The design eccentricity formulae given in most of the building codes can be written in the following general form:

$$e_{fc} = \alpha e + \beta b \qquad (2.1a)$$

$$e_{sc} = \gamma e - \beta b (2.1b)$$

Table 2.1: Design Eccentricity for different International code clause

e_s (m)	Equation 2.1a (m)					Equation 2.1b (m)				
	IS 1893	IBC 2003	FEMA 450	NZS4 203	prEN 1988-1	IS 1893	IBC 2003	FEM A 450	NZS 4203	prEN 1988-1
0.95	1.98 2.38	1.45 1.45	1.38 1.74	2.05 2.85	3.62 4.02	0.4 0	0.45 0.08	0.45 0.08	-0.15 -0.95	0.4 0
1.9	3.4 3.8	2.66 3.22	3.4 3.95	3 3.8	5.45 5.85	1.35 0.95	1.14 0.58	1.14 0.58	0.8 -0.95	1.35 0.95
2.85	4.83 5.23	3.62 4.17	4.74 5.3	3.95 4.75	6.4 6.8	2.3 1.9	2.08 1.53	2.08 1.53	1.75 0.95	2.3 1.9
3.8	6.25 6.65	4.73 5.41	7.37 8.05	4.9 5.7	7.35 7.75	3.25 2.85	2.87 2.19	2.87 2.19	2.7 1.9	3.25 2.85

2.2. STRENGTH DESIGN OF MEMBERS

Previous building codes suggested taking care of the dynamic effect in symmetric as well as asymmetric buildings during seismic excitations in a simplistic manner. According to this concept, the inertia force is assumed to be applied statically to the structure at the centre of mass (CM). Seismic shear on a particular lateral load-resisting element of an asymmetric system can be obtained as:

$$S_i = S\frac{k_i}{\sum k} \pm Se\frac{k_i a_i}{\sum k a^2} \qquad (2.2)$$

However, these older building codes did not consider any dynamic amplification effect. To alleviate this problem, concept of design eccentricity (e_d) has been introduced based on the findings of large numbers of research efforts in this area. This concept suggests to amplify the static eccentricity while deciding the strength of structural members located near the flexible side and to reduce the same for deriving the strength of stiff side members.

2.3. INDIAN STANDARDS IS-1893:2002 (PART 1)

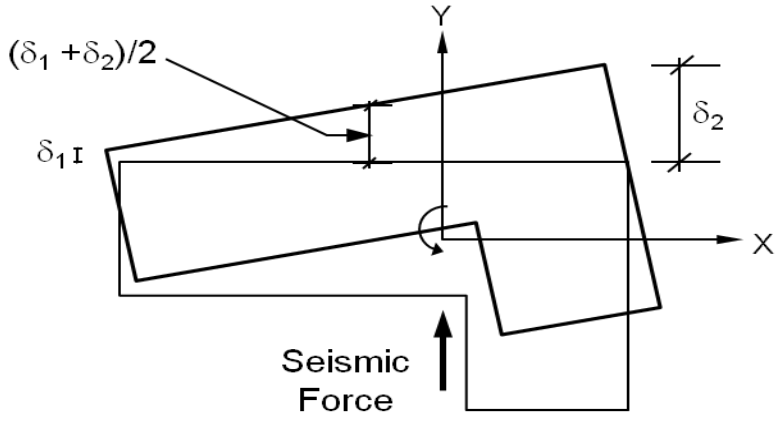

Fig. 2.1: Figure explaining δ_{max} and δ_{avg} in asymmetric building

The torsion design provisions of Indian Standard (IS-1893:2002(Part1)) specify the use of design eccentricity expressions Eq.2.1a and Eq.2.1b with α=1.5, β=0.05 and γ=1. IS 1893:2002 (Part1) does not permit any reduction of lateral strength resulting from negative shear due to the effect of eccentricity. Indian Standard also recommended that dynamic analysis is required to perform for an irregular framed building higher than 12m in Zone IV and Zone V (PGA= 0.24g and 0.36g respectively) and 40m in Zone II and

Zone III (PGA= 0.10g and 0.16g respectively). Building with $\delta_{max}/\ \delta_{avg} \geq 1.2$ are defined as torsional irregular in IS 1893:2002. Where δ_{max} is the maximum displacement of the floor produced by the equivalent static earthquake forces, and $\delta_{avg}=(\delta_1+\delta_2)/2$ is the average of the displacements of the extreme points of the structure. $\delta_{max} =\delta_2$ and δ_{avg}(Fig. 2.1)should be computed with the design eccentricity.

2.4. INTERNATIONAL BUILDING CODE IBC 2003

Eccentricity coefficients specified in IBC 2003 are: α=1.0, $\beta=A_x$ 0.05 and γ=1.0, where A_x is determined from the following equation:

$$A_x = \left(\frac{\delta_{max}}{1.2\delta_{avg}}\right) \tag{2.3}$$

In calculating δ_{max} the effect of accidental torsion must be accounted for but accidental torsion need not be included while calculatingδ_{avg}. If V_0 is applied at a distance $(e + 0.05b$ from ECR δmax can be written as:

$$\delta_{max} = \frac{V_0}{K_y} + \frac{V_0(e + 0.05b)}{K_{\theta R}}\left(\frac{b}{2} + e\right) \tag{2.4}$$

And δ_{avg} be calculated by applying V_0 is through the CM as follows:

$$\delta_{avg} = \frac{V_0}{K_y} + \frac{V_0 \times e^2}{K_{\theta R}} \tag{2.5}$$

Thus A_x can be expanded as:

$$A_x = \left(\frac{\delta_{max}}{1.2\delta_{avg}}\right)^2 = \left(\frac{1 + \frac{1}{\Omega_R^2}\left(\frac{b}{r}\right)^2\left(\frac{e}{b} + 0.05\right)\left(0.5 + \frac{e}{b}\right)}{1.2\left\{1 + \frac{1}{\Omega_R^2}\left(\frac{b}{r}\right)^2\left(\frac{e}{b}\right)^2\right\}}\right)^2 \quad (2.6)$$

Eq.2.6 shows that the design eccentricity depends on three parameters: uncoupled torsional to lateral frequency(Ω_R), floor aspect ratio (b/r) and static eccentricity(e/b). The code also provides that A_x may not be taken as less than 1 and need not be greater than 3. Here *r* represent radius of gyration of the floor.

2.5. FEMA 450:2003(NEHRP)

In FEMA 450:2003, torsional irregularities are subdivided into two categories: torsional irregularity and extreme torsion irregularity. Building with $\delta_{max}/\ \delta_{avg} \geq 1.2$ is classified in the category of torsional irregularity and buildings with $\delta_{max}/\ \delta_{avg} \geq 1.4$ in extreme torsional irregularity. Extreme torsional irregularities are prohibited for structures located very close to major active faults and should be avoided, when possible, in all structures.

For the 1st type of irregularity FEMA 450 recommends to use the procedure explained in Eqs. 2.1a and 2.1b.According to FEMA 450 the amplification factor A_x is applied to both the natural and the accidental torsion components of the design eccentricities, not just to the accidental torsion component. Thus the design eccentricity coefficients are: $\alpha=A_x$, $\beta=0.05A_x$ and $\gamma=1$.

2.6. New Zealand Code NZS 4203:1992

NZS 4203:1992 allows the use of an equivalent static analysis only when one of the following horizontal regularity criteria is satisfied:

i. e≤0.3b and eccentricity does not change its sign over the height of the building;

ii. Under the action of equivalent static loads applied at a distance $e_d = e \pm 0.1b$ from ECR, the ratio of horizontal displacements at the ends of an axis at any horizontal plane transverse to the direction of forces is in the range of 3/7 to 7/3.

NZS 4203:1992 requires three dimensional dynamic analyses for all other cases. For static analysis NZS 4203:1992 uses the design eccentricities as given in Eqs2.1a and 2.1b with α= γ=1 and β=0.1.

2.7. EURO CODEprEN1988-1:2003

The criteria for torsional irregularity defined in prEN 1998-1:2003 includes plan aspect ratio as well as the static eccentricity.

i. Plan aspect ratio,$\lambda = L_{max} / L_{min}$ of the building shall not be higher than 4 for the building to be torsionally regular.

ii. For the building to be regular, static eccentricity$e \leq 0.30 r_x (r_x \geq l_s)$..

The design eccentricity in prEN 1998-1:2003 is slightly different from the others and defined as follows:

$$e_{fc} = (e + e_2) + e_1 \qquad (2.7a)$$

$$e_{sc} = e - e_1 \qquad (2.7a)$$

Here, $e_1 = 0.05b$ is the accidental eccentricity and e is the static eccentricity (i.e., distance between CM and ECR). These two terms are similar to those of other codes. But

an additional eccentricity e_2 is considered here to account for the dynamic effect of simultaneous translational and torsional vibrations. This e_2 is defined as the minimum of following two values:

$$e_2 = 0.1(L+B)\sqrt{(10\times e)/L} \leq 0.1(L+B) \qquad (2.8a)$$

$$e_2 = \frac{1}{2e}\left[l_s^2 - e^2 - r^2 + \sqrt{(l_s^2 - e^2 - r^2) + 4e^2 \times r^2}\right] \qquad (2.8b)$$

2.8. CANADA CODE NBCC 1995

The design eccentricities in NBCC 1995 are obtained from Eqs.2.1a and 2.1b with α=1.5, β=0.1A_x and γ=0.5. NBCC suggests that as an alternative a 3-D dynamic-analysis may be carried out to evaluate the effect of torsion. When a dynamic procedure is used, accidental torsion can be accounted for by applying a torque equal to floor force times 0.1b at each floor. The forces produced by these torques should be added to or subtracted from the forces obtained from 3-D analysis to obtain the maximum design force for each resistance element.

2.9. SUMMARY

The provisions for torsional eccentricity in different international codes are explained in this chapter. It is found that the all the major international codes are using similar function to calculate design eccentricity as shown in Eq. 2.1a and Eq. 2.1b. However, the prescribed values of the coefficients differ from code to code.

CHAPTER 3

STRUCTURAL M.ODELLING

3.1. INTRODUCTION

The first part of thischapter presents a summary of various parameters defining the computational models, the basic assumptions and the building geometries considered for this study.

Accurate modelling of the nonlinear properties of various structural elements is very important in nonlinear analysis. In the present study, frame elements are modelled with inelastic flexural hinges using point plastic model. The second part of this chapter presents the properties of the point plastic hinges, the procedure to generate these hinge properties and the assumptions made.

Finally, this chapter presents the important parameters used for nonlinear time-history analysis and details of the ground motion considered in the analysis.

3.2. COMPUTATIONAL MODEL

Modelling a building involves the modelling and assemblage of its various load-carrying elements. The model must ideally represent the mass distribution, strength, stiffness and deformability. Modelling of the material properties and structural elements used in the present study is discussed below.

3.2.1. Material Properties

M-25 grade of concrete and Fe-415 grade of reinforcing steel are used for all the frame models used in this study. Elastic material properties of these materials are taken as per Indian Standard IS 456: 2000. The short-term modulus of elasticity (E_c) of concrete is taken as:

$$\mathrm{E_c} = 5000\sqrt{f_{ck}}MPa \tag{3.1}$$

f_{ck} is the characteristic compressive strength of concrete cube in MPa at 28-day (25 MPa in this case). For the steel rebar, yield stress (f_y) and modulus of elasticity (E_s) is taken as per IS 456 (2000).

3.2.2. Structural Elements

Beams and columns are modelled by 3D frame elements. The beam-column joints are modelled by giving end-offsets to the frame elements, to obtain the bending moments and forces at the beam and column faces. The beam-column joints are assumed to be rigid (Fig. 3.1). The column end at foundation is considered as fixed for all the models in this study. All the frame elements are modelled with nonlinear properties at the possible yield locations.

The structural effect of slabs due to their in-plane stiffness is taken into account by assigning ‘diaphragm’ action at each floor level. The mass/weight contribution of slab is modelled separately on the supporting beams.

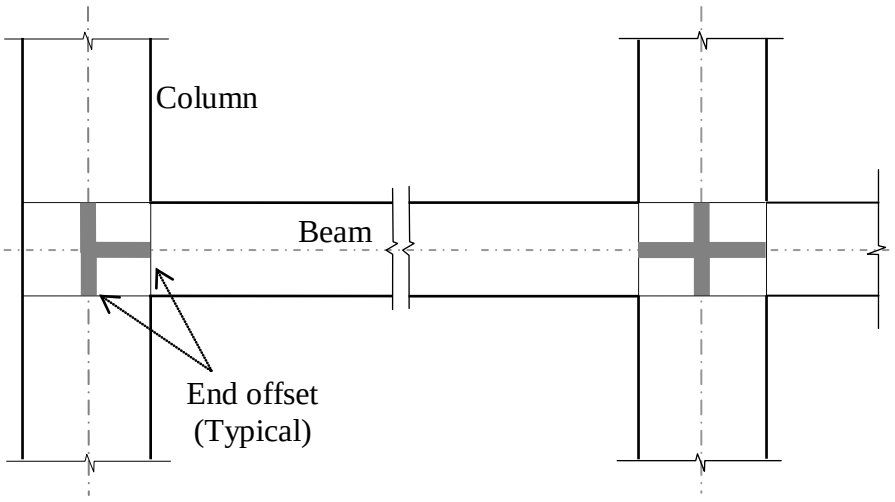

Fig. 3.1: Use of end offsets at beam-column joint

3.3. BUILDING GEOMETRY

A four-storey reinforced concrete frame building (Fig.3.2) with different asymmetry is designed with IS 1893:2002 (Part1); IS 456:2000 and IS 13920: 1993. The building has a uniform storey height of 3 m at each storey. The plan geometry of the building and frame dimensions are taken from literature (Kilar, 2001). The cross sections of the structural members (columns and beams 300 mm×600 mm) are equal in all frames and all stories. The symmetric building variant (SYM) is designed using IS 1893:2002 (Part1), considering an accidental eccentricity equals to ±5% of the relevant plan dimension of the building. Two asymmetric variants are obtained by shifting the centre of masses (CM) in the positive X direction by an amount 0.1L (1.9m). In the first asymmetric variant (ASYM1), the structure remained the same as that of the symmetric building. The second asymmetric variant is redesigned considering mass

eccentricity of 0.1L and accidental eccentricity equals to ±5% of the relevant plan dimension of the building.

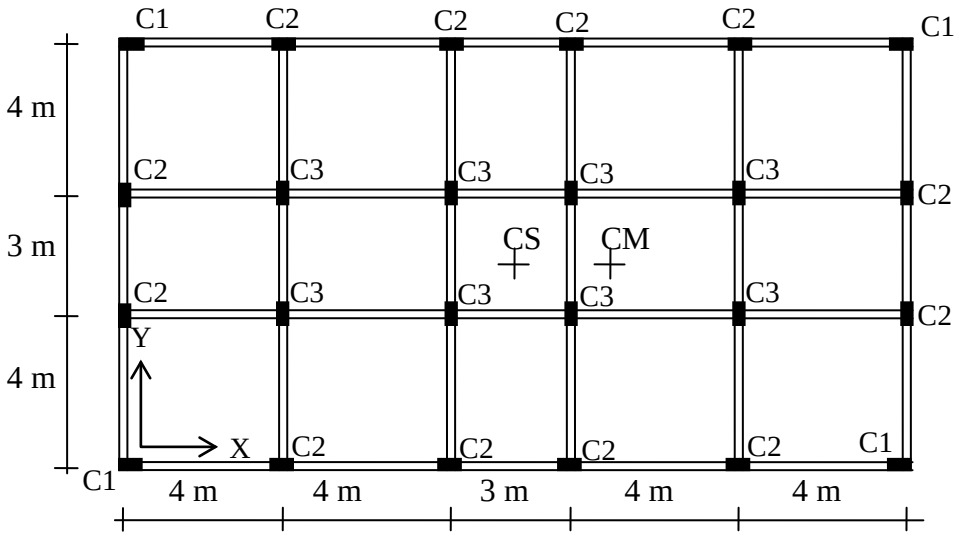

Fig. 3.2(a): Typical floor plan showing columns

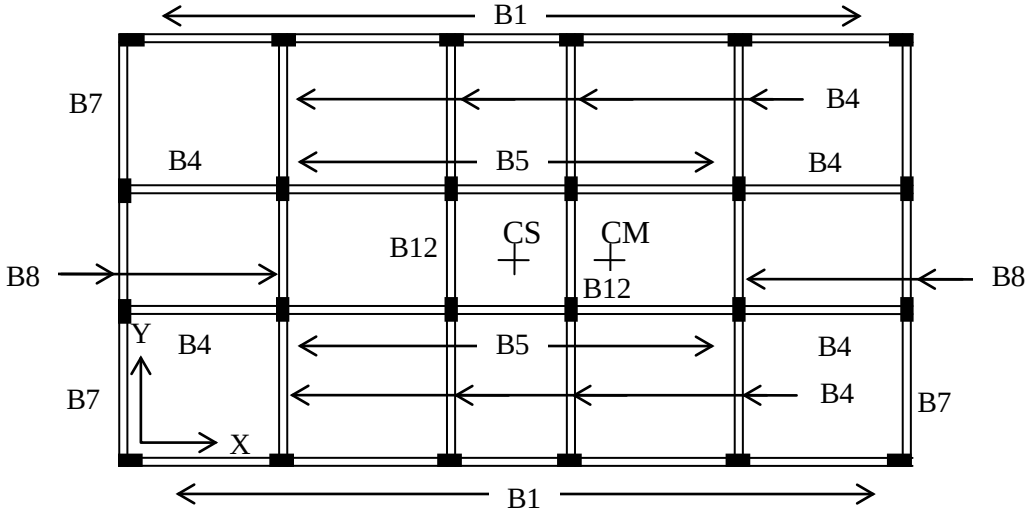

Fig. 3.2(b): Typical floor plan showing beams

For each frame the most unfavourable position of the CM is considered. The design spectrum for medium soil (Type II), with a peak ground acceleration of 0.36g (Zone V),

is used. The response reduction factor, R is equal to 3 (ordinary moment resisting frame). Storey masses to 295 and 237 tonnes in the bottom stories and at the roof level, respectively. The design base shear is equal to 0.15 times the total weight.

Reinforcement of the bottom two stories is different to that in upper two stories. The amount of longitudinal reinforcement in the columns and beams is given in Table 3.1 and Table 3.2, respectively for symmetric and asymmetric building. Beam reinforcement in floor and roof are different. Beam reinforcement at the floor given in Table 3.2 corresponds to Fig. 3.2b for their location. All beams at the roof are same as given in Table 3.2. Refer Annexure A for the details of the earthquake design.

Table 3.1: Longitudinal reinforcement details of column sections

Column No.	Asymmetric building		Symmetric building	
	First two storey	Top two storey	First two storey	Top two storey
C1	4Y16, 6Y12	4Y16, 6Y12	4Y16, 6Y12	4Y16, 6Y12
C2	14Y25	8Y25	10Y25	4Y25, 4Y20
C3	12Y25	4Y25, 4Y20	10Y25	4Y25, 4Y16

Table 3.2: Longitudinal reinforcement details of beam sections

Beam No.		Asymmetric building		Symmetric building	
		Top steel	**Bottom steel**	**Top steel**	**Bottom steel**
Floor Beams	B1	4Y16	3Y16	4Y16	3Y16
	B4	3Y16	2Y16	3Y16	2Y16
	B5	2Y16, 1Y12	2Y16	2Y16, 1Y12	2Y16
	B7	2Y16, 1Y12	2Y16	2Y16	2Y16
	B8	3Y16	2Y16, 1Y12	2Y16	2Y16
	B12	4Y16	3Y16	3Y16	2Y16, 1Y12
Roof Beams		2Y16	2Y16	2Y16	2Y16

3.4. MODELLING OF FLEXURAL PLASTIC HINGES

In the implementation of pushover analysis, the model must account for the nonlinear behaviour of the structural elements.In the present study, a point-plasticity approach is considered for modelling nonlinearity, wherein the plastic hinge is assumed to be concentrated at a specific point in the frame member under consideration.Beam and column elements in this study are modelled with flexure (M3for beams and P-M2-M3 for columns) hinges at possible plastic regionsunder lateral load (i.e., both ends of the beams and columns).Properties of flexure hinges must simulate the actual response of reinforced concrete components subjected to lateral load. Inthe present study the plastic hinge properties are calculated by SAP 2000 (v14). The analytical procedure used to model the flexural plastic hinges are explained below.

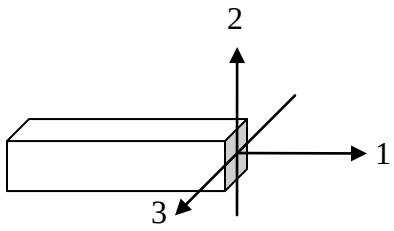

Fig. 3.3: The coordinate system used to define the flexural and shear hinges

Flexural hinges in this study are defined by moment-rotation curves calculated based on the cross-section and reinforcement details at the possible hinge locations. For calculatinghinge properties it is required to carry out moment–curvature analysis of each element.Constitutive relations for concrete and reinforcing steel, plastic hinge length in structural element are required for this purpose. The flexural hinges in beams are

modelled with uncoupled moment (M3) hinges whereas for column elements the flexural hinges are modelled with coupled P-M2-M3 propertiesthat include the interaction of axial force and bi-axial bending moments at the hinge location. Although the axial force interaction is considered for column flexural hinges the rotation values are considered only for axial force associated with gravity load.

3.4.1. Stress-Strain Characteristics for Concrete

The stress-strain curve of concrete in compression forms the basis for analysis of any reinforced concrete section. The characteristic and design stress-strain curves specified in most of design codes (IS 456: 2000, BS 8110) do not truly reflect the actual stress-strain behaviour in the post-peak region, as (for convenience in calculations) it assumes a constant stress in this region (strains between 0.002 and 0.0035). In reality, as evidenced by experimental testing, the post-peak behaviour is characterised by a descending branch, which is attributed to 'softening' and micro-cracking in the concrete. Also, models as per these codes do not account for strength enhancement and ductility due to confinement.However, the stress-strain relation specified in ACI 318M-02 consider some of the important features from actual behaviour. A previousstudy (Chugh, 2004)on stress-strain relation of reinforced concrete section concludes that the model proposed by Panagiotakos and Fardis(2001) represents the actual behaviour best for normal-strength concrete. Accordingly, this model has been selected in the present study for calculating the hinge properties. This model is a modified version of Mander's model (Mander*et. al.*, 1988) where a single equation can generate the stress f_c corresponding to any given strainε_c:

$$f_c = \frac{f_{cc}' xr}{r - 1 + x^r} \tag{3.2}$$

where, $x = \frac{\epsilon_c}{\epsilon_{cc}}; r = \frac{E_c}{E_c - E_{sec}}; E_c = 5000\sqrt{f_{co}'}; E_{sec} = \frac{f_{cc}'}{\varepsilon_{cc}}$ and f'_{cc} is the peak strengthexpressed as follows:

$$f_{cc}' = f_{co}' \left[1 + 3.7 \left(\frac{0.5 k_e \rho_s f_y h}{f_{co}'}\right)^{0.85}\right] \tag{3.3}$$

The expressions for critical compressive strains are expressed in this model as follows:

$$\varepsilon_{cu} = 0.004 + \frac{0.6 \rho_s f_{yh} \epsilon_{sm}}{f_{cc}'} \tag{3.4}$$

$$\varepsilon_{cc} = \epsilon_{co} \left[1 + 5 \left(\frac{f_{cc}'}{f_{co}'} - 1\right)\right] \tag{3.5}$$

The unconfined compressive strength (f'_{co}) is 0.75 f_{ck}, k_e having a typical value of 0.95 for circular sections and 0.75 for rectangular sections.

Fig. 3.4 shows a typical plot of stress-strain characteristics for M-20 grade of concrete as per Modified Mander's model (Panagiotakos and Fardis,2001). The advantage of using this model can be summarized as follows:

- A single equation defines the stress-strain curve (both the ascending and descending branches) in this model.
- The same equation can be used for confined as well as unconfined concrete sections.

- The model can be applied to any shape of concrete member section confined by any kind of transverse reinforcement (spirals, cross ties, circular or rectangular hoops).
- The validation of this model is established in many literatures (*e.g.*, Pam and Ho, 2001).

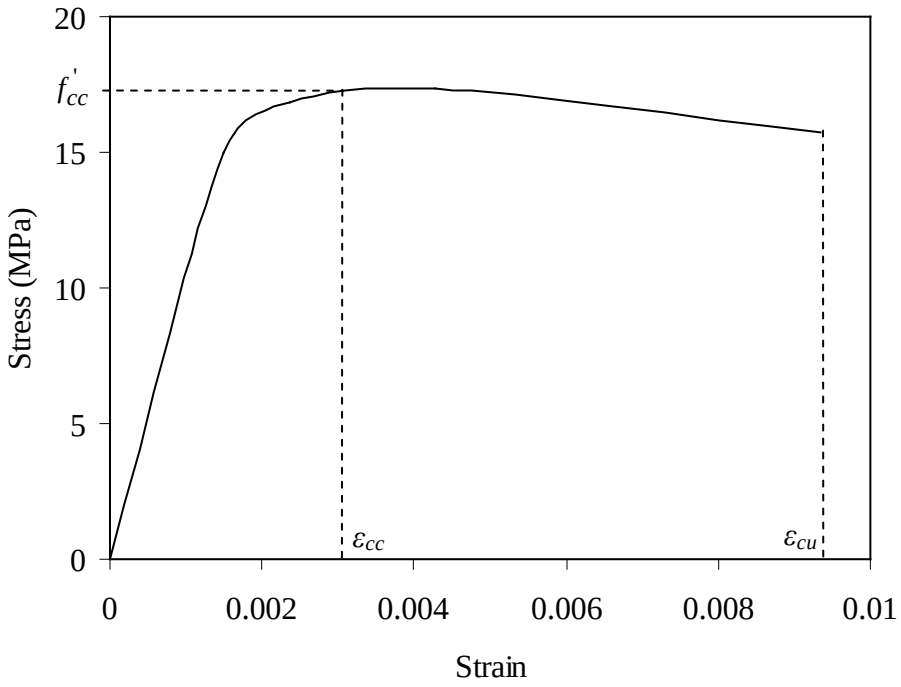

Fig. 3.4: Typical stress-strain curve for M-20 grade concrete (Panagiotakos and Fardis, 2001)

3.4.2. Stress-Strain Characteristics for Reinforcing Steel

The constitutive relation for reinforcing steel given in IS 456 (2000) is well accepted in literature and hence considered for the present study. The 'characteristic' and 'design' stress-strain curves specified by the Code for Fe-415 grade of reinforcing steel (in tension or compression) are shown in Fig. 3.5.

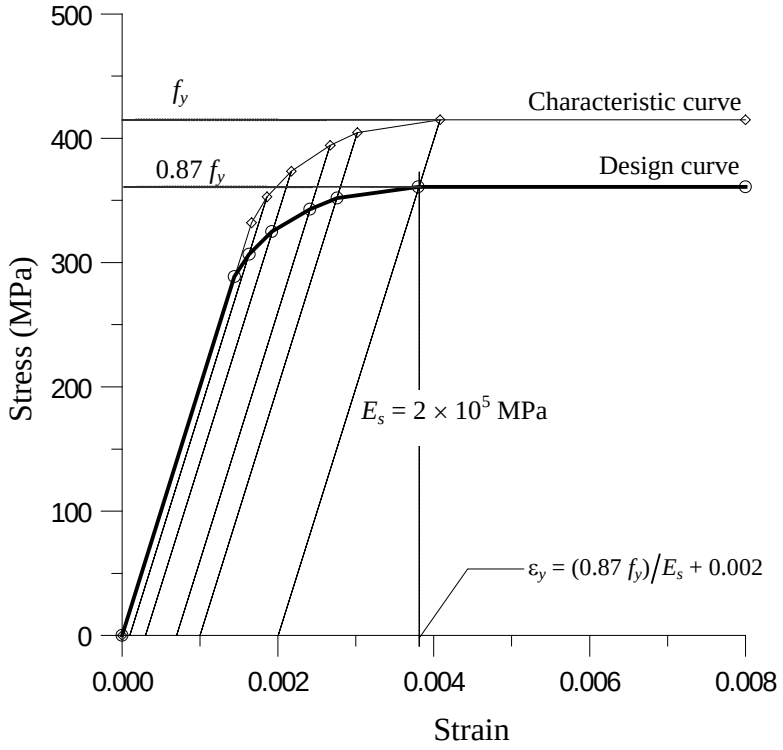

Fig. 3.5: Stress-strain relationship for reinforcement (Fe_{415}) – IS 456 (2000)

3.4.3. Moment-Curvature Relationship

Moment-curvature relation is a basic tool in the calculation of deformations in flexural members. It has an important role to play in predicting the behaviour of reinforced concrete (RC) members under flexure. In nonlinear analysis, it is used to consider secondary effects and to model plastic hinge behaviour.

Curvature (φ) is defined as the reciprocal of the radius of curvature (R) at any point along a curved line. When an initial straight beam segment is subject to a uniform bending moment throughout its length, it is expected to bend into a segment of a circle with a curvature φ that increases in some manner with increase in the applied moment (M). Curvature φ may be alternatively defined as the angle change in the slope of the elastic

curve per unit length$\left(\varphi = 1/R = d\theta/ds\right)$. At any section, using the 'plane sections remain plane' hypothesis under pure bending, the curvature can be computed as the ratio of the normal strain at any point across the depth to the distance measured from the neutral axis at that section (Fig. 3.6).

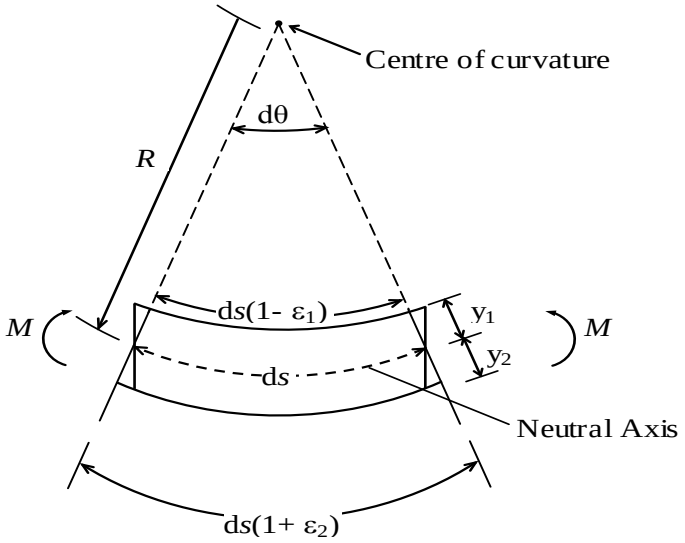

Fig. 3.6: Curvature in an initially straight beam section (Pillai and Menon, 2009)

If the bending produces extreme fibre strains of ε_1 and ε_2 at top and bottom at any section as shown in Fig. 3.6 (compression on top and tension at bottom assumed in this case), then, for small deformations, it can be shown that $\varphi = \left(\varepsilon_1 + \varepsilon_2\right)/D$. If the beam behaviour is linear elastic, then the moment-curvature relationship is linear, and the curvature is obtained as

$$\varphi = \frac{M}{EI} \tag{3.6}$$

The flexural rigidity(EI) of the beam is obtained as a product of the modulus of elasticity *E* and the second moment of area of the section *I*.

When an RC flexural member is subjected to a gradually increasing moment, it's behaviour transits through various stages, starting from the initial un-cracked state to the ultimate limit state of collapse. The stresses in the tension steel and concrete go on increasing as the moment increases. The behaviour at the ultimate limit state depends on the percentage of steel provided, i.e., on whether the section is 'under-reinforced' or 'over-reinforced'. In the case of under-reinforced sections, failure is triggered by yielding of tension steel whereas in over-reinforced section the steel does not yield at the limit state of failure. In both cases, the failure eventually occurs due to crushing of concrete at the extreme compression fibre, when the ultimate strain in concrete reaches its limit. Under-reinforced beams are characterised by 'ductile' failure, accompanied by large deflections and significant flexural cracking. On the other hand, over-reinforced beams have practically no ductility, and the failure occurs suddenly, without the warning signs of wide cracking and large deflections.

In the case of a short column subject to uni-axial bending combined with axial compression, it is assumed that Eq. 3.6 remains valid and that "plane sections before bending remain plane". However, the ultimate curvature (and hence, ductility) of thesection is reduced as the compression strain in the concrete contributes to resisting axial compression in addition to flexural compression.

3.4.4. Modelling of Moment-Curvature in RC Sections

Using the Modified Mander model of stress-strain curves for concrete (Panagiotakos and Fardis,2001)andIndian Standard IS 456 (2000) stress-strain curve for reinforcing steel, for a specific confining steel, momentcurvature relations can be generated for beams and columns (for different axial load levels). The assumptions and procedure used in generating the moment-curvature curves are outlined below.

Assumptions

i. The strain is linear across the depth of the section ('plane sections remain plane').

ii. The tensile strength of the concrete is ignored.

iii. The concrete spalls off at a strain of 0.0035.

iv. The initial tangent modulus of the concrete, E_c is adopted from IS 456 (2000), as $5000\sqrt{f_{ck}}$.

v. In determining the location of the neutral axis, convergence is assumed to be reached within an acceptable tolerance of 1%.

Algorithm for Generating Moment-Curvature Relation

i. Assign a value to the extreme concrete compressive fibre strain (normally starting with a very small value).

ii. Assume a value of neutral axis depth measured from the extreme concrete compressive fibre.

iii. Calculate the strain and the corresponding stress at the centroid of each longitudinal reinforcement bar.

iv. Determine the stress distribution in the concrete compressive region based on the Modified Mander stress-strain model for given volumetric ratio of confining steel. The resultant concrete compressive force is then obtained by numerical integration of the stress over the entire compressive region.

v. Calculate the axial force from the equilibrium and compare with the applied axial load (for beam element both of these will be zero). If the difference lies within the specified tolerance, the assumed neutral axis depth is adopted. The moment capacity and the corresponding curvature of the section are then calculated. Otherwise, a new neutral axis is determined from the iteration (using bisection method) and steps (iii) to (v) are repeated until it converges.

vi. Assign the next value, which is larger than the previous one, to the extreme concrete compressive strain and repeat steps (ii) to (v).

vii. Repeat the whole procedure until the complete moment-curvature is obtained.

3.4.5. Moment-Rotation Parameters

Moment-rotation parameters are the actual input for modelling the hinge properties and this can be calculated from the moment-curvature relation. This can be explained with a simple cantilever beam AB shown in Fig. 3.7(a) with a concentrated load applied at the free end B. To determine the rotation between the ends an idealized inelastic curvature distribution and a fully cracked section in the elastic region may be assumed. Figs. 3.7(b)

and 3.7(c) represent the bending moment diagram and probable distribution of curvature at the ultimate moment.

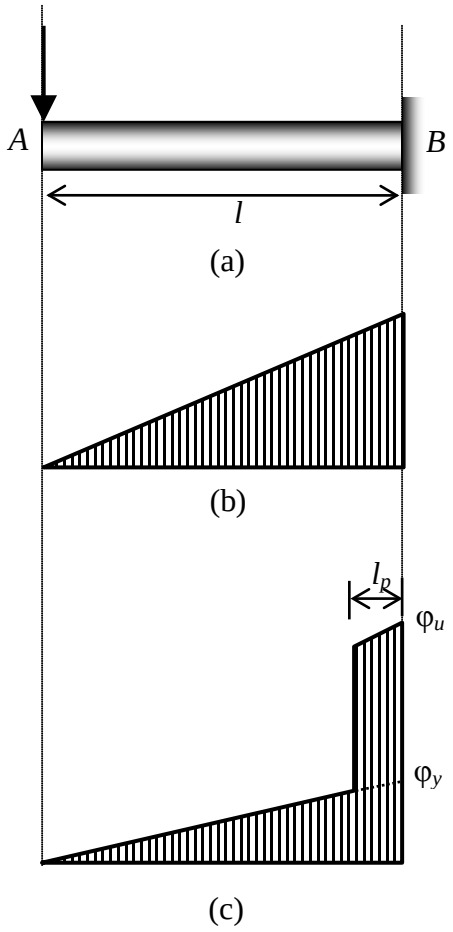

Fig. 3.7: (a) cantilever beam, (b) Bending moment distribution, and (c) Curvature distribution (Park and Paulay 1975)

The rotation between *A* and *B* is given by

$$\theta = \int_{A}^{B} \varphi \, dx \tag{3.7}$$

The ultimate rotation is given by,

$$\theta_u = \varphi_y \frac{1}{2} + (\varphi_u - \varphi_y) l_p \tag{3.8}$$

The yield rotation is,

$$\theta_y = \varphi_y \frac{1}{2} \tag{3.9}$$

And the plastic rotation is,

$$\theta_p = (\varphi_u - \varphi_y) l_p \tag{3.10}$$

l_p is equivalent length of plastic hinge over which plastic curvature is considered to be constant.The physical definition of the plastic hinge length, considering the ultimate flexural strength developing at the support, is the distance from the support over which the applied moment exceeds the yield moment. A good estimate of the effective plastic hinge length may be obtained from the following equation (Paulay and Priestley, 1992)

$$l_p = 0.08l + 0.15 d_b f_y \tag{3.11}$$

The yield strength of the longitudinal reinforcement should be in 'ksi'. For typical beam and column proportions Eq. 3.11 results in following equation (FEMA-274; Paulay and Priestley, 1992) where *D* is the overall depth of the section.

$$l_p = 0.5D \tag{3.12}$$

The moment-rotation curve can be idealised as shown in Fig. 3.8, and can be derived from the moment-curvature relation. The main points in the moment-rotation curve shown in the figure can be defined as follows:

- The point 'A' corresponds to the unloaded condition.

- The point 'B' corresponds to the nominal yield strength and yield rotation θ_y.
- The point 'C' corresponds to the ultimate strength and ultimate rotation θ_u, following which failure takes place.
- The point 'D' corresponds to the residual strength, if any, in the member. It is usually limited to 20% of the yield strength, and ultimate rotation, θ_u can be taken with that.
- The point 'E' defines the maximum deformation capacity and is taken as $15\theta_y$ or θ_u, whichever is greater.

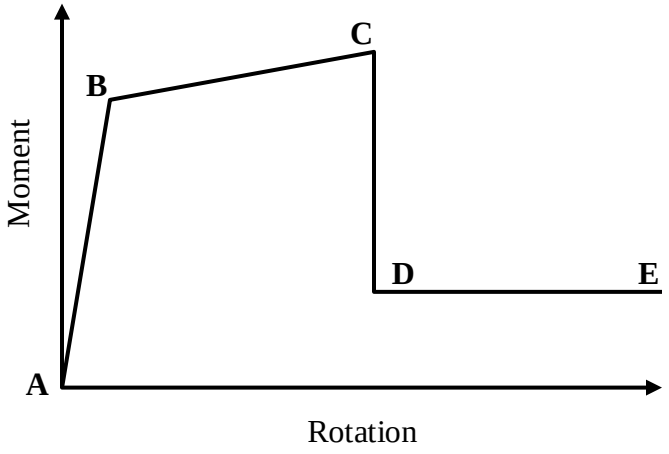

Fig. 3.8: Idealised moment-rotation curve of RC elements

While applying Eqs. 3.8and3.9 to determine the ultimate and yield rotations, care must be taken to adopt the correct value of the length *l*, applicable for cantilever action. In the case of a frame member in a multi-storey frame subject to lateral loads, it may be conveniently assumed that the points of contra flexure are located (approximately) at the mid-points of the beams and columns. In such cases, an approximate value of *l* is given by half the span of the member under consideration.

3.5. NONLINEAR TIME HISTORY ANALYSIS

Time-history analysis is a step-by-step analysis of the dynamical response (in time domain) of a structure subjected to a specified ground motion. This section explains the nonlinear parameters, input ground motion, time integration and damping used in the present study. The dynamic input has been given as a ground acceleration time-history which is applied uniformly at all the points of the base of the structure; only one horizontal component of the ground motion has been considered. Fifteen input time histories, consisting of five artificially generated accelerogram and ten natural records, are employed for the dynamic analysis of the study. Computer software SAP2000 (v14)is used for carrying out nonlinear time-history analysis.

To maintain the similarity between the dynamic analysis and the pushover analysis, standard hinges are used to model nonlinearity in the frame through nonlinear links. Also, soil-structure interaction effect and P-Δ effects are neglected in both pushover and dynamic analysis. The limitation of this model is that it does not consider the stiffness and strength degradation in cyclic loading.

The damping matrix is calculated as a linear combination of the stiffness matrix scaled by a coefficient, and the mass matrix scaled by a second coefficient. These coefficients are not specified directly,butare computed by specifying equivalent fractions of critical modal damping at two different periods.

Table 3.3: Characteristics of the selected ground motion

No.	Earthquake	Magnitude	Epicentre Distance (KM)	Duration (sec)	PGA (g)
1	Imperial Valley Earthquake, May 18, 1940	6.9	16.9	12	0.32
2	Loma Prieta-Oakland, October 17, 1989	7.1	3.5	40	0.28
3	Loma Prieta-Corralitos, October 17, 1989	7.1	7	40	0.63
4	Northridge-Santa Monica, January 17, 1994	6.7	23	60	0.37
5	Northridge-Sylmar, January 17, 1994	6.7	16	60	0.84
6	Northridge-Century City, January 17, 1994	6.7	20	60	0.22
7	Landers-Lucerne Valley, June 28, 1992	7.3	42	48	0.68
8	Sierra Madre-Altadena, June 28, 1991	5.6	12.6	40	0.44
9	Imperial Valley Earthquake-El Centro, October 15,1979	6.6	13.2	40	0.37
10	Morgan Hill-Gilroy 4, April 24, 1984	6.2	37.4	60	0.18

'Hilber-Hughes-Taylor alpha' (HHT) method is used for performing direct-integration time-history analysis. The HHT method is an implicit method and is popular due to its intrinsic stability. The HHT method uses a single parameter (alpha) whose value is bounded by 0 and -1/3.

3.5.1. Natural Record of Earthquake Ground Motion

Fifteen natural ground acceleration time histories have been used for the dynamic analysis of the structural models. All these acceleration data are collected from Strong Motion Database available in the website of Center for Engineering Strong Motion Data, USA (http://www.strongmotioncenter.org/) and are scaled to peak ground acceleration 0.3g. The main characteristics of the input motion used are summarized in Table 3.3 above.

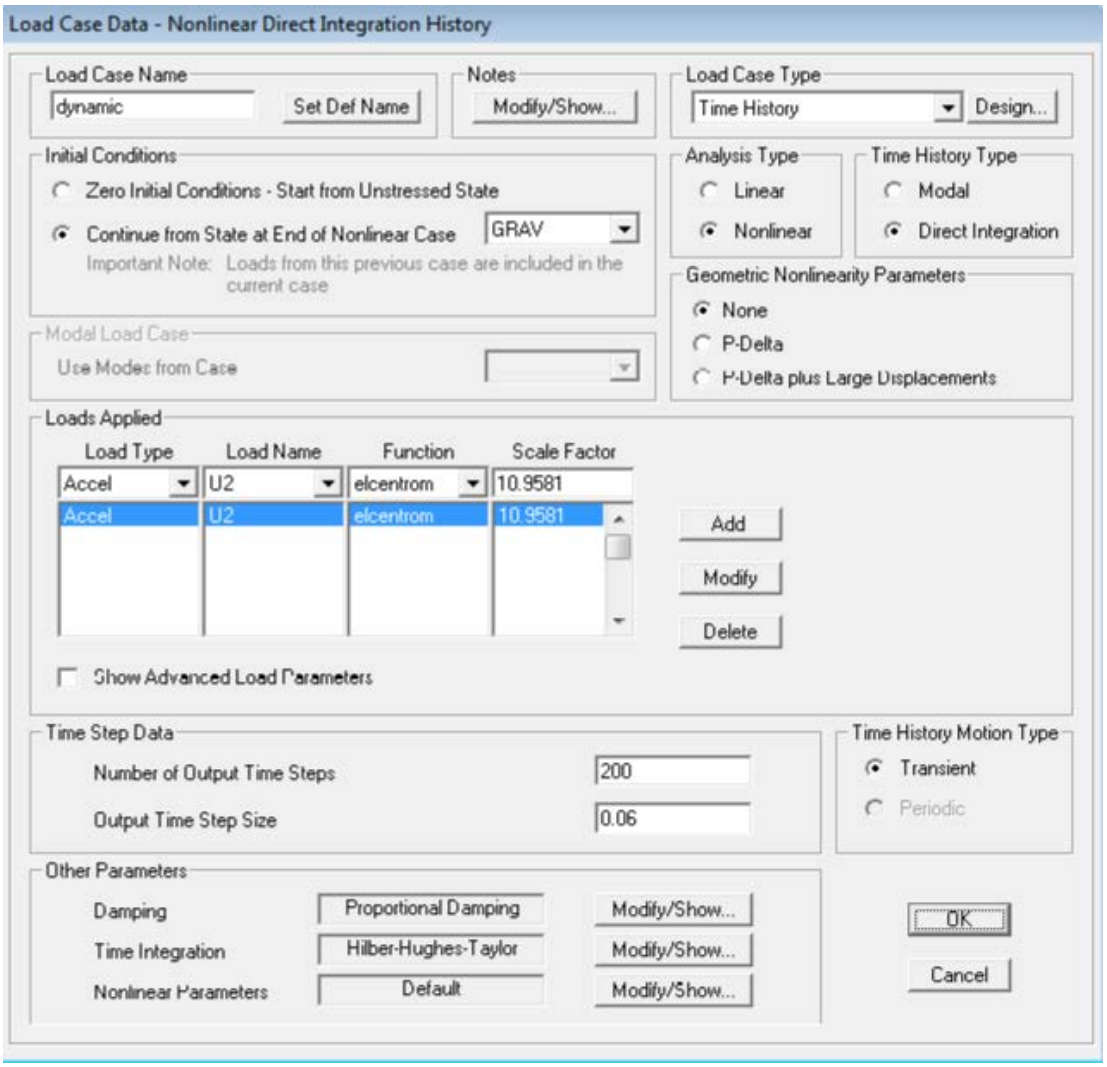

Fig 3.9:SAP Window showing the nonlinear time history load case

The scaling is done by using scale factors which is entered at the time of creating nonlinear dynamic analysis load case. Fig. 3.9 presents a typical SAP window to show how the scaling has been done. The proportional damping considered is 5% for both first and second mode and total number of output steps keptas 200 for all the dynamic analyses. Geometric nonlinearity is not considered in the analysis. Building is loaded first with gravity load and the nonlinear time history analysis is done on the stressed structure due to gravity to simulate the actual situation. All the selected natural earthquake ground motion is presented in Annexure C (ref Fig. C.1)

3.5.2. Spectral consistent earthquake data

Five uncorrelated spectrum-consistentartificially generated earthquake acceleration histories, consistent with design spectrum given in Indian standard IS 1893:2002 (Part1), are used as input ground acceleration. These artificial earthquake motions are generated using a computer program SIMQKE-I (Vanmarcke*et. al.,* 1990) and are expected to have characteristics in terms of frequency and energy contents intended through the well accepted design spectrum. The target design spectrum as well as the elastic response spectrum obtained from these time histories for 5% damping are presented in Fig. 3.10. The figure shows that the response spectra of all the artificial ground motion (A, B, C, D and E) have very little deviation from the target design spectrum (IS-1893 RS). All the generated earthquake ground motion is presented in Annexure C (ref Fig. C.2). Refer Annexure D for input and output details of computer program SIMQKE-I.

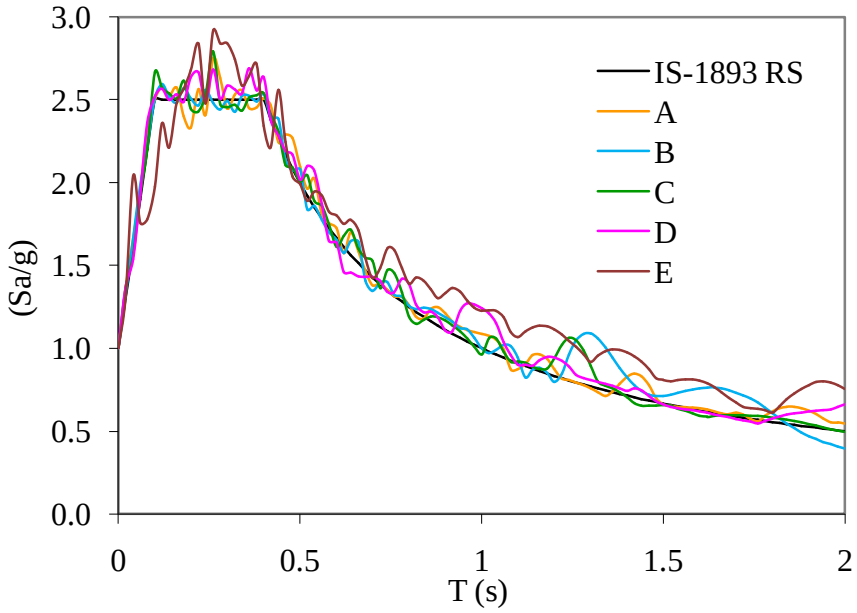

Fig. 3.10: Acceleration spectra for the artificial accelerograms (5% damping)

3.6. SUMMARY

This chapter presents details of the basic modelling technique for the linear and nonlinear analyses of the selected framed buildings. It also describes the selected building geometries used in the present study. The remaining sections of this chapter deal with plastic flexure hinge modelling used for the present study. Finally, the important parameters for nonlinear time-history analysisincluding the input ground motions (natural and generated) used in the present study are described.

CHAPTER 4

NONLINEAR STATIC (PUSHOVER) ANALYSIS

4.1. INTRODUCTION

Pushover analyses of the selected buildingsarecarried out as per FEMA 356. Details of the pushover analysis procedures are described in Annexure B. First total gravity load (Dead load and 25% live load) is applied in a load controlled pushover analysis followed by lateral load pushover analyses using displacement control.An invariant parabolic load pattern similar to IS 1893:2002 (Part1) equivalent static analyses is considered for all the pushover analyses carried out here. This chapter presents the results obtained from the pushover analyses and discusses the nonlinear behaviour of the three selected buildings.

4.2. MODAL ANALYSIS

Often a modal analysis is used to get insight about the regularity of a building. The three building models (SYM, ASYM1 and ASYM2) are first analysed using modal analysis to know the change in elastic modal properties due to the presence of asymmetry. Table 4.1 presents the period and the corresponding participating mass ratios for the first three modes in Y-direction. The mass and the stiffness distribution are identical for the two asymmetric building variants. The only difference between these two buildings is the reinforcement design. Therefore no changes found in the modal properties of the two structures. Table 4.1 shows that there is a slight decrease in the periods for all three modes in the asymmetric building variants. It is also found that the cumulative mass participation in the first three modes decreases due to the presence of asymmetry. This

indicates that the contribution of higher mode is slightly the more in case of asymmetric building. However, from the table it is clear that there are no considerable changes in the elastic modal properties of the building for the asymmetry.

Table 4.1: Modal properties of the selected buildings for first three modes

Mode	SYM			ASYM1 and ASYM2		
	T (s)	UY (%)	Cum UY (%)	T (s)	UY (%)	Cum UY (%)
1	0.542	88.19	88.19	0.553	87.31	87.31
2	0.176	9.18	97.37	0.180	9.09	96.40
3	0.102	2.19	99.56	0.104	2.17	98.57

4.3. PUSHOVER ANALYSIS

All the three building models are then analysed using non-linear static (pushover) analysis. At first, the pushover analysis is done for the gravity loads (DL+0.25LL) incrementally under load control. The lateral pushover analysis (in Y-direction) is followed after the gravity pushover, under displacement control. The building is pushed in lateral directions until the formation of collapse mechanism. The capacity curve (base shear versus roof displacement) is obtained from the analysis.

Fig. 4.1 presents the capacity curves for all three building variants. It is found that all three building models followed the same path. However, both the asymmetric building variants collapsed in a non-ductile manner (ductility factor = 2.6) whereas the symmetric building model collapsed after significant plastic deformation (ductility factor = 12.6). It is interesting to observe that the reinforcement design as per current standard

(IS 1893:2002 (Part1)) for ASYM2 did not reflect in the capacity curve as shown in Fig. 4.1.

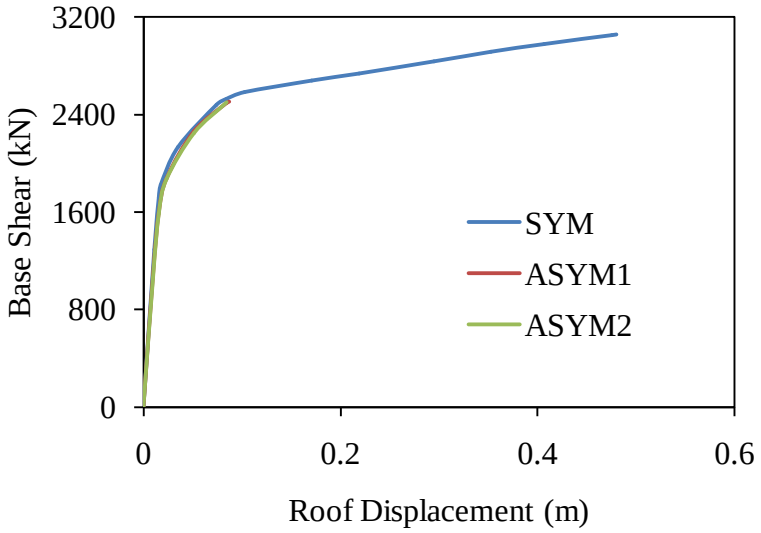

Fig. 4.1: Comparison of capacity curves of the three buildings

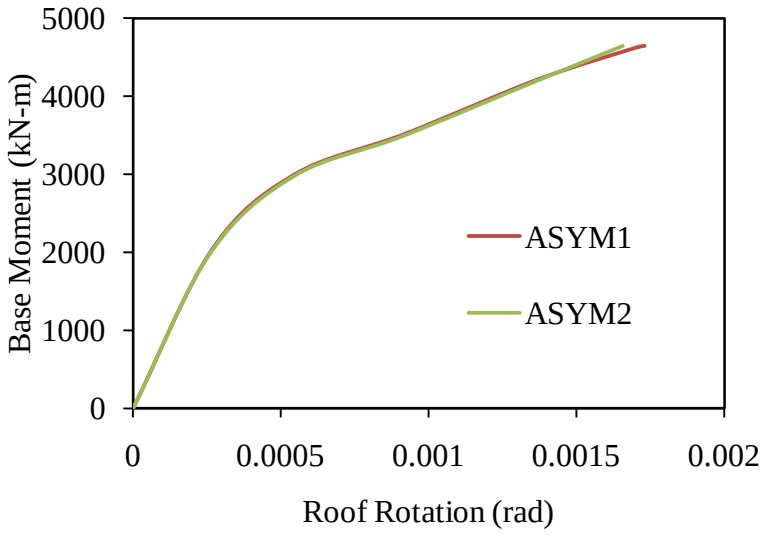

Fig. 4.2: Base moment versus roof rotation relation for the asymmetric buildings

Fig. 4.2 presents the base moment (about the elastic centre of stiffness) versus the roof rotation curve for the two asymmetric building. Since the application of the load

issymmetric in the symmetric building there is no significant rotation found for the structure. Also, no significant base moment for the symmetric building is found during the non-linear analysis. As per Fig. 4.2 there is no difference in two buildings with regard to base moment and roof rotation. This figure also do not justify the clauses given in IS 1893:2002 (Part1) for torsion.

Provisions in IS 1893:2002 (Part1) uses elastic centre of rigidity as benchmark for calculation of static eccentricity and design eccentricity. Centre of rigidity for a structure changes as the formation of plastic hinges progresses in the structure. Although both of asymmetric buildings collapsed at a very early stage of plastic deformation it is found that the centre of rigidity moved up to 40 mm from the original position (elastic).

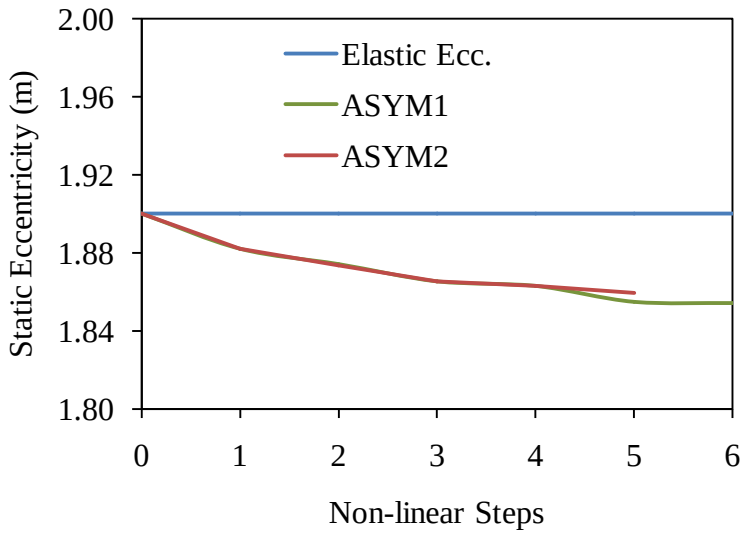

Fig. 4.3: Variation in the static eccentricity in different nonlinear steps

Considering that all the building structures will undergo inelastic deformation under an expected earthquake it is meaningless to relate the design criterion to the elastic centre of

rigidity. It is to be noted that the variation of the static eccentricity in different nonlinear steps are identical for both the asymmetric buildings.

Figs. 4.4 and 4.5 present the distribution of hinges at collapse for ASYM1 and ASYM2, respectively. Two frames in *YZ* direction from each building is taken for this discussion: first one is at the right most edge of the building (X = 19m) and the other one is the left edge of the building. This two figure shows that there will be uneven yielding in the two edge-frames of the building due to torsion and the frame closer to the centre of mass has the maximum yielding.

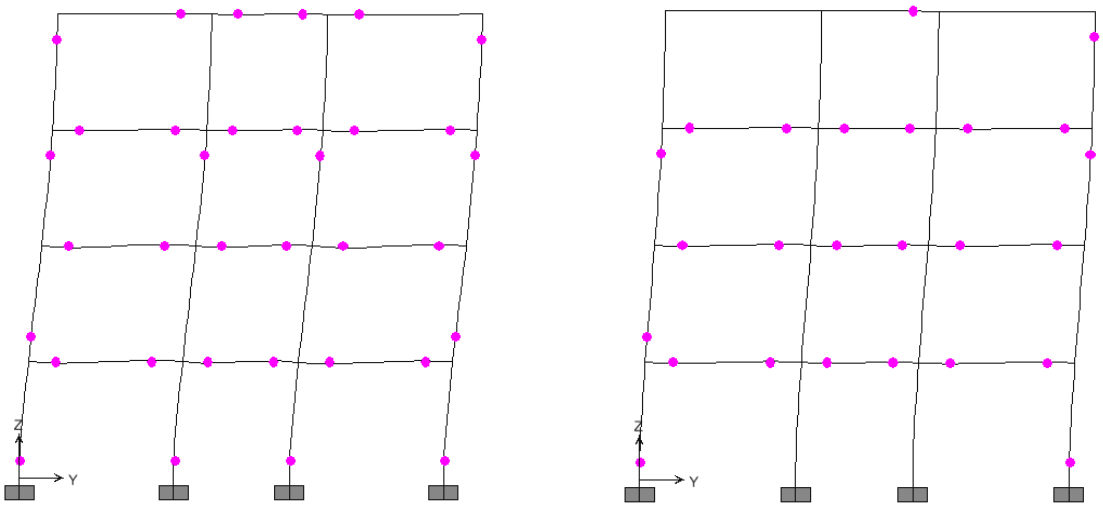

YZ frame at X = 19m *YZ* frame at X = 0m

Fig. 4.4: Hinge distribution at collapse for two XY frames of ASYM1

It is also noticed that there are no considerable difference in the hinge pattern for the two asymmetric buildings except two extra hinges in the second floor columns for ASYM1 (building designed without considering the provision given in IS 1893:2002). It has been

found that 165 numbers of sections in ASYM1 formed plastic hinges out of a total 496 possible locations. In case of ASYM2 numbers of hinges formed are only 113.

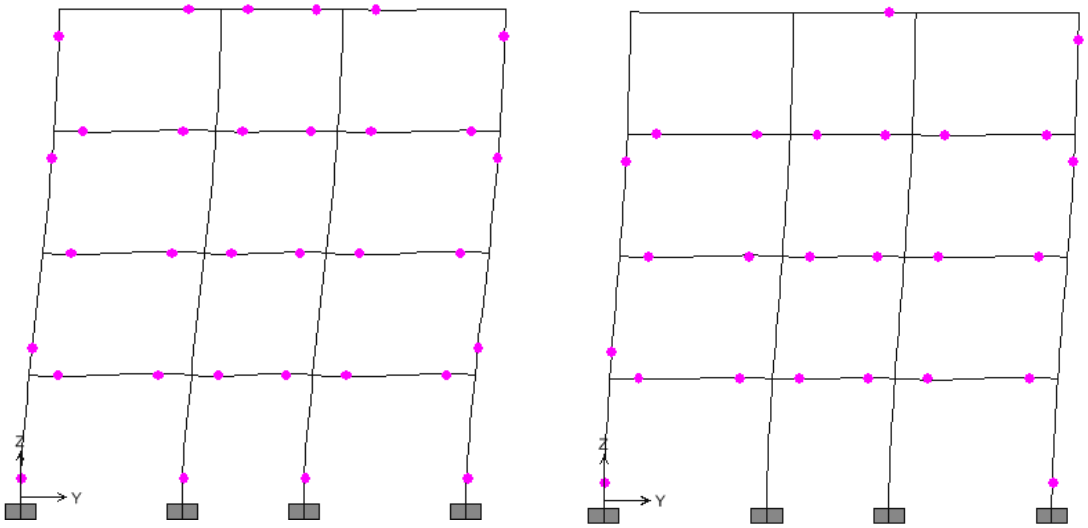

YZ frame at X = 19m

YZ frame at X = 0m

Fig. 4.5: Hinge distribution at collapse for two XY frames of ASYM2

\

4.4. SUMMARY

This chapter presents the modal properties of structure and peculiarities seen in modal analysis of asymmetric structure compare to symmetric structure. Nonlinear static analysis (Pushover analysis) results for the three structural variant is discussed in this chapter. The hinge pattern obtained in pushover analysis is also discussed for the clarity of conclusions.

CHAPTER 5

NONLINEAR DYNAMIC ANALYSIS

5.1. INTRODUCTION

To confirm the results obtained from nonlinear static analyses a more rigorous nonlinear dynamic analyses of the three selected building models are carried out for 15 selected ground motions. 10 of these ground motions are natural records and the remaining five are generated records consistent with Indian Standard IS 1893:2002 (Part1) design response spectrum. These analyses are carried out using the same nonlinear point plastic building models using SAP2000 (v14). Details of the modelling and analysis parameters, and selected ground motions are explained in Chapter 3. All of these 15 records are scaled to 0.3g for analysis. This Chapter presents the results obtained from the nonlinear dynamic analyses and discusses the nonlinear dynamic behaviour of the three selected building models. Additional results from nonlinear dynamic analyses can be available in Annexure C (ref. Section C.2 for detail)

5.2. BASE SHEAR VERSUS ROOF DISPLACEMENT

Base shear-versus-roof displacements curve is an important parameter to understand the difference between three buildings with different level of asymmetry. Base shear-versus-roof displacement curves obtained from time history analyses of these three buildings (SYM, ASYM1 and ASYM2)are presentedtogether in the same plot for individual ground motion records. Results of natural and generated ground motion data are

presented separately for convenience. Figs. 5.1 to 5.15 present base shear-versus-roof displacement curves for the 15 selected ground motion data.

5.2.1. Results obtained from Natural Ground Motion Data

Ten strong motion natural data (refer Section 3.5.1 for details) normalised to peak ground acceleration of 0.3g are taken for the nonlinear dynamic analyses. Figs. 5.1 to 5.10 present the cyclic base shear-versus-roof displacement data for ten natural records. Each figures presents results for symmetric building (SYM), asymmetric building designed without code provisions (ASYM1) and asymmetric building designed with Indian Standard IS 1893:2002 (Part1) provisions (ASYM2)

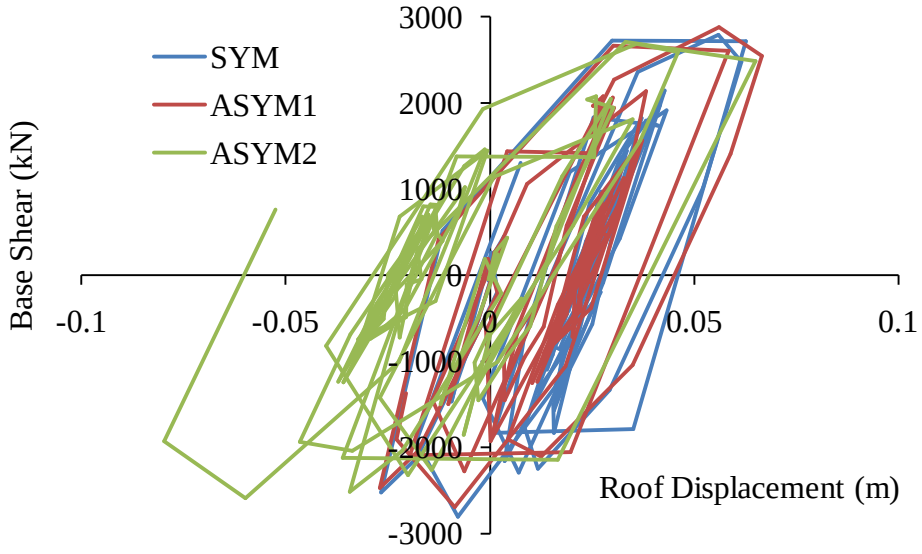

Fig. 5.1: Base shear-versus-roof displacement data for Imperial Valley Eq. (1940)

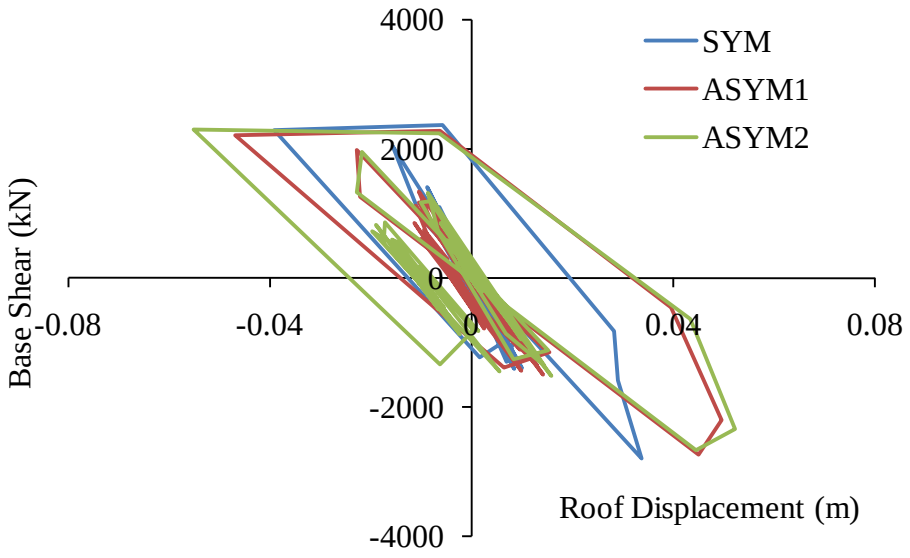

Fig. 5.2: Base shear-versus-roof displacement data for Loma Prieta – Oakland (1989)

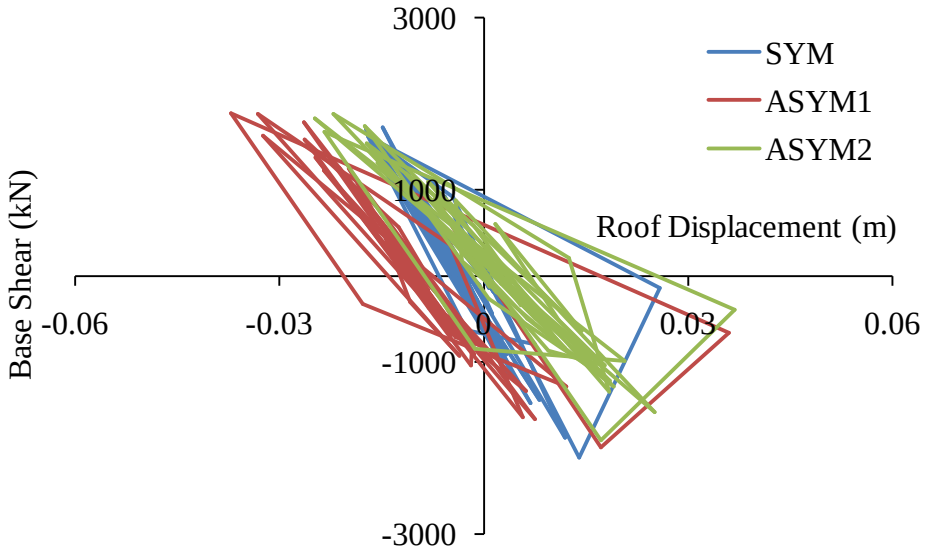

Fig. 5.3: Base shear-versus-roof displacement data for Loma Prieta - Corralitos (1989)

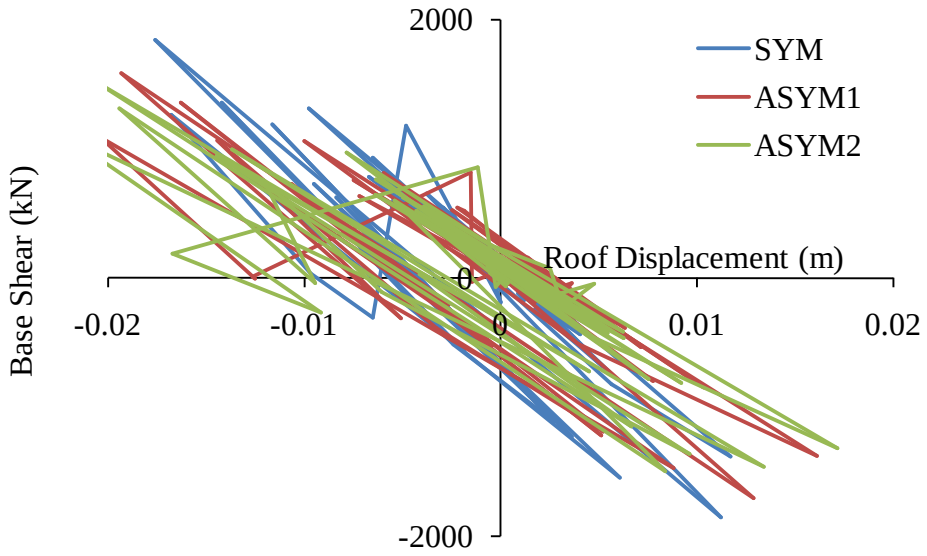

Fig. 5.4: Base shear-versus-roof displacement data for Northridge – Santa Monica (1994)

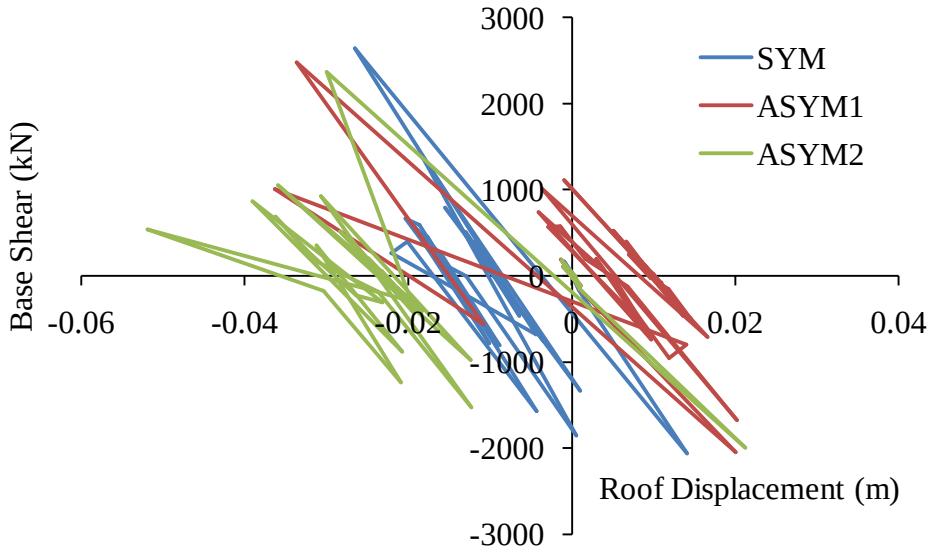

Fig. 5.5: Base shear-versus-roof displacement data for Northridge – Sylmar (1994)

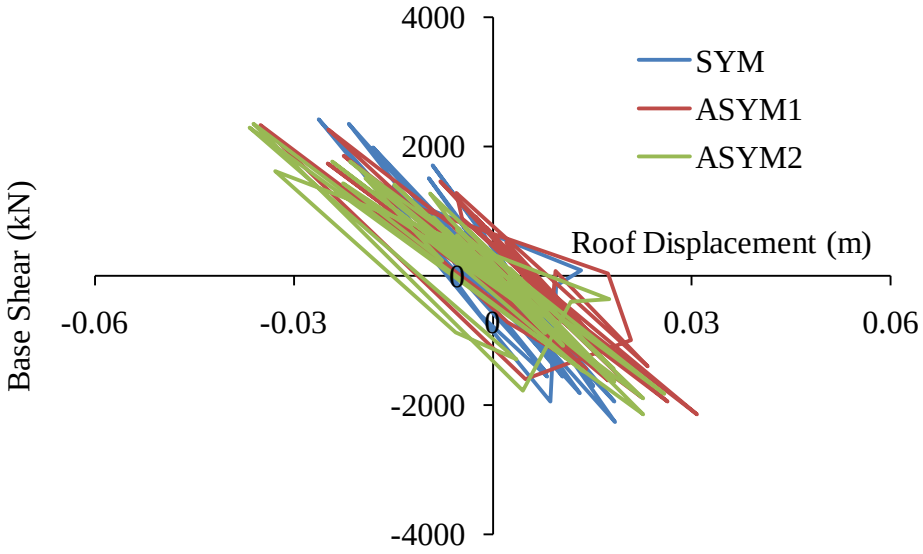

Fig. 5.6: Base shear-versus-roof displacement data for Northridge Century City (1994)

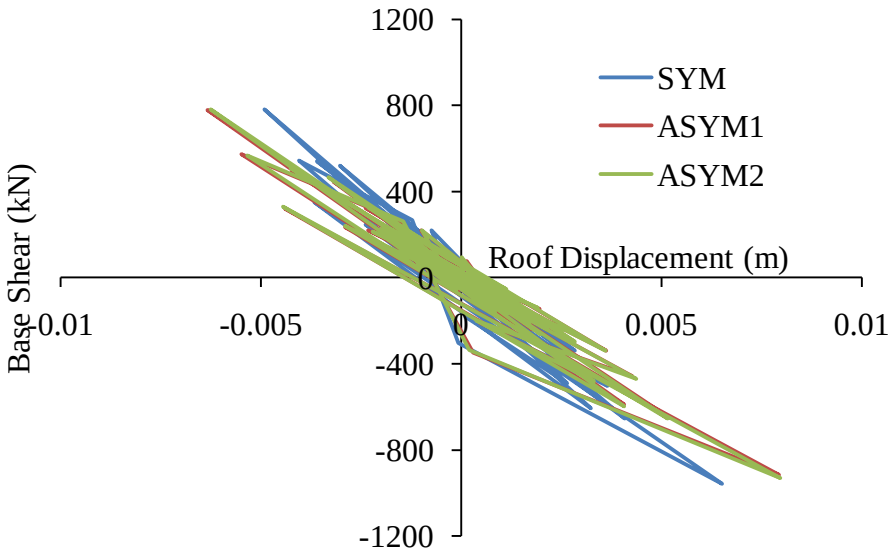

Fig. 5.7: Base shear-versus-roof displacement data for Landers – Lucerne Valley (1992)

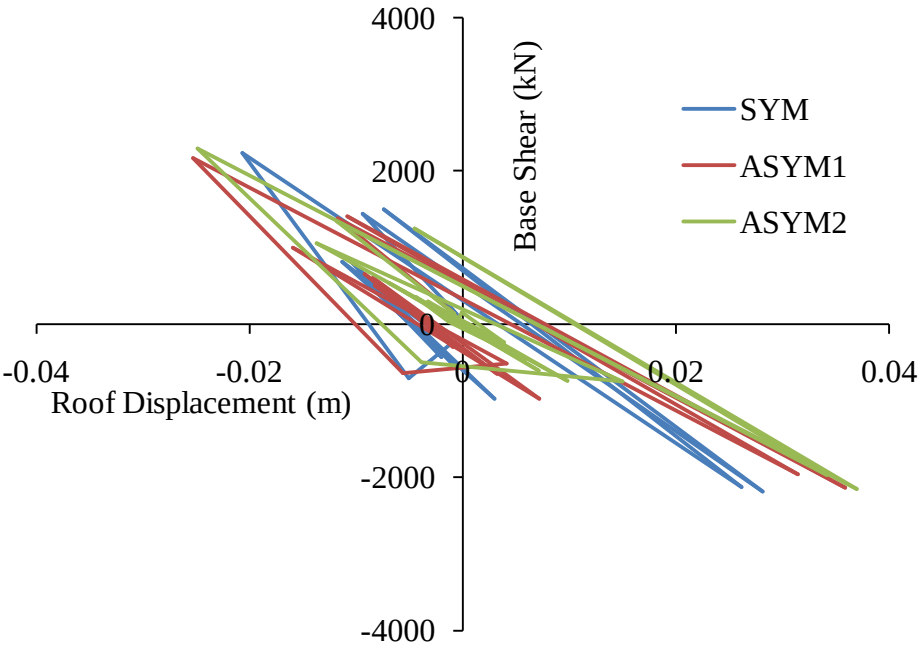

Fig. 5.8: Base shear-versus-roof displacement data for Sierra Madre – Altadena (1991)

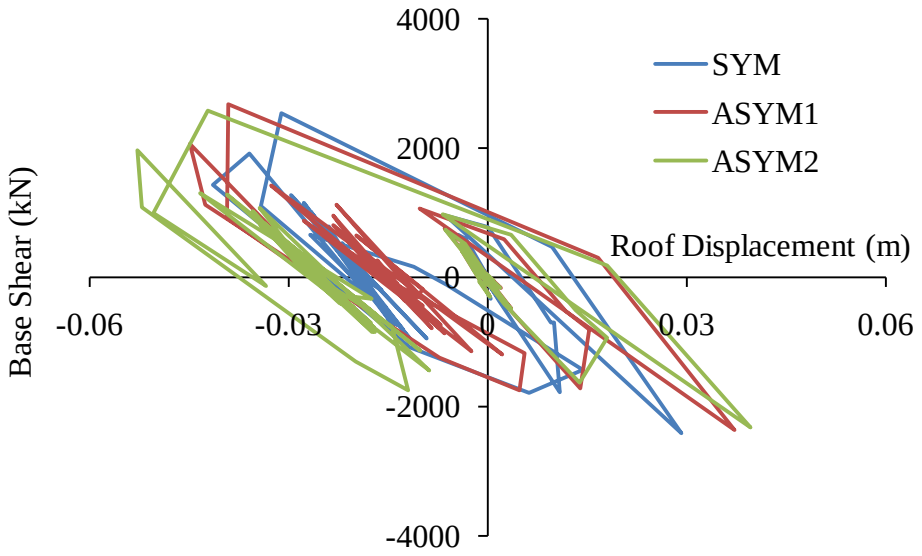

Fig. 5.9: Base shear-versus-roof displacement data for Imperial Valley Eq. (1979)

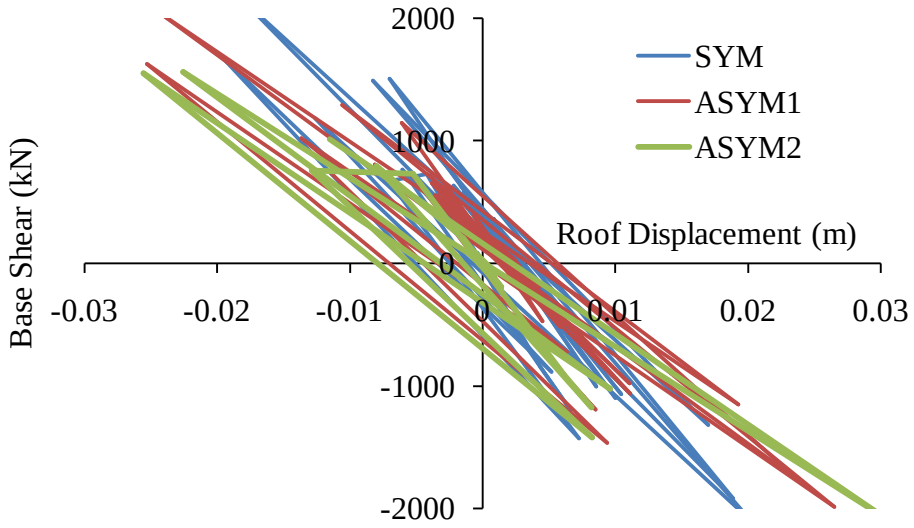

Fig. 5.10: Base shear-versus-roof displacement data for Morgan Hill – Gilroy4 (1984)

Table 5.1: Maximum response of the building subjected to natural ground motion

GroundMotion Data	SYM		ASYM1		ASYM2	
	Max.Base Shear(kN)	Max.Roof Disp.(mm)	Max.Base Shear(kN)	Max.Roof Disp.(mm)	Max.Base Shear(kN)	Max.Roof Disp.(mm)
Imperial Valley	2801	63	2879	67	2709	80
Loma Prieta-Oakland	2796	39	2739	50	2670	55
Loma Prieta-Corralitos	2112	26	1988	37	1907	37
Northridge-Santa Monica	1853	18	1703	20	1511	22
Northridge-Sylmar	2641	27	2482	36	2367	51
Northridge-Century City	2420	26	2337	35	2352	27
Landers-Lucerne Valley	956	7	915	8	929	8
Sierra Madre-Altadena	2236	28	2171	36	2291	37
Imperial Valley Earthquake-El Centro	2539	41	2684	45	2584	53
Morgan Hill-Gilroy 4	2168	20	2038	27	2069	30
Average	**2252**	**29**	**2194**	**36**	**2139**	**40**

Figs. 5.1-5.10 and Table 5.1 presented here show that the maximum base shear demands

for the three building variant are very similar for all the ten earthquake ground motion (variation within 5%). However, symmetric building variant consistently experiences a slightly higher base shear demand compared to the asymmetric buildings.

Table 5.1 shows that there is a considerable variation with regard to the maximum roof displacement demands for the three building variants. Average maximum roof displacement demand for ASYM1 is about 22% higher than that of the similar regular (SYM) building. This is over 35% in case of ASYM2 building.

It is found from Figs. 5.1-5.10 that the base shear versus roof displacement hysteresis curves for three buildings are matching very closely for all the ground motion studied here except Loma Prieta and Northridge – Sylmar ground motion record. When subjected to Northridge – Sylmar ground motion record ASYM-2 building experience more displacement at roof compared to other two building variants. The figures presented here do not clearly show any significant difference even between symmetric and asymmetric buildings. This may be because of the fact that many of the nonlinear dynamic analyses do not lead to the collapse of the buildings analysed for ground motion with PGA = 0.3g.

5.2.2. Results obtained from Generated Ground Motion Data

Five ground acceleration data (A, B, C, D and E) are generated (refer Section 3.5.2 for details) using computer software SIMQKEconsistent to Indian Standard IS 1893:2002 design spectrum. These acceleration data normalised to peak ground acceleration of 0.3g are taken for the nonlinear dynamic analyses. Figs. 5.11 to 5.15 present the cyclic base shear-versus-roof displacement data for five generated ground motions.

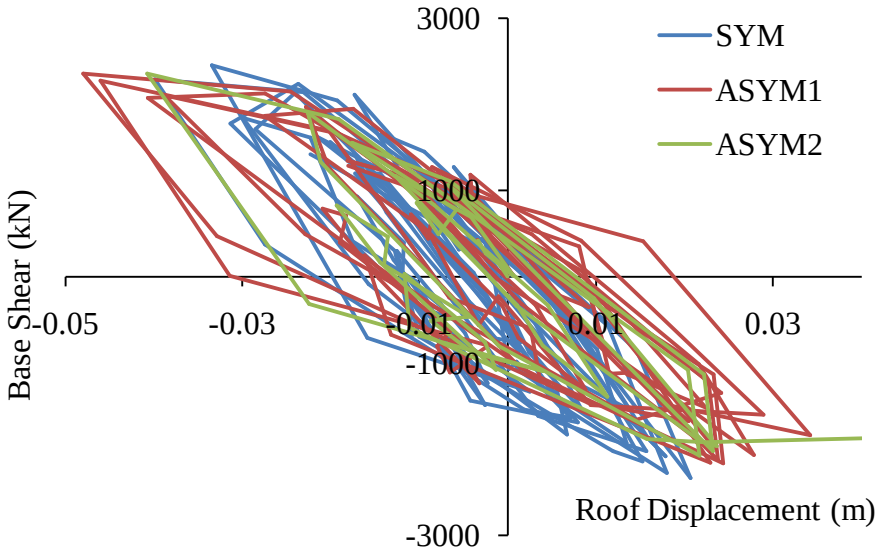

Fig. 5.11: Base shear-versus-roof displacement data for Data-A

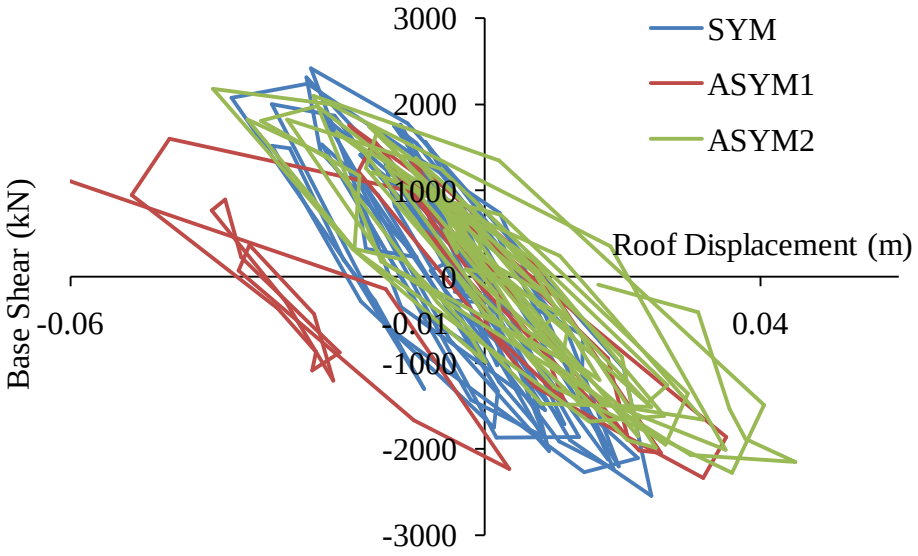

Fig. 5.12: Base shear-versus-roof displacement data for Data-B

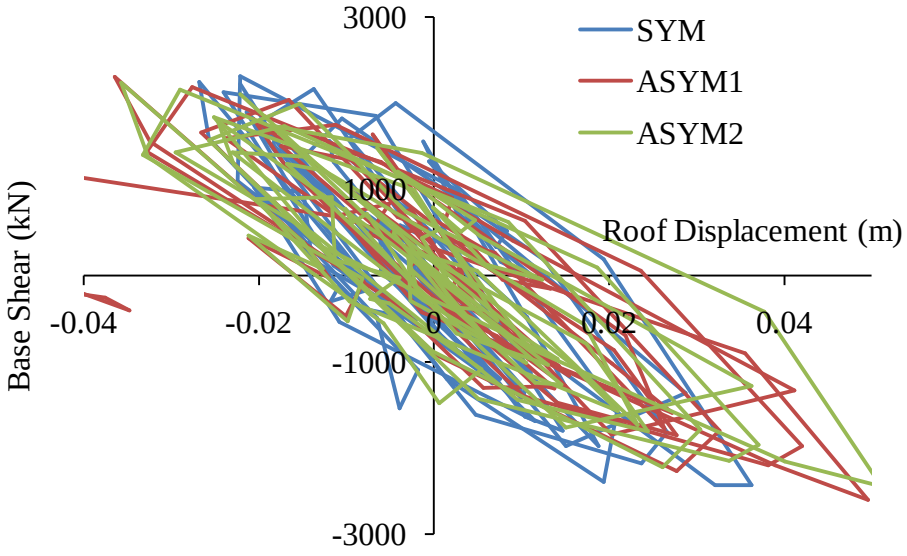

Fig. 5.13: Base shear-versus-roof displacement data for Data-C

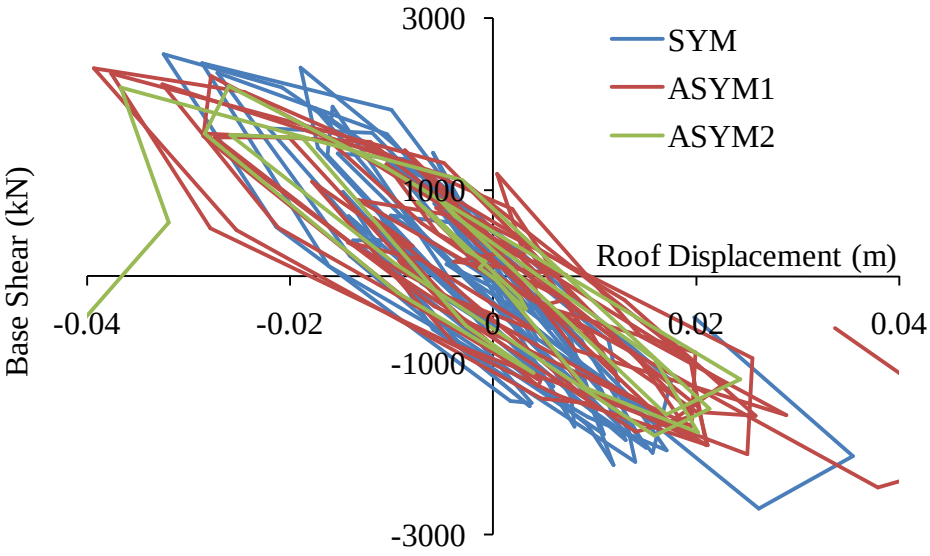

Fig. 5.14: Base shear-versus-roof displacement data for Data-D

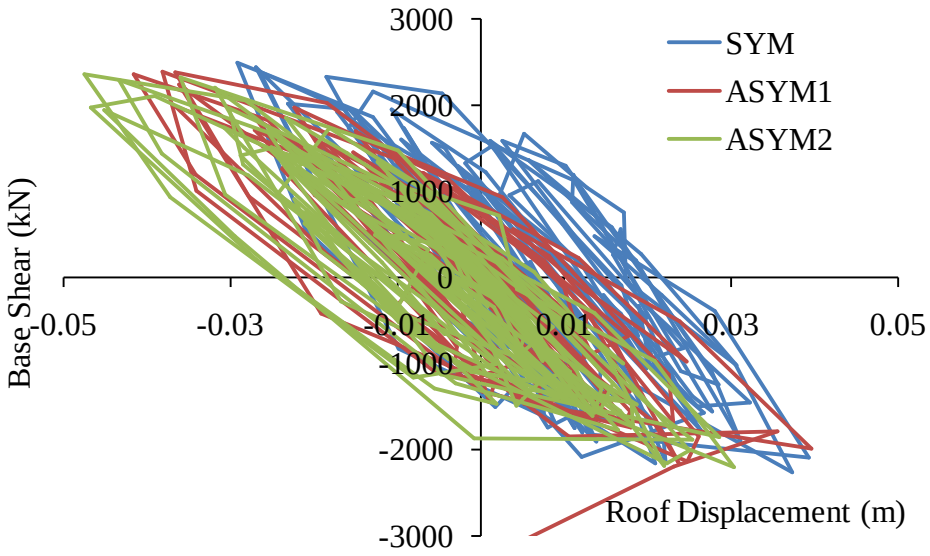

Fig. 5.15: Base shear-versus-roof displacement data for Data-E

Table 5.2 summarises the results presented graphically in Figs. 5.11-5.15.This table shows that the maximum base shear demands for the three building variant aresimilar for all the generated earthquake ground motion (within 6.5%variation). However, Symmetric building variants show slightly higher base shear demand compared to other two asymmetric variants consistently.Among the two asymmetric variants ASYM2 has always lesser base shear demand although variation is very less.

It is found from Table 5.2 that there is a considerable amount of variation in the maximum roof displacement responses of the three building variants subjected to generated earthquake ground motion (as high as 28%variation). The maximum roof displacement responses for symmetric building variants are found to be lesser compared to the two asymmetric buildings for all the cases studied.

Also, it is found from the Figs. 5.11-5.15 that the base shear versus roof displacement

hysteresis curves for two asymmetric buildings ASYM1 and ASYM2 are matching very closely for all the ground motion studied here except Data-B ground motion record. When subjected to Data-B ground motion record, ASYM-2 building found to be dissipating more energy compared to ASYM1. Except this case there is no behavioural difference found between two asymmetric buildings ASYM1 and ASYM2.

Table 5.2: Maximum response of the building subjected to generated ground motion

Ground Motion Data	SYM		ASYM1		ASYM2	
	Max. Base Shear (kN)	Max. Roof Disp. (mm)	Max. Base Shear (kN)	Max. Roof Disp. (mm)	Max. Base Shear (kN)	Max. Roof Disp. (mm)
A	2452	40	2362	48	2362	41
B	2542	37	2337	51	2276	45
C	2435	36	2600	49	2448	51
D	2697	35	2450	50	2208	37
E	2491	39	2389	42	2485	47
Average	**2523**	**37**	**2428**	**48**	**2356**	**44**

5.3. BASE MOMENT VERSUS ROOF ROTATION

Another important parameter that can be useful to explain the behaviour of torsionally irregular asymmetric building is base moment versus roof rotation relation.To understand the difference between the behaviour of three buildings with different asymmetry base moment versus roof rotation hysteresis data obtained from dynamic analyses of the three buildings subjected to all 15 ground motion records. Similar to the previous case results of natural and generated ground motion data are presented separately.

5.3.1. Results obtained from Natural Ground Motion Data

Figs. 5.16 to 5.24 present the cyclic base moment-versus-roof rotation data for ten natural records. Each figures presents results for symmetric building (SYM), asymmetric building designed without code provisions (ASYM1) and asymmetric building designed with Indian Standard IS 1893:2002 (Part1) provisions (ASYM2)

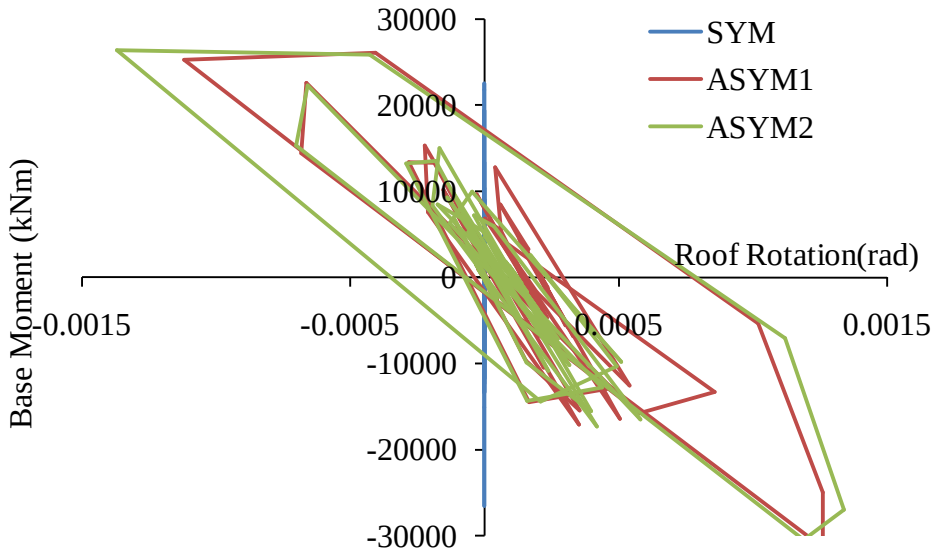

Fig. 5.16: Base moment -versus-roof displacement data for Loma Prieta – Oakland (1989)

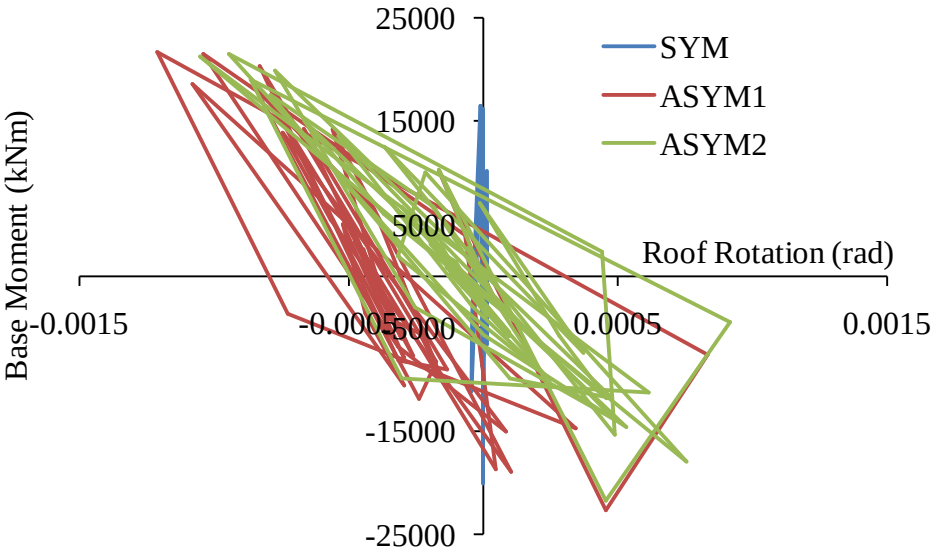

Fig. 5.17: Base moment -versus-roof displacement data for Loma Prieta - Corralitos (1989)

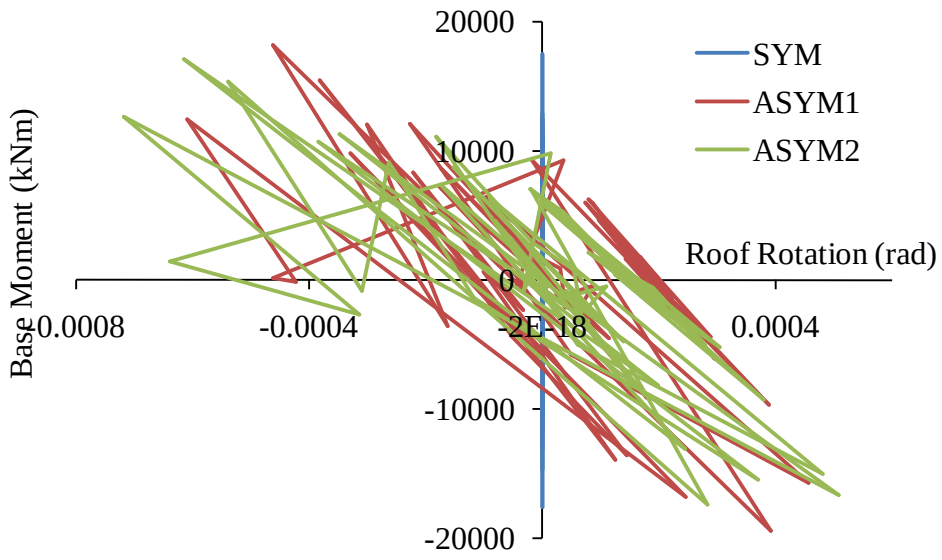

Fig. 5.18: Base moment -versus-roof displacement data for Northridge – Santa Monica (1994)

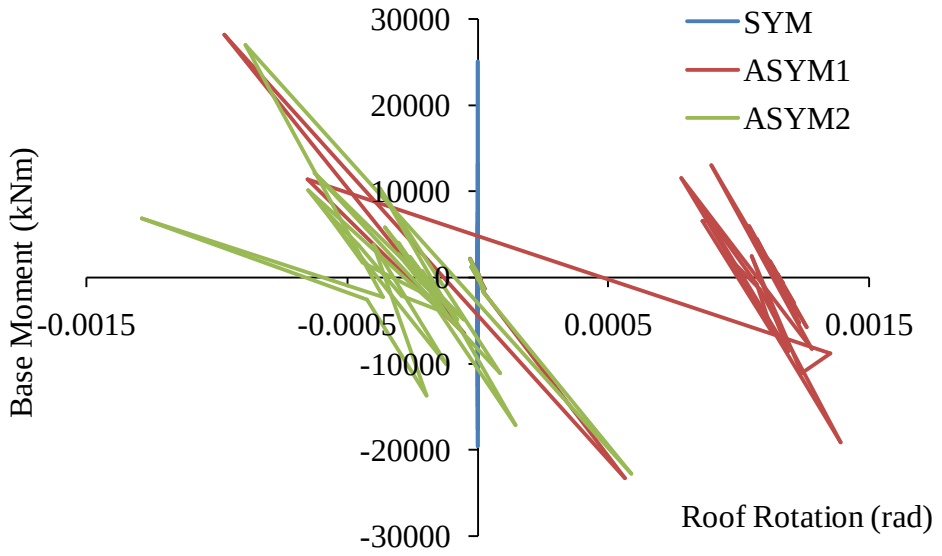

Fig. 5.19: Base moment -versus-roof displacement data for Northridge – Sylmar (1994)

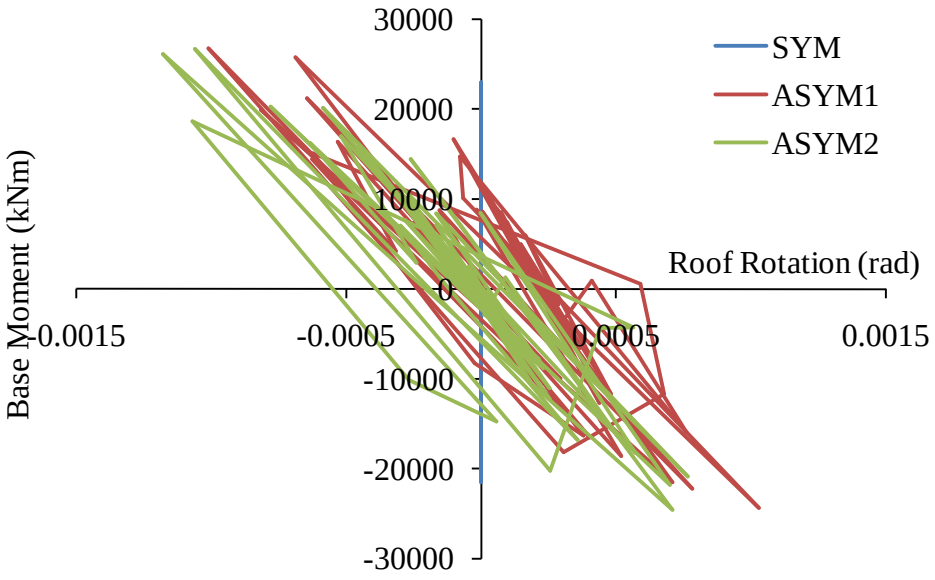

Fig. 5.20: Base moment -versus-roof displacement data for Northridge Century City (1994)

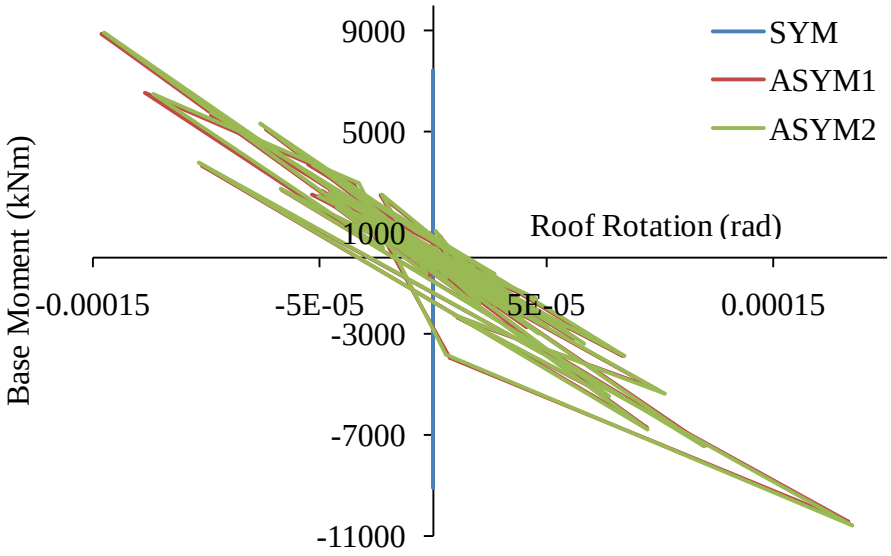

Fig. 5.21: Base moment versus-roof displacement data for Landers – Lucerne Valley (1992)

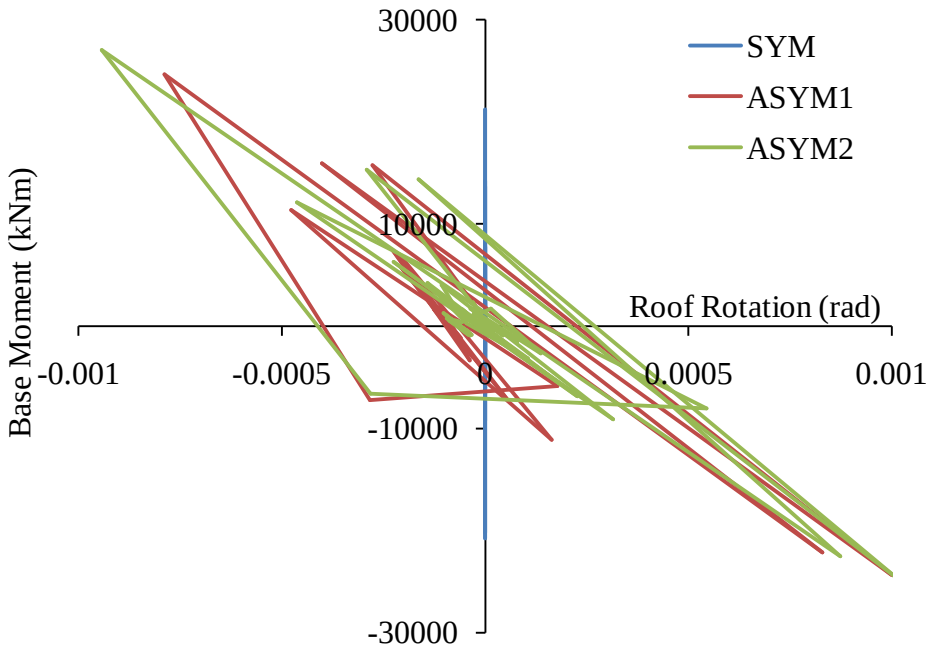

Fig. 5.22: Base moment -versus-roof displacement data for Sierra Madre – Altadena (1991)

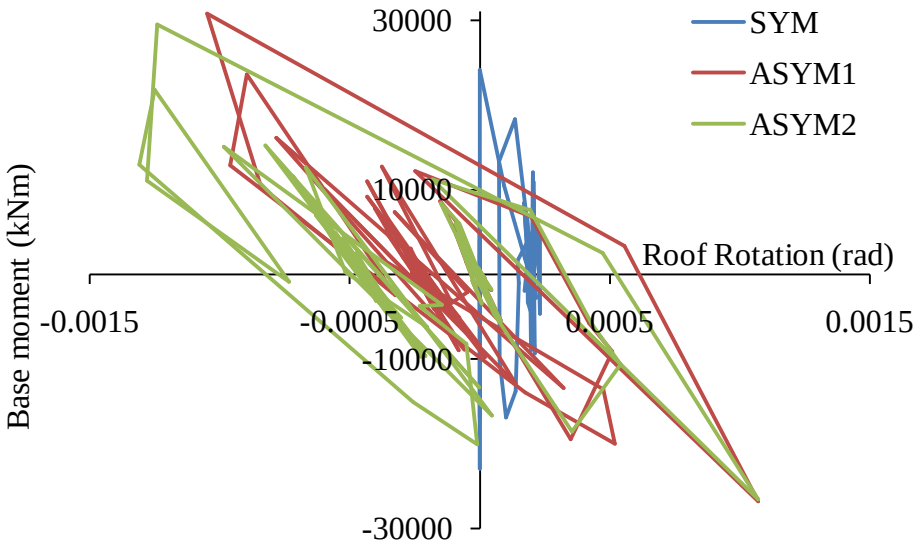

Fig. 5.23: Base moment -versus-roof displacement data for Imperial Valley Eq. (1979)

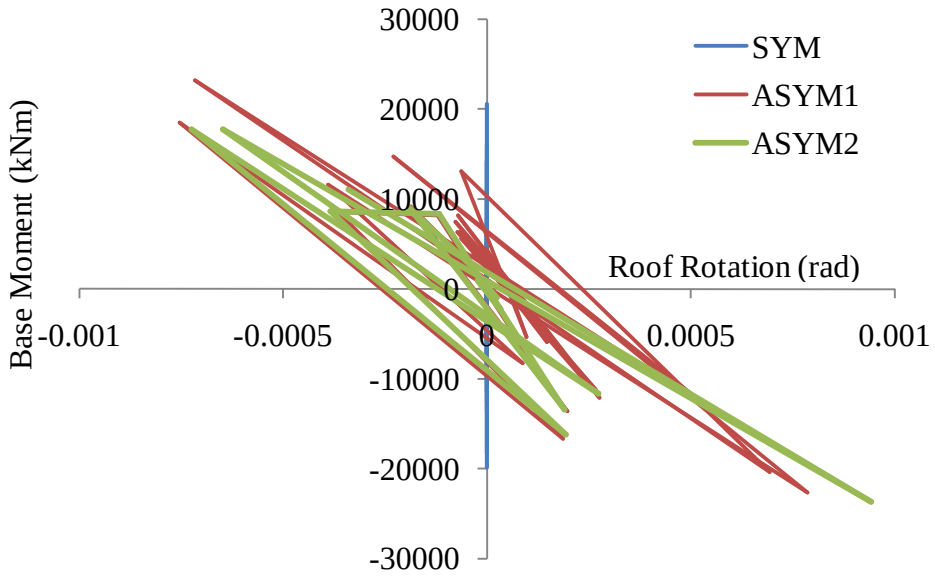

Fig. 5.24: Base moment -versus-roof displacement data for Morgan Hill – Gilroy4 (1984)

Followings are the important observations from Figs. 5.16-5.24 presented above:

i) It is found in most of the cases that symmetric building does not undergo rotation even after yielding. This means that the yielding is taking place symmetrically for symmetric building subjected to earthquake ground motion. However, the results show that for Loma Prieta and Imperial Valley earthquake symmetric building also rotate, although less in magnitude, about a vertical axis few steps after yielding.

ii) Base moment demand is almost same for both of the two asymmetric buildings for all the cases studied here.

iii) ASYM2 building found to have a more roof rotation demand compared to ASYM1 building consistently.

iv) When building is within the elastic range the base moment – roof rotation

hysteresis behaviour of two asymmetric buildings exactly match together (ref. Fig. 5.21 for Landers – Lucerne Valley Earthquake)

v) It is found in most of the cases that base moment – roof rotation relation is very similar for both the asymmetric buildings with small translational/rotation shift.

5.3.2. Results obtained from Generated Ground Motion Data

Figs. 5.25 to 5.29 present the cyclic base moment versus roof rotation (about the vertical axis) data for five generated ground motions. Identical observations can be made from these figures.

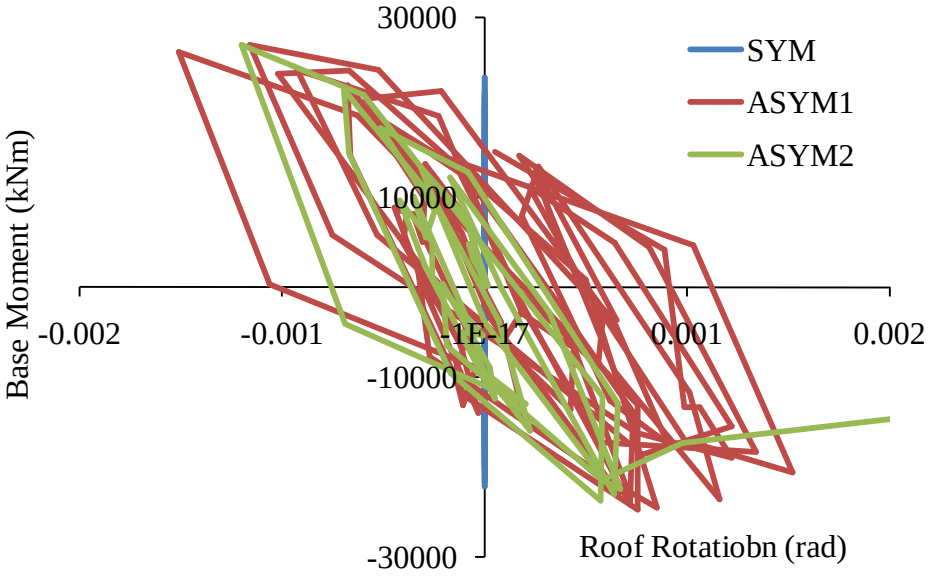

Fig. 5.25: Base moment -versus-roof displacement data for Data-A

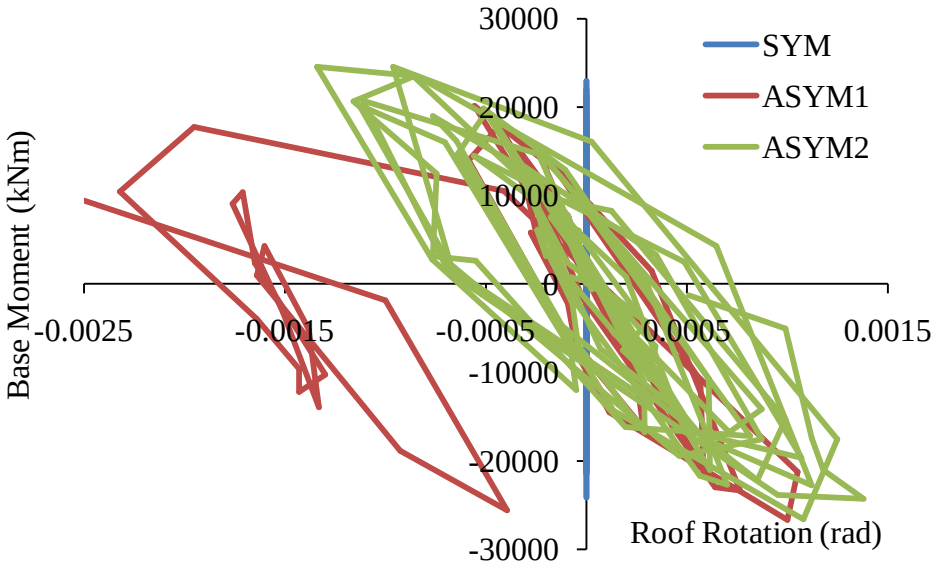

Fig. 5.26: Base moment -versus-roof displacement data for Data-B

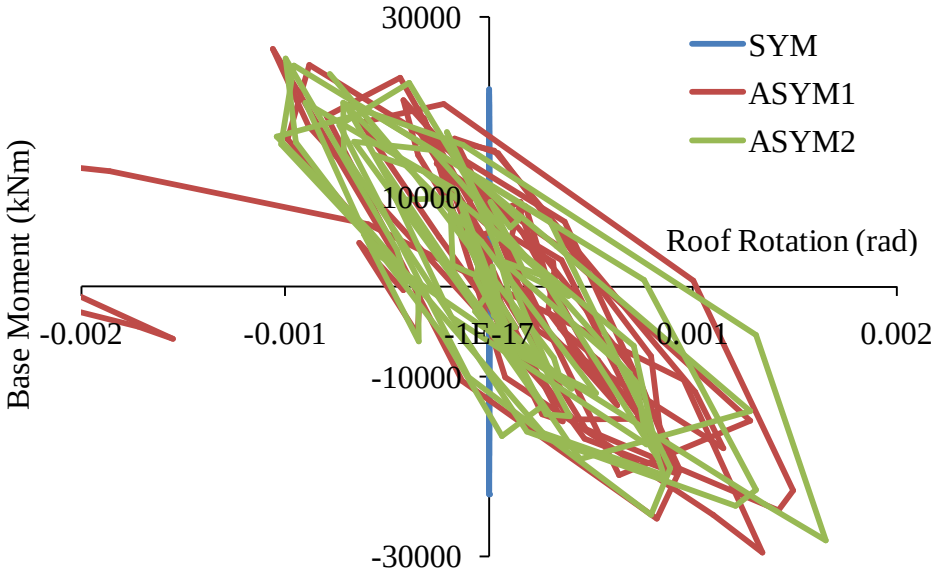

Fig. 5.27: Base moment -versus-roof displacement data for Data-C

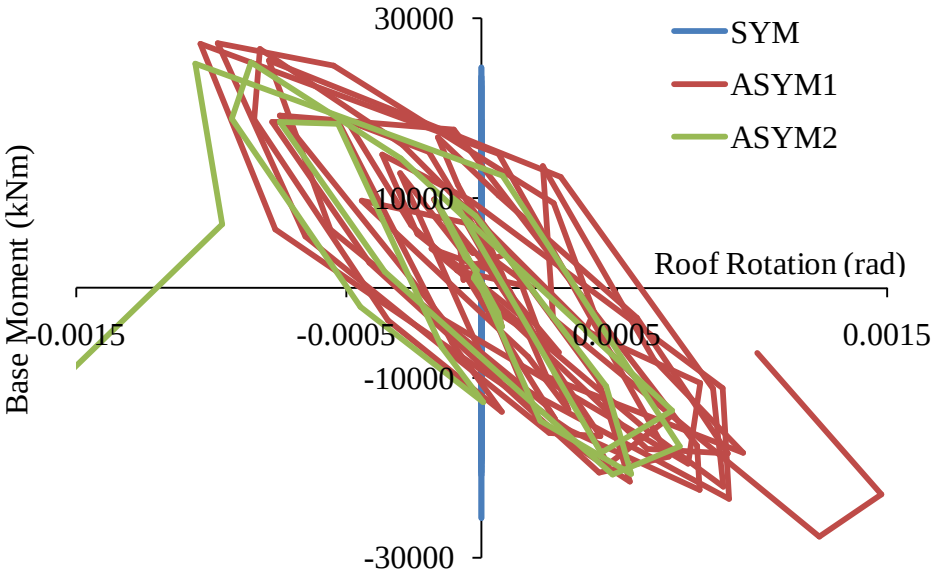

Fig. 5.28: Base moment -versus-roof displacement data for Data-D

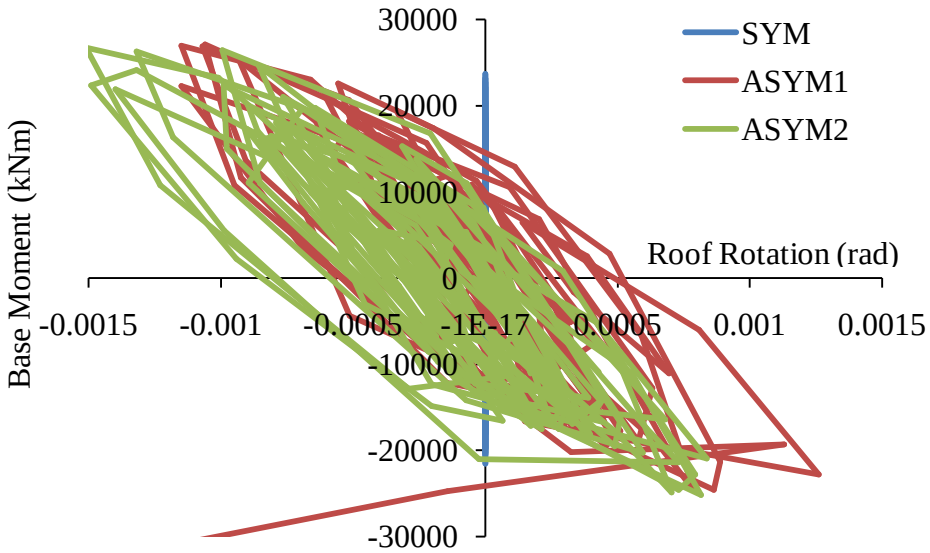

Fig. 5.29: Base moment -versus-roof displacement data for Data-E

The figure presented here (Figs. 5.25-5.29) and before (Figs. 5.11-5.15) shows that the energy dissipated during the motion is very high when the building is subjected to generated ground motion compared to that of natural ground motion record. This may be due to the fact that the number of times the ground acceleration reaching its peak is

considerably high for the generated ground motion compared to recorded motion. Because of this fact the yielding (or failure) is more for the case of generated ground motion that leads to an increased structural damping for the case of generated ground motion compared to recorded motion. Otherwise the observations made in the previous article (i.e., for Fig. 5.16-5.24) are true for these cases also.

5.4. VARIATION OF ECCENTRICITY DURING NONLINEAR ANALYSIS

As evident from Chapter 2 all the major international design codes rely on static eccentricity (*i.e.*, distance between centre of mass and elastic centre of rigidity) for analysis and design of asymmetric building.

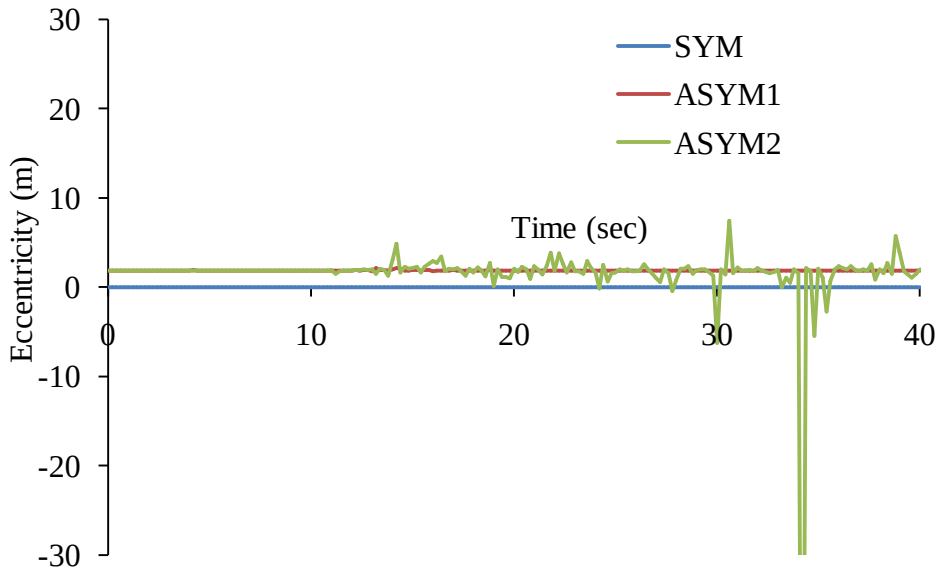

Fig. 5.30: Eccentricity -versus-time data for Loma Prieta – Oakland (1989)

However, as the current earthquake design philosophy allows yielding in building structure under design earthquake the static eccentricity is bound to change once yielding starts. It is interesting to study how the eccentricity between centre of mass and yielded

centre of rigidity changes at different nonlinear steps. Figs. 5.30 to 5.38 present the variation of eccentricity with time for natural ground motions whereas Figs. 5.39 to 5.43 present the same for generated ground motions.

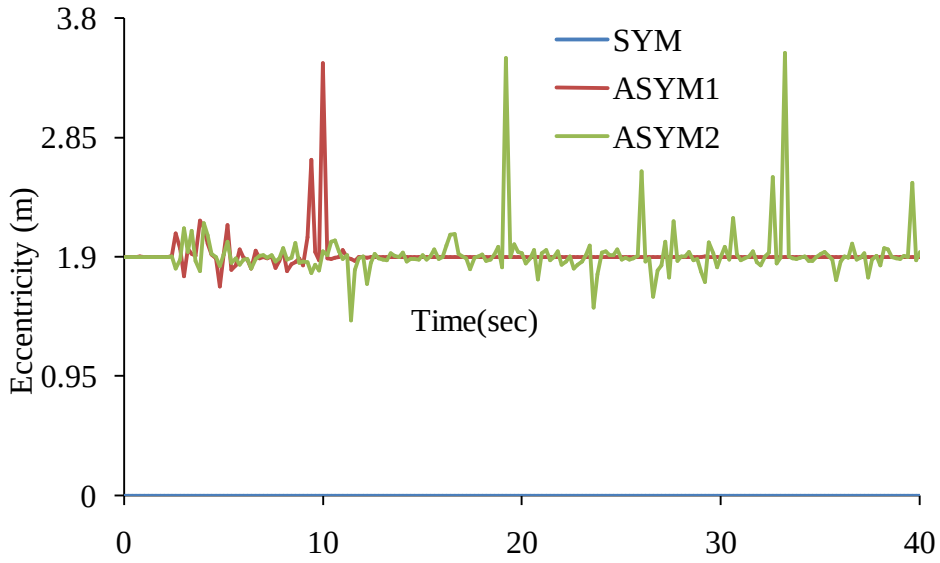

Fig. 5.31: Eccentricity -versus-time data for Loma Prieta - Corralitos (1989)

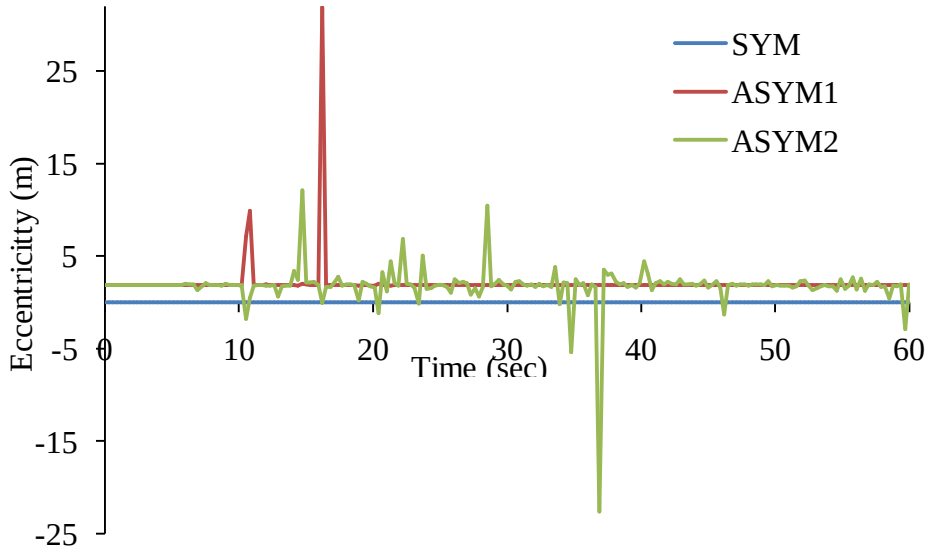

Fig. 5.32: Eccentricity -versus-time data for Northridge – Santa Monica (1994)

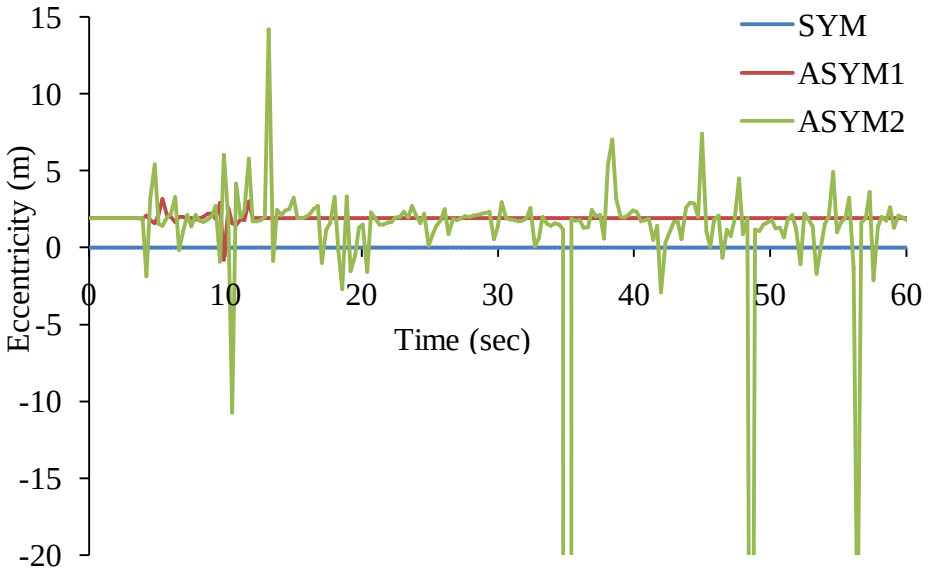

Fig. 5.33: Eccentricity -versus-time data for Northridge – Sylmar (1994)

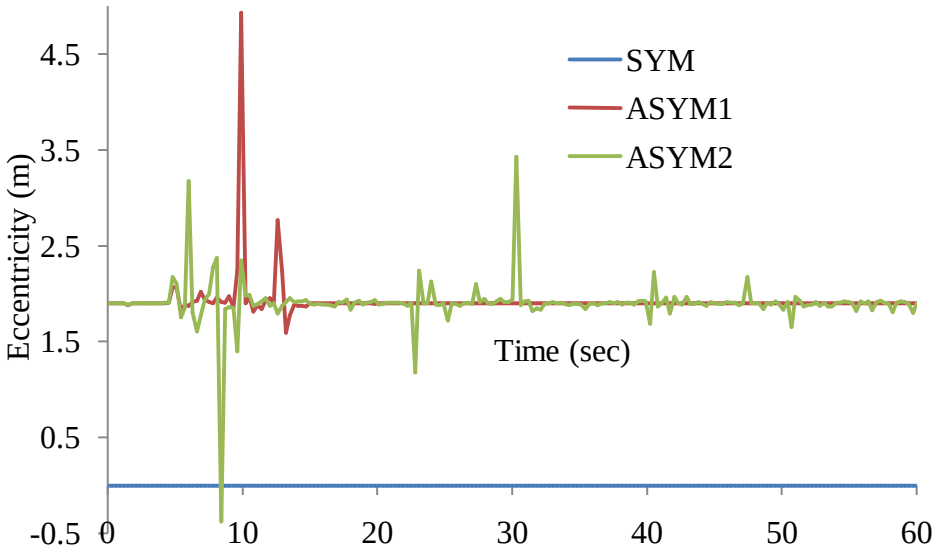

Fig. 5.34: Eccentricity -versus-time data for Northridge Century City

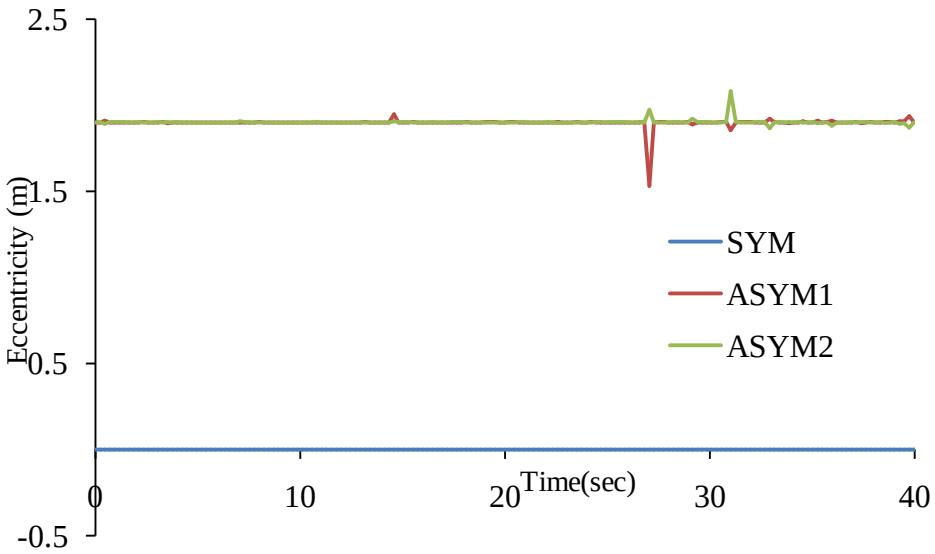

Fig. 5.35: Eccentricity -versus-time data for Landers – Lucerne Valley (1992)

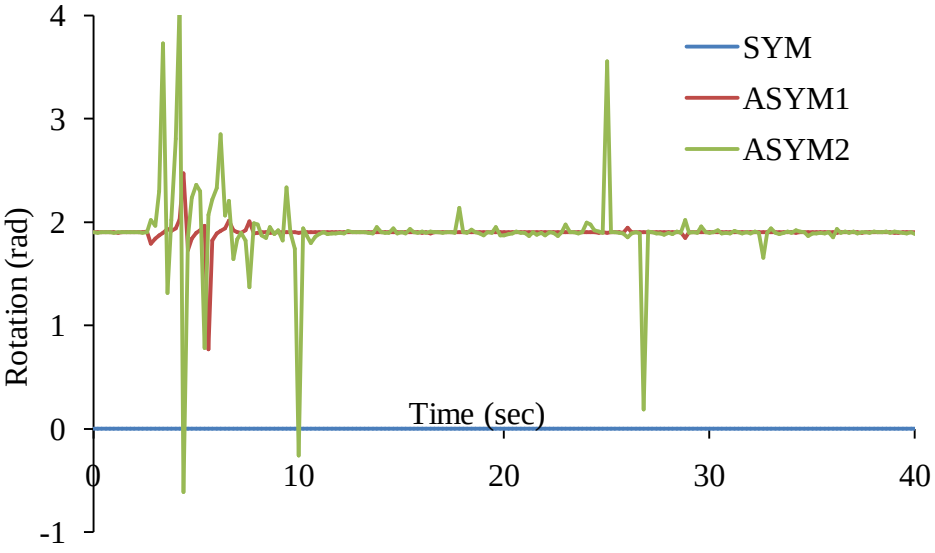

Fig. 5.36: Eccentricity -versus-time data for Sierra Madre – Altadena (1991)

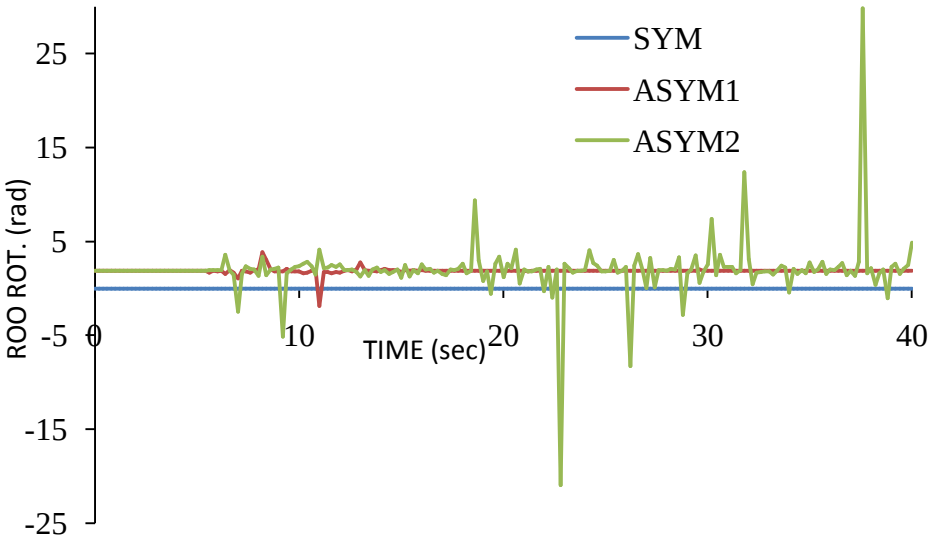

Fig. 5.37: Eccentricity -versus-time data for Imperial Valley Eq. (1979)

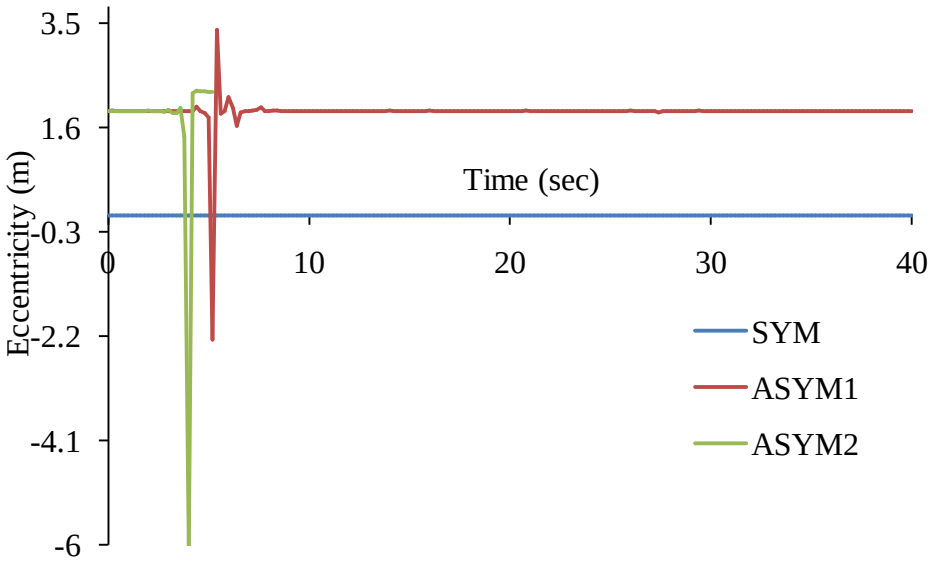

Fig. 5.38: Eccentricity -versus-time data for Morgan Hill – Gilroy4 (1984)

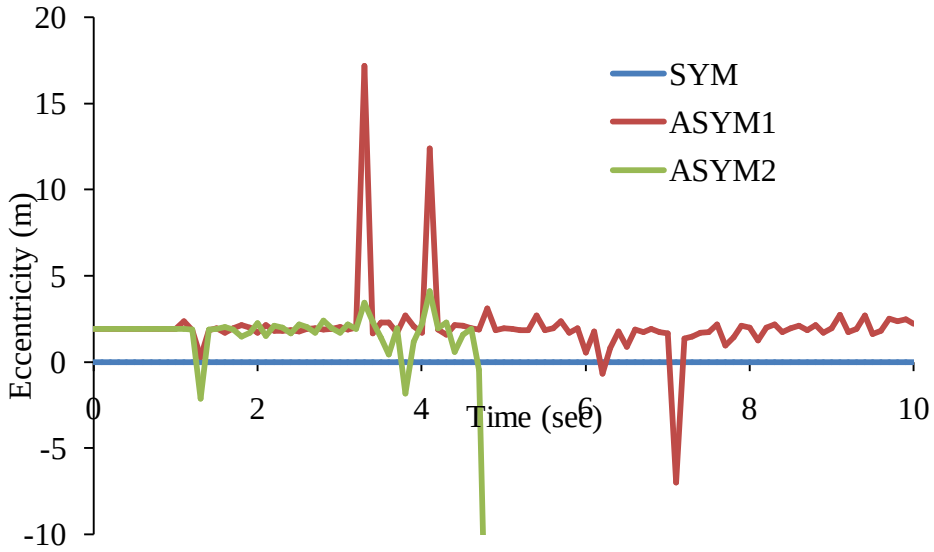

Fig. 5.39: Eccentricity -versus-time data for Data-A

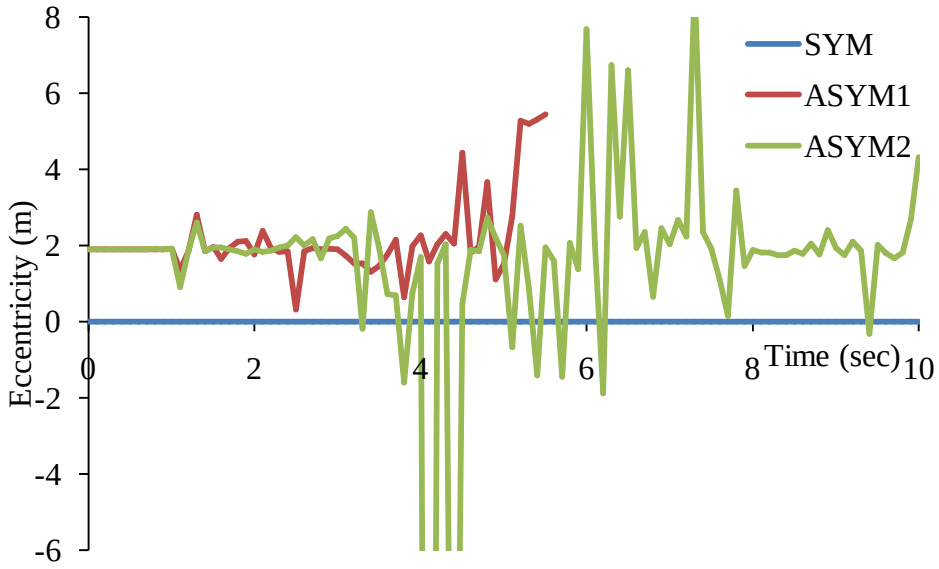

Fig. 5.40: Eccentricity -versus-time data for Data-B

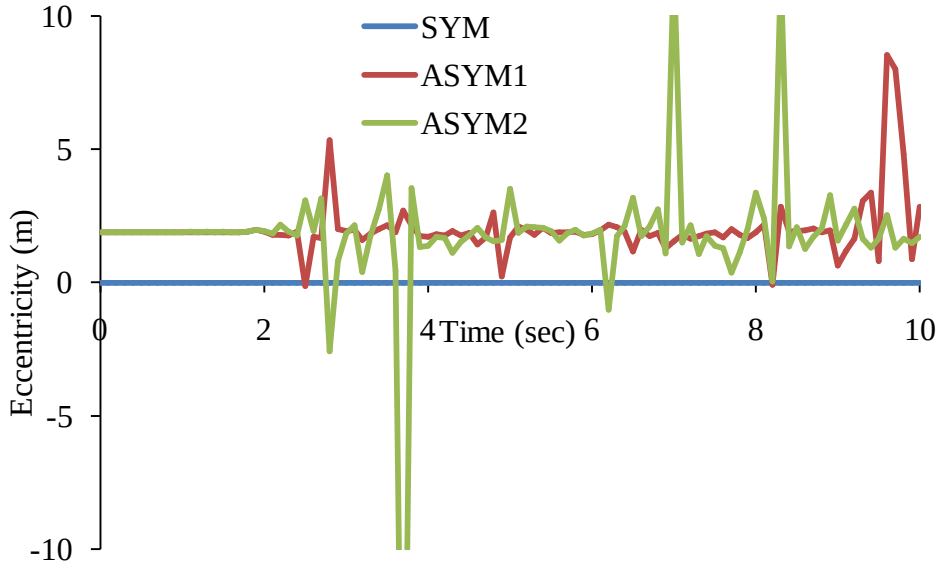

Fig. 5.41: Eccentricity -versus-time data for Data-C

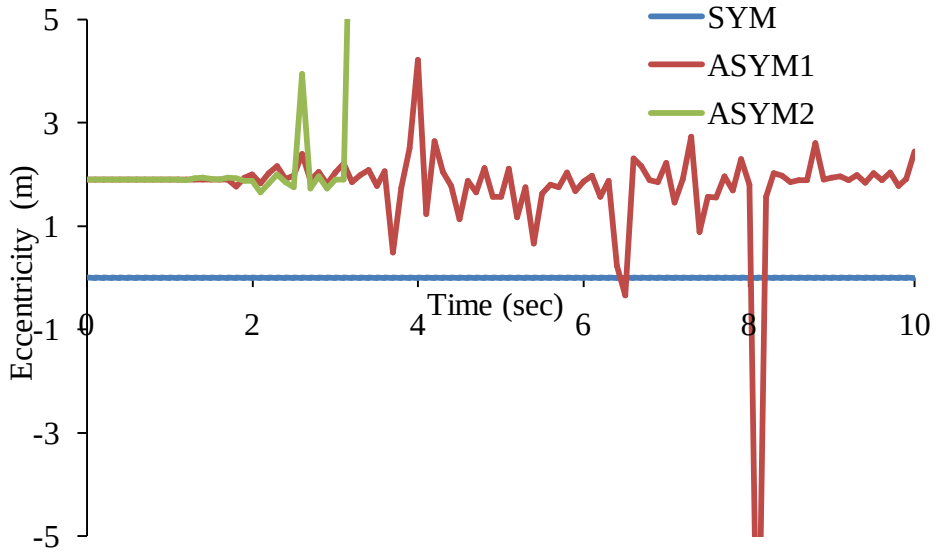

Fig. 5.42: Eccentricity -versus-time data for Data-D

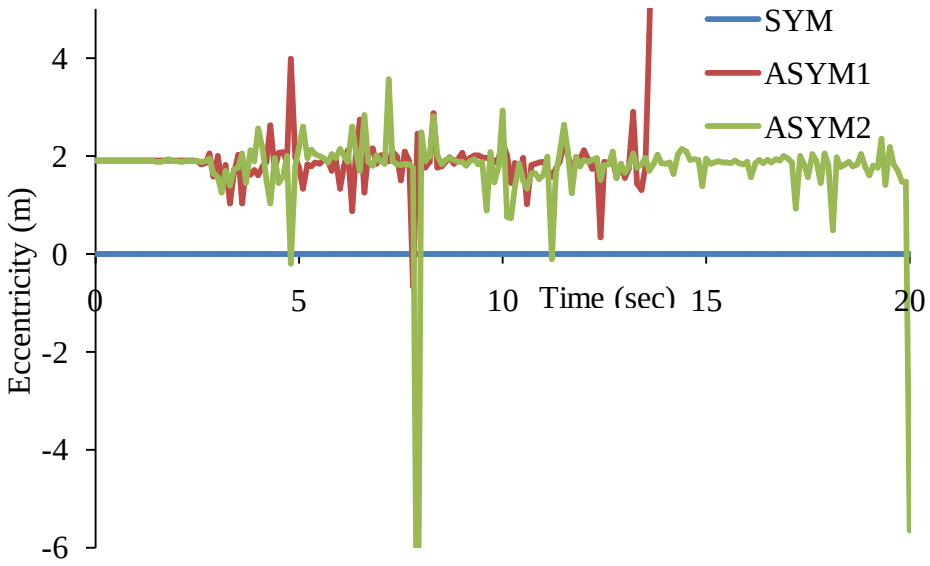

Fig. 5.43: Eccentricity -versus-time data for Data-E

Followings are the important observation made from the Figs. 5.30-5.43 presented above:

i) The eccentricity of the building is same as the static eccentricity till the first yielding (or any significant yielding) occurs.

ii) These figures clearly show that the yielding for both the asymmetric building occurs at the same time step of the dynamic analyses even though ASYM2 has a greater strength compared to ASYM1.

iii) The value of eccentricity for both the asymmetric buildings oscillates about the static elastic eccentricity (e = 1.9m for this case). However, there is no trend found in the change of the eccentricity value.

iv) The value of eccentricity for ASYM2 changes in nonlinear analysis steps more frequently and with more amplitude as compared to ASYM1.

5.5. SUMMARY

This Chapter presents the results obtained from the nonlinear dynamic analyses of the three selected building models. Three important parameters are considered to study the nonlinear dynamic behaviour of the three buildings: (a) base shear versus roof displacement relation, (b) base moment versus roof rotation about the vertical axis and (c) variation of the building eccentricity in nonlinear time step. It is found from these results that the maximum base shear demands for the three building variant are almost same when subjected to earthquake ground motion. However, there is a considerably higher roof displacementdemand for asymmetric building variants compared to similar symmetric building. The yielding in symmetric building subjected to earthquake ground motion is found to occur symmetrically. Among the two asymmetric building variants ASYM2 has more roof rotation demand compared to ASYM1. It is foundthat the yielding for both the asymmetric building occurs at the same time stepof the dynamic analyses after following the same elastic eccentricity even though ASYM2 has a greater strength compared to ASYM1.

CHAPTER 6

SUMMARY AND CONCLUSIONS

6.1. GENERAL

Seismic damage surveys and analyses conducted on modes of failure of building structures during past severe earthquakes concluded that most vulnerable building structures are those, which are asymmetric in nature. However asymmetric building structures are almost unavoidable in modern construction due to various types of functional and architectural requirements. With this background one question becomes important: is the clause to safeguard torsional force arising out of plan asymmetry during an earthquake given in IS 1893:2002 (Part1) adequate? The structures are analyzed with pushover analysis and time history analyses with tennaturaland five spectral consistent ground motions data for checking the validity of the code clause.

6.2. SUMMARY

The step-by-step progress of the entire project work carried out to achieve the objectives of the present study is presented here as follows:

i) The main objective of the present study is to check the validity of IS 1893:2002 (Part1) with regard to torsional irregularity of asymmetric buildings. Two similar asymmetric building has been considered for this study: one of them is designed considering the code recommendation (ASYM2)whereas the other one is designed neglecting this recommendation (ASYM1). A symmetric building variant (SYM) is designed using IS

1893:2002 (Part1), considering an accidental eccentricity equals to ±5% of the relevant plan dimension of the building. In the first asymmetric variant (ASYM1), the structure remained the same as that of the symmetric building. The second asymmetric variant (ASYM2)is redesigned considering mass eccentricity of 0.1L and accidental eccentricity equals to ±5% of the relevant plan dimension of the building.

ii) Beams and columns in the present study aremodelled as frame elements with the centrelines joined at nodes using commercial software SAP2000 (v14). The rigid beam-column joints aremodelled by using end offsets at the joints. The floor slabs are assumed to act as diaphragms, which ensure integral action of all the vertical lateral load-resisting elements. The weight of the slab is distributed as triangular and trapezoidal load to the surrounding beams. M 25 grade of concrete and Fe 415 grade of reinforcing steel are used to design the building. The column end at foundation is considered as fixed for all the models in this study.

iii) The flexural hinges in beams are modelled with uncoupled moment (M3) hinges whereas for column elements the flexural hinges are modelled with coupled P-M2-M3 properties based on the interaction of axial force and bi-axial bending moments at the hinge location.

iv) The three building models (SYM, ASYM1 and ASYM2) are first analysed using modal analysis to know the change in elastic modal properties due to the presence of asymmetry.

v) All the three building models are then analysed using non-linear static (pushover) analysis. At first, the pushover analysis is done for the gravity loads (DL+0.25LL) incrementally under load control. The lateral pushover analysis (in Y-direction) is followed after the gravity pushover, under displacement control.

vi) Direct integration time-history analyses of building models with point plastic hingesarecarried out with ten natural and five generated earthquake data normalised to a PGA of 0.3g.

vii) Five uncorrelated spectrum-consistent artificially generated earthquake acceleration histories, consistent with design spectrum given in Indian standard IS 1893:2002 (Part1), are used as input ground acceleration. These are generated using commercial software SIMQKE 2000.

viii) The seismic behaviour of these two asymmetric building found to be almost identical. This is concludes that the requirement of additional strength in the frame elements to safeguard the torsional force is not proper.

6.3. CONCLUSIONS AND RECOMMENDATIONS

From the present study following point-wise salient conclusions can be drawn:

i) Nonlinear static analysesrevealsthat the plan asymmetry in the building makes it non-ductile even after design with code provision.

ii) Nonlinear dynamic analyses show that the maximum base shear demands for the three building variant are almost same. This is because the fundamental

periods of all the three building are almost identical. However, symmetric building variant consistently experiences a slightly higher base shear demand compared to the asymmetric buildings as the fundamental period of the symmetric building is slightly less.

iii) The maximum roof displacement responses of the three building variants have considerable amount of variation subjected to generated earthquake ground motion (as high as 28%variation). The maximum roof displacement responses for symmetric building variants are found to be lesser compared to the two asymmetric buildings for all the cases studied here.

iv) It is found in most of the cases that symmetric building does not undergo rotation about the vertical axis even after yielding. This means that the yielding is taking place symmetrically for symmetric building subjected to earthquake ground motion.

v) Base moment demand obtained from nonlinear dynamic analyses is almost same for both of the two asymmetric buildings for all the cases studied here.

vi) In most of the cases base shear – roof displacement and base moment – roof rotation hysteresis curves are found to be similar for both the asymmetric buildings with small translational/rotation shift.

vii) A close look on the base shear – roof displacement and base moment – roof rotation hysteresis curves reveals that the energy dissipated during the motion is very high when the building is subjected to generated ground motion compared to that of natural ground motion record. This may be due to the fact that the number of times the ground acceleration reaching its peak is

considerably high for the generated ground motion compared to recorded motion. Because of this fact the yielding (or failure) is more for the case of generated ground motion that leads to an increased structural damping for the case of generated ground motion compared to recorded motion.

viii) It is found that the yielding for both the asymmetric building occurs at the same time stepof the dynamic analyses after following the same elastic eccentricity even though ASYM2 (designed with code provision) has a greater strength compared to ASYM1 (designed without code provision).

ix) Considering that all the building structures will undergo inelastic deformation under an expected earthquake it is meaningless to relate the design criterion to the elastic centre of rigidity.

x) Design criterion given in IS 1893:2002 (Part-1) with regard to plan asymmetry seems to be not very efficient.

xi) Code criterion for plan asymmetry recommends increasing the strength distribution in the building but it does not look for changing the stiffness distribution of the building.Change in the stiffness distribution to reduce eccentricity can be a useful for such buildings.

6.4. SCOPE FOR FUTURE WORK

i) The present study is based on a case study of a four storeyed RC framed building. Only mass eccentricity is considered in the present study. This study can be extended considering stiffness eccentricity of building. Also,

there is a scope of studying the effect of building height and plan dimensions on the asymmetric behaviour of the building.

ii) The present study considers only one eccentricity value (10% of the plan dimension). This study can be extended to consider various other possible eccentricities.

iii) The present study considers mass eccentricityonly in one direction although eccentricity in both the horizontal orthogonal directions in asymmetric building is more general. Therefore, there is a scope of analyzing building models with bi-directional eccentricity subjected to bi-directional ground motion.

iv) Soil-structure interaction can be studied for mass- and stiffness- eccentric buildings.

ANNEXURE-A

EARTHQUAKE ANALYSIS

A.1. INTRODUCTION

The seismic analysis of a structure involves evaluation of the earthquake forces acting at various level of the structure during an earthquake and the effect of such forces on the behavior of the overall structure. The analysis may be static or dynamic in approach as per the code provisions.

Thus broadly we can say that analysis of structures to compute the earthquake forces is commonly based on one of the following three approaches.

1. An equivalent lateral procedure in which dynamic effects are approximated by horizontal static forces applied to the structure. This method is quasi-dynamic in nature and is termed as the *Seismic Coefficient Method* in the IS code.
2. *The Response Spectrum Approach* in which the effects on the structure are related to the response of simple, single degree of freedom oscillators of varying natural periods to earthquake shaking.
3. *Response History Method* or *Time History Method* in which direct input of the time history of a designed earthquake into a mathematical model of the structure using computer analyses.

First of the above three methodsofanalysis,*i.e*. Seismic Coefficient Method of Analysis, is considered for the design of buildings studied here. Details of this method are described in the following section.

A.2. LOAD COMBINATION

Load combination used for the earthquake analysis of structure is explained in the IS: 1893, 2002 (Part1). In the limit state design of reinforced and prestressedconcrete structures, the following load combinationsshall be accounted for:

COMB1 = 1.5(DL+IL)
COMB2 = 1.2(DL+IL+EL)
COMB3 = 1.2(DL+IL −EL)
COMB4 = 1.5(DL+EL)
COMB5 = 1.5(DL−EL)
COMB6 = 0.9DL+1.5EL
COMB7 = 0.9DL−1.5EL

Here, *DL*≡ Dead load, *IL*≡ Live load, and *EL*≡ Earthquake Load. The dead load and the live load are taken as per IS 875, 1987. When the lateral load resisting elements are not orthogonally oriented, the design forces along two horizontal orthogonal directions (X- and Y-) should be considered. One method to consider this is the following.

(a) 100% of the design forces in X-direction and 30% of the design forces in Y-direction.

(b) 100% of the design forces in Y-direction and 30% of the design forces in X-direction.

An alternative method to consider the effect of the forces along X- and Y- directions is the square root of the sum of the squares (SRSS) basis.

$$EL = \sqrt{EL_x^2 + EL_y^2} \qquad (A.1)$$

The vertical component is considered only for special elements like horizontal cantilevers in Zones IV and V. The maximum value of a response quantity from the above load combinations gives the demand.

A.3. LINEAR ANALYSIS METHODS

The two different linear analysis methods recommended in IS 1893: 2002 (Part1) are explained in this Section. Any one of these methods can be used to calculate the expected seismic demands on the lateral load resisting elements.

A.3.1. Equivalent static method

In the equivalent static method, the lateral force equivalent to the design basis earthquake is applied statically. The equivalent lateral forces at each storey level are applied at the design 'centre of mass' locations. It is located at the design eccentricity from the calculated 'centre of rigidity (or stiffness)'.

A.3.1.1. Centre of mass

The centre of mass is the point where the total mass of the floor level is assumed to be lumped. The centre of mass can be calculated for each floor by taking moments of the axial forces (from gravity load analysis of that floor only) in the columns about an assumed reference axis.

$$CM_x = \frac{\sum W_i x_i}{\sum W_i}; \qquad CM_y = \frac{\sum W_i y_i}{\sum W_i} \tag{A.2}$$

$$x^1 = -{(\vartheta_z)_x}\Big/{(\vartheta_z)_z} \tag{A.3a}$$

$$y^1 = -{(\vartheta_z)_y}\Big/{(\vartheta_z)_z} \tag{A.3b}$$

The static eccentricity of the centre of mass with respect of centre of rigidity is given as follows.

$$e_{six} = CM_x - CR_x \qquad (A.4a)$$

$$e_{siy} = CM_y - CR_y \qquad (A.4a)$$

A.3.1.2. Effect of torsion

The design eccentricity of the centre of mass (e_{dix},e_{diy}) is calculated considering a dynamic amplification factor and an additional eccentricity of 5% of the dimension of the building perpendicular to the direction of the seismic force. For either of X- or Y- directions,

$$e_{di} = 1.5e_{si} + 0.05b \qquad (A.5a)$$

$$e_{di} = e_{si} - 0.05b (A.5b)$$

There can be four possible locations of the design centre of mass. To reduce computation, only two diagonal locations can be considered.

A.3.1.3. Seismic weight

The seismic weight of each floor of the structure includes the dead load and fraction of the live load (as per Table 8 of IS 1893: 2002(Part1)) acting on the floor. The weight of the columns and walls (up to the tributary height) are to be included. The tributary height is between the centreline of the storey above and centre line of the storey below.

A.3.1.4. Lumped mass

The lumped mass is the total mass of each floor that is lumped at the design centre of mass of the respective floor. The total mass of a floor is obtained from the seismic weight of that floor.

A.3.1.5. Calculation of lateral forces

The base shear ($V = V_B$) is calculated as per Clause 7.5.3 of IS 1893: 2002.

$$V_B = A_h W \qquad (A.6)$$

$$A_h = \frac{Z}{2}\frac{I}{R}\frac{S_a}{g} \qquad (A.7)$$

Where

Z= Zone factor, is for the Maximum Considered Earthquake (MCE) and service life of structure in a zone. The factor 2 in the denominator of Z is used so as to reduce the Maximum Considered Earthquake (MCE) zone factor to the factor for Design Basis Earthquake (DBE).

I = Important factor, depending upon the functional use of the structures, characterized by hazardous consequences of its failure, post-earthquake functional needs, historical value, or economic importance.

R = Response factor, depending on the perceived seismic damage performance of the structure, characterized by ductile or brittle deformations. However, the ratio (I/R) shall not be greater than 1.0.

Fig. A.1, corresponding to an approximate time period (T_a) which is given by

For RC moment resisting frame without masonry infill,

$$T_a = 0.075h^{0.75} \qquad (A.8a)$$

For RC moment resisting frame with masonry infill,

$$T_a = \frac{0.09h}{\sqrt{d}} \qquad (A.8b)$$

The base dimension of the building at the plinth level along the direction of lateral forces is represented as *d* (in meters) and height of the building from the support is represented as *h* (in meters). The response spectra functions can be calculated as follows:

For Type I soil (rock or hard soil sites):

$$\frac{S_a}{g} = \begin{cases} 1 + 15T & 0.00 \leq T \leq 0.10 \\ 2.5 & 0.10 \leq T \leq 0.40 \\ \dfrac{1}{T} & 0.40 \leq T \leq 4.00 \end{cases} \qquad (A.9a)$$

For Type II soil (medium soil):

$$\frac{S_a}{g} = \begin{cases} 1 + 15T & 0.00 \leq T \leq 0.10 \\ 2.5 & 0.10 \leq T \leq 0.55 \\ \dfrac{1.36}{T} & 0.55 \leq T \leq 4.00 \end{cases} \qquad (A.9b)$$

For Type III soil (soft soil):

$$\frac{S_a}{g} = \begin{cases} 1 + 15T & 0.00 \leq T \leq 0.10 \\ 2.5 & 0.10 \leq T \leq 0.67 \\ \dfrac{1.67}{T} & 0.67 \leq T \leq 4.00 \end{cases} \qquad (A.9c)$$

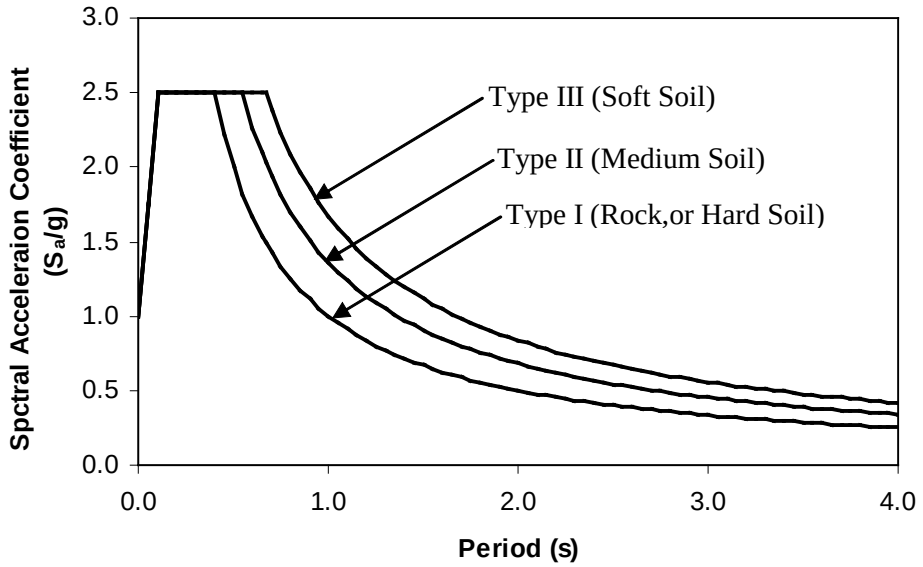

Fig. A.1: Response spectra for 5 percentdamping (IS 1893: 2002 (Part1))

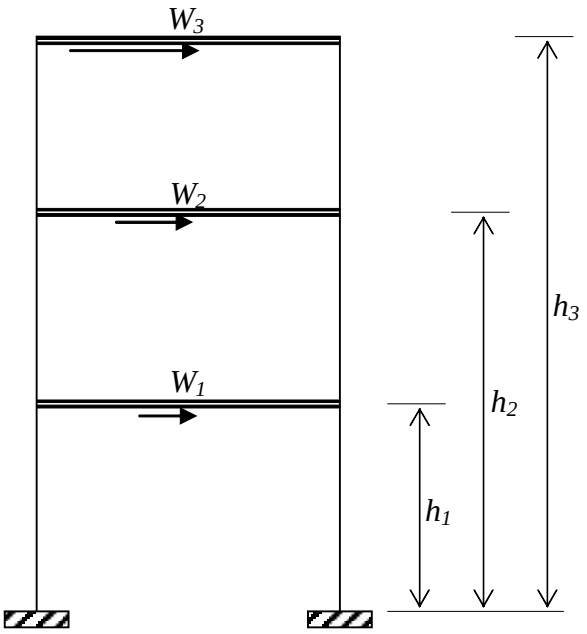

Fig. A.2: Building model under seismic load

The design base shear is to be distributed along the height of building as per Clause 7.7.1 of IS 1893: 2002 (Part1).

The design lateral force at floor *i* is given as follows,

$$Q_i = V_B \frac{W_i h_i^2}{\sum_{j=1}^{n} W_j h_j^2} \qquad (A.10)$$

A.4. RESPONSE SPECTRUM ANALYSIS

The equations of motion associated with the response of a structure to ground motion are given by:

$$\ddot{u}(t)_n + 2\zeta_n \omega_n \dot{u}(t)_n + \omega_n^2 u(t)_n = p_{ni} \ddot{u}(t)_g \qquad (A.11)$$

Where p_{ni} the Mode Participation Factor are defined by modal participation factor of mode i of vibration is the amount by which mode k contributes to the overall vibration of the structure under horizontal and vertical earthquake ground motions.

For a specified ground motion$\ddot{u}(t)_g$, damping value and assumingp_{ni}. It is possible to solve above equation at various values of ω and plot a curve of maximum peak response $u(\omega)_{MAX}$. For this acceleration input, the curve is defined as Displacement Response Spectrum for earthquake motion. A different curve will exist for each different value of damping.

A plot of ω $u(\omega)_{MAX}$ is defined as the pseudo-velocity spectrum and plot of $\omega^2 u(\omega)_{MAX}$ is defined as the pseudo-acceleration spectrum. These pseudo values have minimum significance and are not essentially a part of a response spectrum analysis. The true values for maximum velocity and acceleration must be calculated from the solution of above equation. There is a mathematical relationship, however, between the pseudo-acceleration spectrum and the total acceleration spectrum. The total acceleration of the unit mass, single degree-of-freedom system is given by,

$$\ddot{u}(t)_T = \ddot{u}(t) + \ddot{u}(t)_g \qquad (A.12)$$

$\ddot{u}(t)$from first equation is substituted in the above equation which yields,

$$\ddot{u}(t)_T = -2\zeta_n \omega \dot{u}(t) - \omega^2 u(t) \qquad (A.13)$$

Therefore, for the special case of zero damping, the total acceleration of the system is equal to $\omega^2 u(t)$. For this reason, the displacement response spectrum curve is normally not plotted as modal displacement ω vs $u(\omega)_{MAX}$. It is standard to present the curve in terms of $S(\omega)_n$ vs a period T in seconds.

Where,

$$S(\omega)_n = \left(\frac{2\pi}{T}\right)^2 u(\omega)_{MAX} \qquad (A.14)$$

The pseudo-acceleration spectrum, $S(\omega)_n$ curve has units of acceleration vs period which has some physical significance for zero damping only. It is apparent that all response spectrum curves represent the properties of the earthquake at specific site and are not a function of the properties of the structural system. After estimation is made of linear viscous damping properties of the structure, a specific response spectrum curve is selected.

A.4.1. Calculation of Modal Response

The maximum modal displacement, for a structural model, can now be calculated for a typical node n with period T_n and corresponding spectrum response value $S(\omega)_n$. The maximum modal response associated with period T_n is given by,

$$u(T)_{MAX} = \frac{S(\omega)_n}{\omega_n^2} \qquad (A.15)$$

The maximum modal displacement of response of the structure model is calculated from,

$$u_n = u(T_n)_{MAX}\,\phi_n \qquad (A.16)$$

The corresponding internal modal forces are calculated from standard matrix structural analysis using the same equations as required in static analysis.

A.4.2. Modal combination

The peak response quantities (for example, member forces, displacements, storey forces, storey shears and base reactions) shall be combined as per CompleteQuadratic Combination (CQC) method.

$$\lambda = \sqrt{\sum_{i=1}^{r}\sum_{j=1}^{r} \lambda_i \rho_{ij} \lambda_j} \qquad (A.17)$$

Where,

$$\rho_{ij} = \frac{8\zeta^2(1+)\beta^{1.5}}{(1+\beta^2)^2 + 4\zeta^2\beta(1+\beta)^2} \qquad (A.18)$$

β= Frequency ratio=ω_j/ω_i .

If the structure does not have closely spaced mode then the peak response quantity due to all modes considered shall be obtained as:

$$\lambda = \sqrt{\sum_{k=1}^{r} (\lambda_k)^2} \qquad (A.19)$$

A.4.3. Modal Mass

The structure is to be modeled as a system of masses lumped at the floor levels with each mass having one degree of freedom that of lateral displacement in the direction under consideration and the modal mass is given by:

$$M_k = \frac{(\sum_{i=1}^{n} W_i \phi_{ik})^2}{g \sum_{i=1}^{n} W_i (\phi_{ik})^2} \qquad (A.20)$$

A.4.4. Modal Participation factor

The modal participation factor of mode *k* is given by,

$$P_k = \frac{\sum_{i=1}^{n} W_i \phi_{ik}}{\sum_{i=1}^{n} W_i (\phi_{ik})^2} \qquad (A.21)$$

A.4.5. Design Lateral Force in Each Mode

The peak lateral force Q_{ik}at floor *i* in mode *k* is given by,

$$Q_{ik} = A_k \phi_{ik} P_k W_i \qquad (A.22)$$

Where,

A_k= Design Horizontal acceleration spectrum value using the natural period of vibration T_k of mode k.

A.4.6. Shear Force in Each Mode

The peak shear force V_{ik} acting in storey *i* in mode *k* is given by,

$$V_{ik} = \sum_{j=i+1}^{n} Q_{ik} \qquad (A.23)$$

A.4.6.1. Storey Shear Force due to All Modes Considered

The peak storey force V_i in storey *i* due to all modes considered is obtained by approximate modal combination.

A.4.6.2. Lateral Force at Each Storey due to All Modes Considered

The design lateral forces $F_{roof}$and F_i and at floor *I,*

$$F_{roof} = V_{roof}$$

$$F_i = V_i - V_{i+1}$$

A.5. DYNAMIC ANALYSIS

All real physical structure, when subjected to loads or displacements, behave dynamically. The additional inertia forces, from Newton's second law, are equal to mass times the acceleration. If the loads or displacements are applied very slowly then the inertia forces can

be neglected and static load analysis can be justified. Hence, dynamic analysis is a simple extension of static analysis.

All real structures potentially have an infinite number of displacements. Therefore, the most critical phase of a structural analysis is to create a computer model with a finite number of mass less members and finite number of node (joint) displacement that will stimulate the behavior of real structure. The mass of structure system, which can be accurately estimated, is lumped at nodes. Also for linear elastic structures the stiffness properties of members, with the aid of experimental data, can be approximated with a high degree of confidence. However, the dynamic loading, energy dissipation properties and boundary conditions for many structures are difficult to estimate. This is always true for the case of seismic input. To reduce the error that may be caused by the approximations, it is necessary to conduct many different dynamic analyses using different models, loading and boundary conditions.

A.5.1. Determination of Structural Properties

- Mass Matrix:

  Mass matrix for the modal shown can be written as:

$$M = \frac{1}{g}\begin{bmatrix} W_1 & 0 & \dots & \dots & 0 \\ 0 & W_2 & \dots & \dots & 0 \\ \dots & \dots & \dots & \dots & \dots \\ \dots & \dots & \dots & \dots & \dots \\ 0 & 0 & \dots & \dots & W_n \end{bmatrix} \qquad (A.4)$$

- Stiffness Matrix:

$$K = \begin{bmatrix} K_1 + K_2 & -K_2 & 0 & 0 & \dots & \dots & 0 \\ -K_2 & K_2 + K_3 & -K_3 & 0 & \dots & \dots & 0 \\ 0 & -K_3 & K_3 + K_4 & -K_4 & \dots & \dots & 0 \\ \dots & \dots & \dots & \dots & \dots & \dots & \dots \\ \dots & \dots & \dots & \dots & \dots & \dots & \dots \\ 0 & 0 & 0 & 0 & K_{n-1} & K_{n-1} + K_n & -K_n \\ 0 & 0 & 0 & 0 & \dots & -K_n & K_n \end{bmatrix} \qquad (A.5)$$

- Frequencies and Mode Shapes:

  Frequencies and mode shapes are calculated using the standard eigen function,

$$[K]\phi = \lambda[M]\phi \qquad (A.6)$$

  Where, $\lambda = \omega^2$

  ω being the frequency

The resulted eigen values represent the square of the frequencies whereas the obtained eigen vectors do furnish the mode shapes.

The force equilibrium of multi-degree of freedom lumped mass system as a function of time can be expressed by the following relationship:

$$F(t)_I + F(t)_D + F(t)_S = F(t) \qquad (A.7)$$

The above equation is based on physical laws and is valid for both linear and nonlinear systems if equilibrium is formulated with respect to the deformed geometry of the structure. For many structural systems, the approximation of linear structural behavior is made in order

to convert the physical equilibrium statement to the following set of second order linear differential equation,

$$u(t) + C\dot{u}(t) + K\ddot{u(t)} = -M_x\ddot{u}(t)_{xg} - M_y\ddot{u}(t)_{yg} - M_z\ddot{u}(t)_{zg} \qquad (A.8)$$

Dynamic analysis may be performed either by the Time History Method or by the Response Spectrum Method.

ANNEXURE B

PUSHOVER ANALYSIS

The present study is based on the nonlinear static and dynamic analyses of a class of RC framed building. Nonlinear static analysis, popularly known as Pushover Analysis, is widely used to evaluate existing buildings and also to the check the new design. The analysis procedure given in FEMA 356:2000 is used in the presents study. This Annexure presents the step-by-step procedure to carry out pushover analysis as per FEMA 356:2000. This analysis has two major parts: (a) generating pushover curve (base shear versus roof displacement curve) and (b) Calculation of target displacement from the pushover curve. Although the present study only generates of capacity curve of the selected buildings and does not use the second part of this analysis this annexure explains entire method to run pushover analysis of RC framed buildings.

B.1. INTRODUCTION

The use of the nonlinear static analysis (pushover analysis) came in to practice in 1970's but the potential of the pushover analysis has been recognized for last 10-15 years. This procedure is mainly used to estimate the strength and drift capacity of existing structure and the seismic demand for this structure subjected to selected earthquake. This procedure can be used for checking the adequacy of new structural design as well. The effectiveness of pushover analysis and its computational simplicity brought this procedure in to several seismic guidelines (ATC 40 and FEMA 356) and design codes (Euro code 8 and PCM 3274) in last few years.

Pushover analysis is defined as an analysis wherein a mathematical model directly incorporating the nonlinear load-deformation characteristics of individual components and elements of the building shall be subjected to monotonically increasing lateral loads representing inertia forces in an earthquake until a 'target displacement' is exceeded. Target displacement is the maximum displacement (elastic plus inelastic) of the building at roof expected under selected earthquake ground motion. Pushover analysis assesses the structural performance by estimating the force and deformation capacity and seismic demand using a nonlinear static analysis algorithm. The seismic demand parameters are global displacements (at roof or any other reference point), storey drifts, storey forces, and component deformation and component forces. The analysis accounts for geometrical nonlinearity, material inelasticity and the redistribution of internal forces. Response characteristics that can be obtained from the pushover analysis are summarised as follows:

a) Estimates of force and displacement capacities of the structure. Sequence of the member yielding and the progress of the overall capacity curve.

b) Estimates of force (axial, shear and moment) demands on potentially brittle elements and deformation demands on ductile elements.

c) Estimates of global displacement demand, corresponding inter-storey drifts and damages on structural and non-structural elements expected under the earthquake ground motion considered.

d) Sequences of the failure of elements and the consequent effect on the overall structural stability.

e) Identification of the critical regions, where the inelastic deformations are

expected to be high and identification of strength irregularities (in plan or in elevation) of the building.

Pushover analysis delivers all these benefits for an additional computational effort (modeling nonlinearity and change in analysis algorithm) over the linear static analysis. Step by step procedure of pushover analysis is discussed next.

B.1.1. Pushover Analysis Procedure

Pushover analysis is a static nonlinear procedure in which the magnitude of the lateral load is increased monotonically maintaining a predefined distribution pattern along the height of the building (Fig. B.1 (a)). Building is displaced till the 'control node' reaches 'target displacement' or building collapses. The sequence of cracking, plastic hinging and failure of the structural components throughout the procedure is observed. The relation between base shear and control node displacement is plotted for all the pushover analysis (Fig. B.1(b)). Generation of base shear – control node displacement curve is single most important part of pushover analysis. This curve is conventionally called as pushover curve or capacity curve. The capacity curve is the basis of 'target displacement' estimation. So the pushover analysis may be carried out twice: (a) first time till the collapse of the building to estimate target displacement and (b) next time till the target displacement to estimate the seismic demand. The seismic demands for the selected earthquake (storey drifts, storey forces, and component deformation and forces) are calculated at the target displacement level.

The seismic demand is then compared with the corresponding structural capacity or predefined performance limit state to know what performance the structure will exhibit.

Independent analysis along each of the two orthogonal principal axes of the building is permitted unless concurrent evaluation of bi-directional effects is required

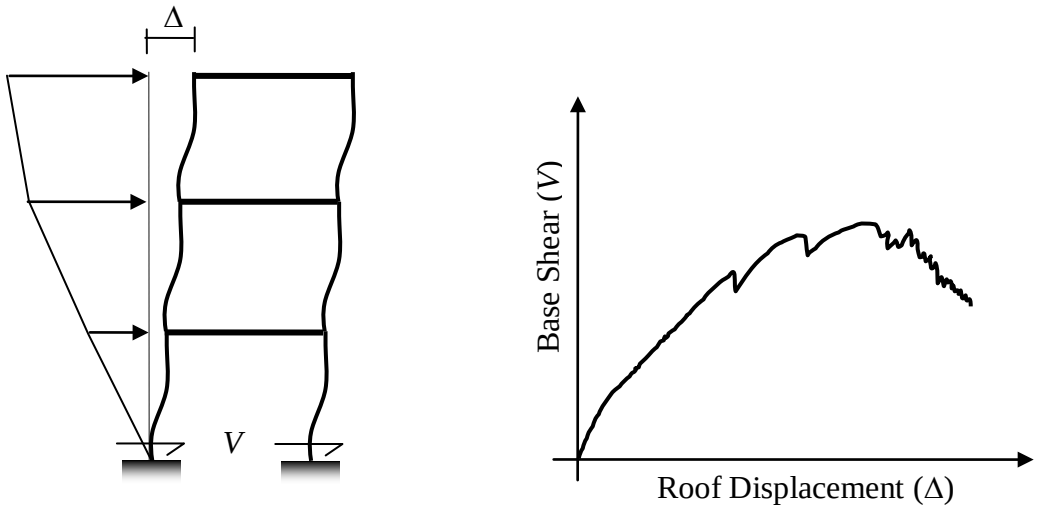

a) Building model b) Pushover curve

Fig. B.1: Schematic representation of pushover analysis procedure

The analysis results are sensitive to the selection of the control node and selection of lateral load pattern. In general, the centre of mass location at the roof of the building is considered as control node. For selecting lateral load pattern in pushover analysis, a set of guidelines as per FEMA 356 is explained in Section B.1.2. The lateral load generally applied in both positive and negative directions in combination with gravity load (dead load and a portion of live load) to study the actual behavior.

B.1.2. Lateral Load Profile

In pushover analysis the building is pushed with a specific load distribution pattern along the height of the building. The magnitude of the total force is increased but the

pattern of the loading remains same till the end of the process. Pushover analysis results (*i.e.*, pushover curve, sequence of member yielding, building capacity and seismic demand) are very sensitive to the load pattern. The lateral load patterns should approximate the inertial forces expected in the building during an earthquake. The distribution of lateral inertial forces determines relative magnitudes of shears, moments, and deformations within the structure. The distribution of these forces will vary continuously during earthquake response as the members yield and stiffness characteristics change. It also depends on the type and magnitude of earthquake ground motion. Although the inertia force distributions vary with the severity of the earthquake and with time, FEMA 356 recommends primarily invariant load pattern for pushover analysis of framed buildings.

Several investigations (Mwafy and Elnashai, 2000; Gupta and Kunnath, 2000) have found that a triangular or trapezoidal shape of lateral load provide a better fit to dynamic analysis results at the elastic range but at large deformations the dynamic envelopes are closer to the uniformly distributed force pattern. Since the constant distribution methods are incapable of capturing such variations in characteristics of the structural behavior under earthquake loading, FEMA 356 suggests the use of at least two different patterns for all pushover analysis. Use of two lateral load patterns is intended to bind the range that may occur during actual dynamic response. FEMA 356 recommends selecting one load pattern from each of the following two groups:

1. Group – I:

i) Code-based vertical distribution of lateral forces used in equivalent static

analysis (permitted only when more than 75% of the total mass participates in the fundamental mode in the direction under consideration).

ii) A vertical distribution proportional to the shape of the fundamental mode in the direction under consideration (permitted only when more than 75% of the total mass participates in this mode).

iii) A vertical distribution proportional to the story shear distribution calculated by combining modal responses from a response spectrum analysis of the building (sufficient number of modes to capture at least 90% of the total building mass required to be considered). This distribution shall be used when the period of the fundamental mode exceeds 1.0 second.

2. Group – II:

i) A uniform distribution consisting of lateral forces at each level proportional to the total mass at each level.

ii) An adaptive load distribution that changes as the structure is displaced. The adaptive load distribution shall be modified from the original load distribution using a procedure that considers the properties of the yielded structure.

Instead of using the uniform distribution to bind the solution, FEMA 356 also allows adaptive lateral load patterns to be used but it does not elaborate the procedure. Although adaptive procedure may yield results that are more consistent with the characteristics of the building under consideration it requires considerably more analysis effort. Fig. B.2 shows the common lateral load pattern used in pushover analysis.

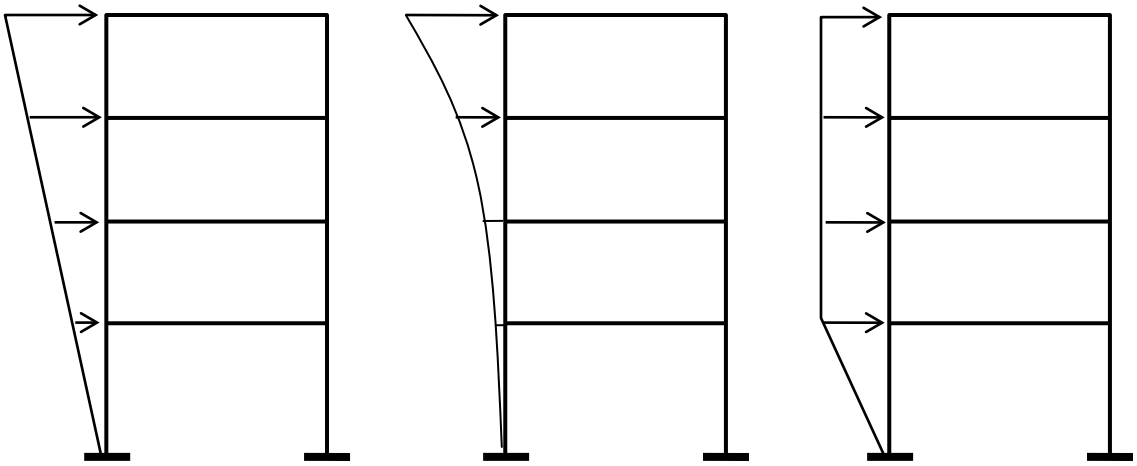

(a) Triangular (b) IS Code Based (c) Uniform

Fig. B.2: Lateral load pattern for pushover analysis as per FEMA 356
(Considering uniform mass distribution)

B.1.3. Target Displacement

Target displacement is the displacement demand for the building at the control node subjected to the ground motion under consideration. This is a very important parameter in pushover analysis because the global and component responses (forces and displacement) of the building at the target displacement are compared with the desired performance limit state to know the building performance. So the success of a pushover analysis largely depends on the accuracy of target displacement. There are two approaches to calculate target displacement:

(a) Displacement Coefficient Method (DCM) of FEMA 356 and

(b) Capacity Spectrum Method (CSM) of ATC 40.

Both of these approaches use pushover curve to calculate global displacement demand on the building from the response of an equivalent single-degree-of-freedom (SDOF) system.

The only difference in these two methods is the technique used.

B.1.3.1. Displacement Coefficient Method (FEMA 356)

This method primarily estimates the elastic displacement of an equivalent SDOF system assuming initial linear properties and damping for the ground motion excitation under consideration. Then it estimates the total maximum inelastic displacement response for the building at roof by multiplying with a set of displacement coefficients.

The process begins with the base shear versus roof displacement curve (pushover curve) as shown in Fig. B.3(a). An equivalent period (T_{eq}) is generated from initial period (T_i) by graphical procedure. This equivalent period represents the linear stiffness of the equivalent SDOF system.The peak elastic spectral displacement corresponding to this period is calculated directly from the response spectrum representing the seismic ground motion under consideration (Fig. B.3 (b)).

$$S_d = \frac{T_{eq}^2}{4\pi^2} S_a \qquad (B.1)$$

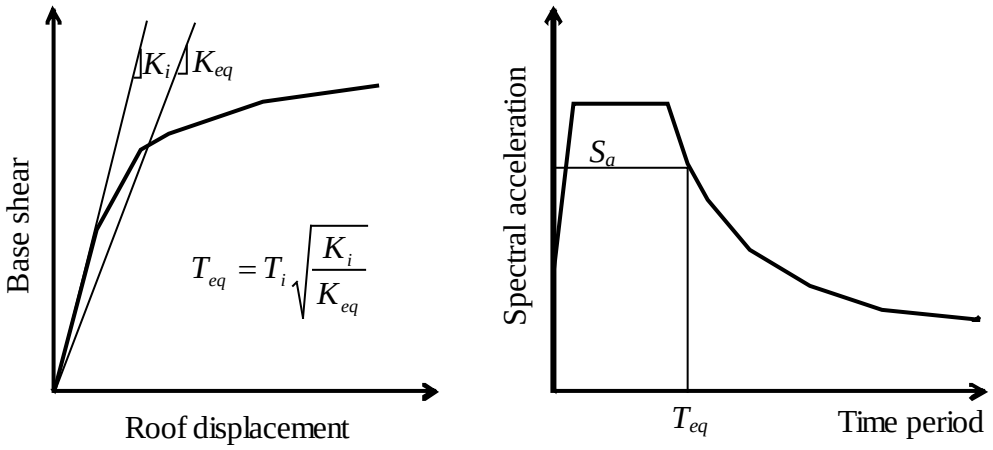

(a) Pushover Curve (b) Elastic Response Spectrum

Fig. B.3: Schematic representation of Displacement Coefficient Method (FEMA 356)

Now, the expected maximum roof displacement of the building (target displacement) under the selected seismic ground motion can be expressed as:

$$\delta_t = C_o C_1 C_2 C_3 S_d = C_o C_1 C_2 C_3 \frac{T_{eq}^2}{4\pi^2} S_a \qquad (B.2)$$

C_0 = a shape factor (often taken as the first mode participation factor) to convert the spectral displacement of equivalent SDOF system to the displacement at the roof of the building.

C_1 = the ratio of expected displacement (elastic plus inelastic) for an inelastic system to the displacement of a linear system.

C_2 = a factor that accounts for the effect of pinching in load deformation relationship due to strength and stiffness degradation

C_3 = a factor to adjust geometric nonlinearity (P-Δ) effects

These coefficients are derived empirically from statistical studies of the nonlinear response history analyses of SDOF systems of varying periods and strengths and given in FEMA 356.

B.1.3.2. Capacity Spectrum Method (ATC 40)

The basic assumption in Capacity Spectrum Method is also the same as the previous one. That is, the maximum inelastic deformation of a nonlinear SDOF system can be approximated from the maximum deformation of a linear elastic SDOF system with an equivalent period and damping.

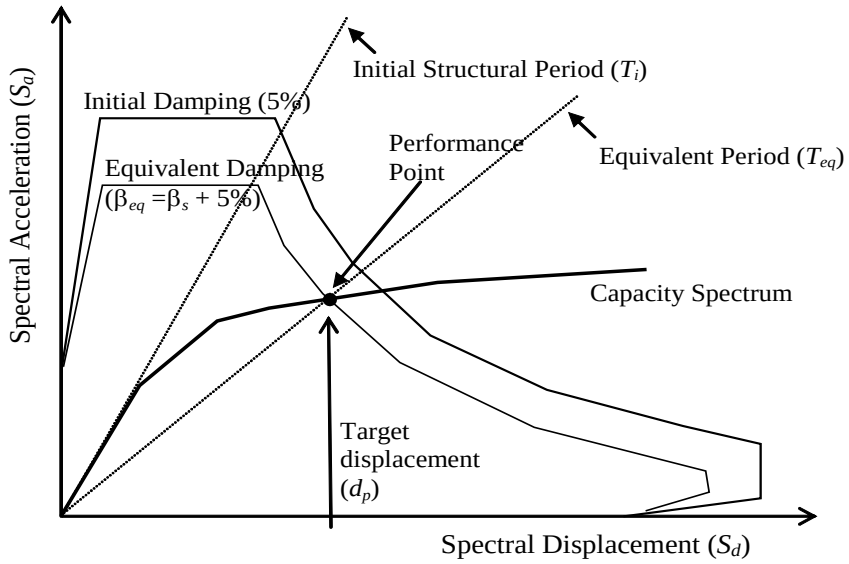

Fig. B.4: Schematic representation of Capacity Spectrum Method (ATC 40)

This procedure uses the estimates of ductility to calculate effective period and damping. This procedure uses the pushover curve in an acceleration-displacement response spectrum (ADRS) format. This can be obtained through simple conversion using the dynamic properties of the system. The pushover curve in an ADRS format is termed a 'capacity spectrum' for the structure. The seismic ground motion is represented by a response spectrum in the same ADRS format and it is termed as demand spectrum (Fig. B.4).

The equivalent period (T_{eq}) is computed from the initial period of vibration (T_i) of the nonlinear system and displacement ductility ratio (μ). Similarly, the equivalent damping ratio (β_{eq}) is computed from initial damping ratio (ATC 40 suggests an initial elastic viscous damping ratio of 0.05 for reinforced concrete building) and the displacement ductility ratio (μ). ATC 40 provides the following equations to calculate equivalent time period (T_{eq}) and equivalent damping (β_{eq}).

$$T_{eq} = T_i \sqrt{\frac{\mu}{1 + \alpha\mu - \alpha}} \qquad (B.3)$$

$$\beta_{eq} = \beta_i + k\frac{2(\mu - 1)(1 - \alpha)}{\pi\mu(1 + \alpha\mu - \alpha)} = 0.05 + \kappa\frac{2(\mu - 1)(1 - \alpha)}{\pi\mu(1 + \alpha\mu - \alpha)} \qquad (B.4)$$

Where α is the post-yield stiffness ratio and κ is an adjustment factor to approximately account for changes in hysteretic behavior in reinforced concrete structures.

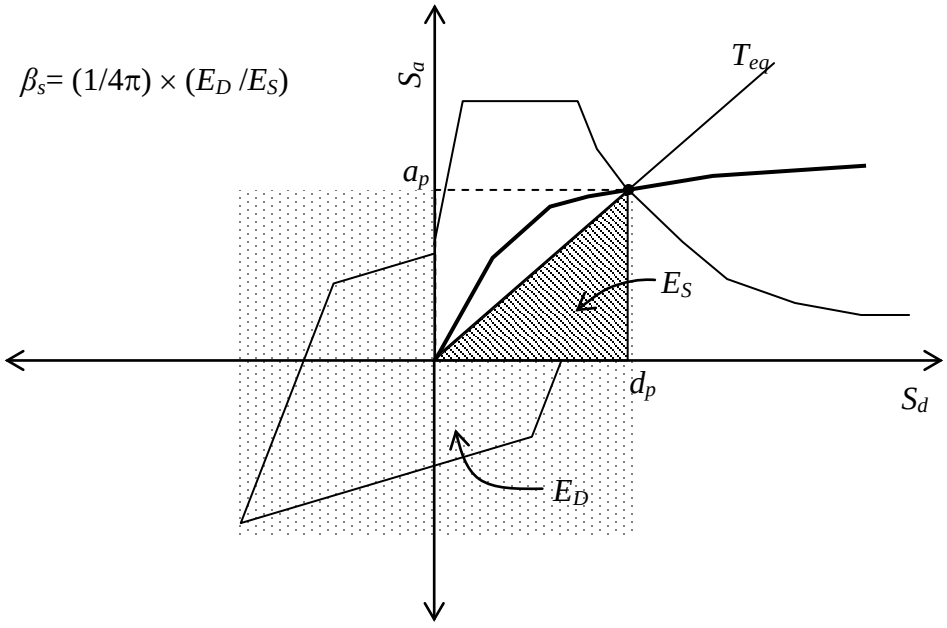

Fig. B.5: Effective damping in Capacity Spectrum Method (ATC 40)

ATC 40 relates effective damping to the hysteresis curveFig. B.5 and proposes three hysteretic behavior types that alter the equivalent damping level. Type A hysteretic behavior is meant for new structures with reasonably full hysteretic loops, and the corresponding equivalent damping ratios take the maximum values. Type C hysteretic behavior represents severely degraded hysteretic loops, resulting in the smallest equivalent damping ratios. Type B hysteretic behavior is an intermediate hysteretic

behavior between types A and C. The value of κ decreases for degrading systems (hysteretic behavior types B and C).

The equivalent period in Eq. B.3 is based on a lateral stiffness of the equivalent system that is equal to the secant stiffness at the target displacement. This equation does not depend on the degrading characteristics of the hysteretic behavior of the system. It only depends on the displacement ductility ratio (μ) and the post-yield stiffness ratio (α) of the inelastic system.

ATC 40 provides reduction factors to reduce spectral ordinates in the constant acceleration region and constant velocity region as a function of the effective damping ratio. The spectral reduction factors are given by:

$$SR_A = \frac{3.21 - 0.68ln(100\beta_{eq})}{2.2} \qquad (B.5)$$

$$SR_V = \frac{2.31 - 0.41ln(100\beta_{eq})}{1.65} \qquad (B.6)$$

Where$SR_A$is the spectral reduction factor to be applied to the constant acceleration region, and $SR_V$is the spectral reduction factor to be applied to the constant velocity region (descending branch) in the linear elastic spectrum.

Since the equivalent period and equivalent damping are both functions of the displacement ductility ratio (Eqs. B.3 and B.4), it is required to have prior knowledge of displacement ductility ratio. However, this is not known at the time of evaluating a structure. Therefore, iteration is required to determine target displacement. ATC 40 describes three iterative procedures with different merits and demerits to reach the solution.

ANNEXURE C

TIME HISTORY ANALYS

C.1. TIME HISTORY DATA

The un-scaled earthquake data used for the nonlinear dynamic analysis, specified in the Table 3.3 is graphically presented in Figs. C.1 and C.2.This includes ten natural ground motions and five generated ground motion data. All the natural acceleration data are collected from Strong Motion Database available in the website of Center for Engineering Strong Motion Data, USA (http://www.strongmotioncenter.org/) and the generated data is obtained from computer software SIMQKE 2000.

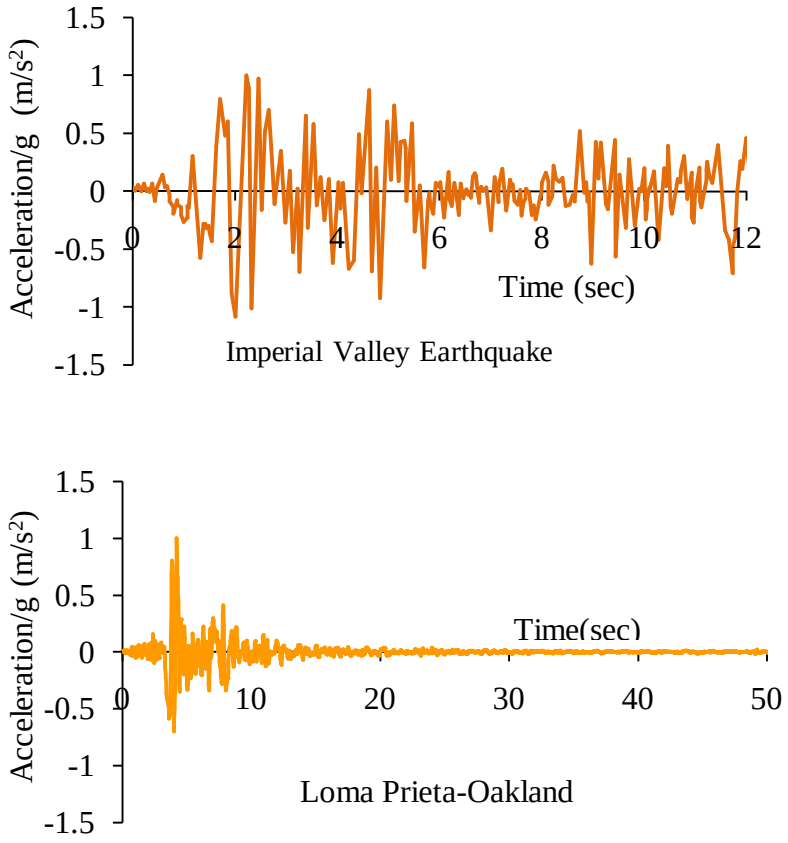

Fig. C.1: Natural ground motions used for nonlinear analysis

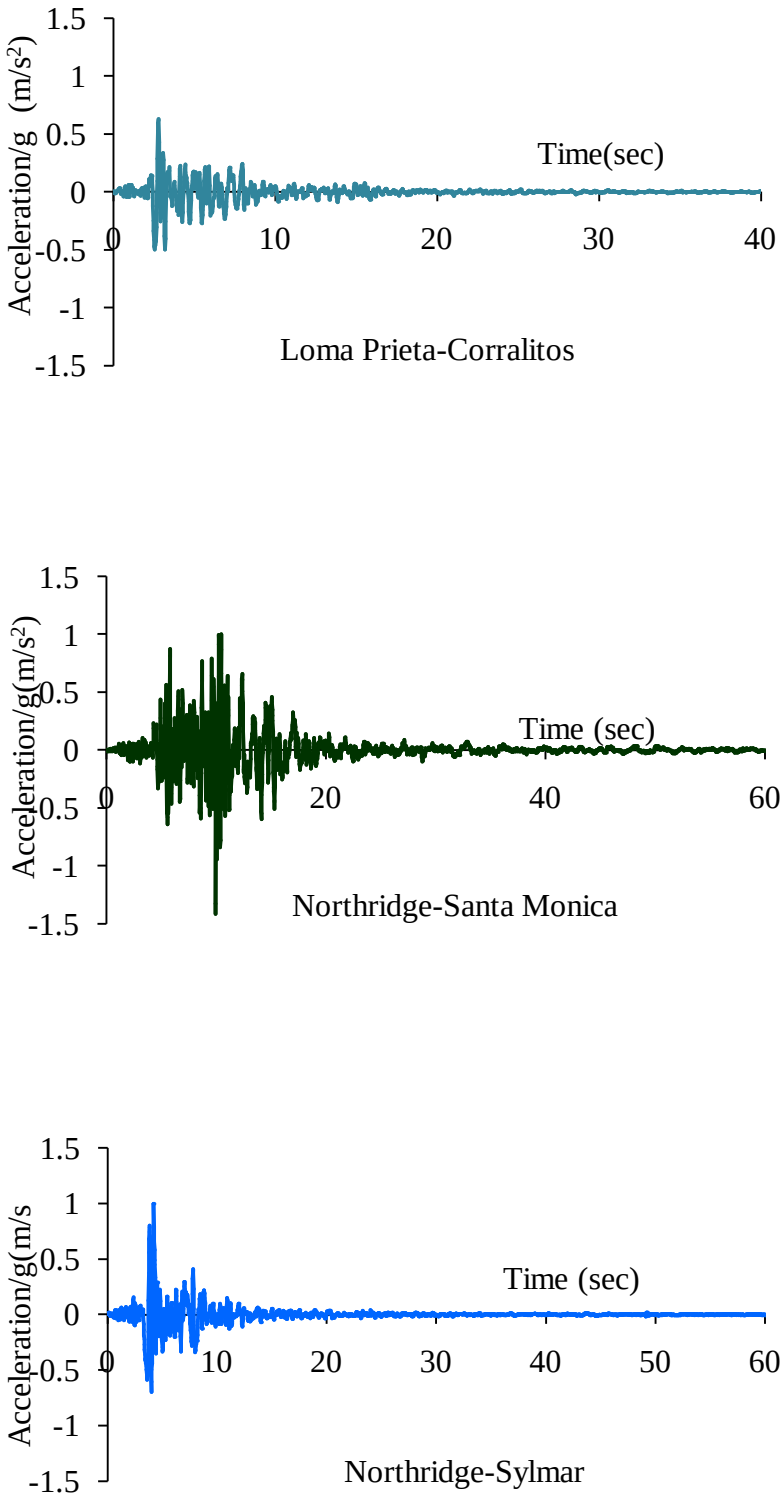

Fig. C.1 (contd.): Natural ground motions used for nonlinear analysis

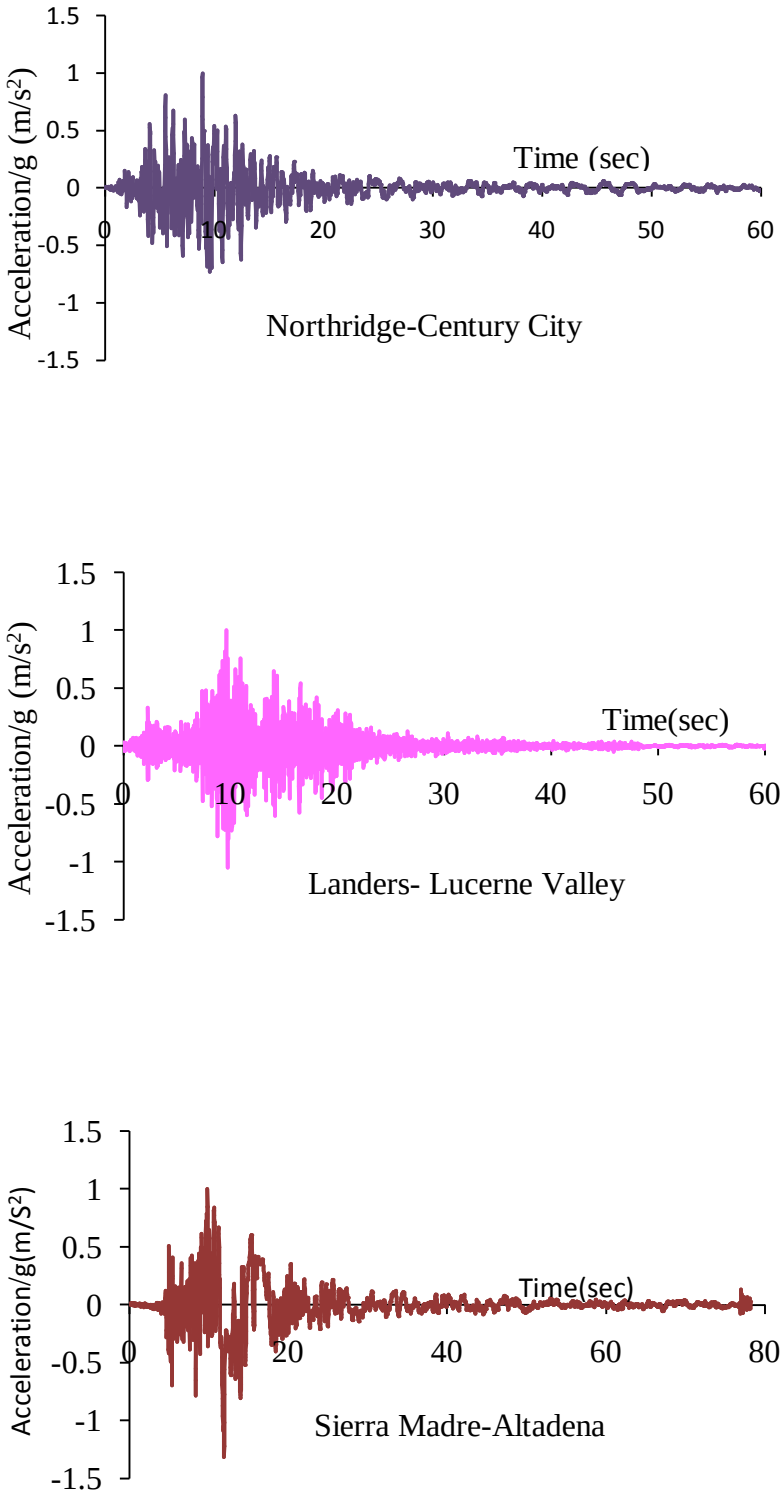

Fig. C.1 (contd.): Natural ground motions used for nonlinear analysis

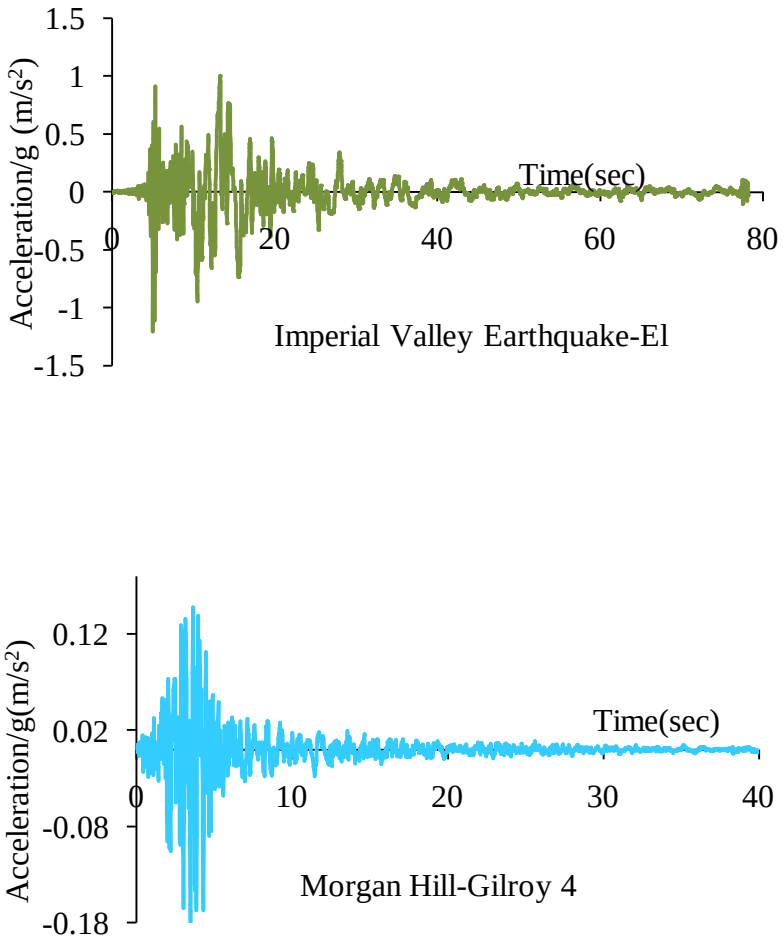

Fig. C.1 (contd.): Natural ground motions used for nonlinear analysis

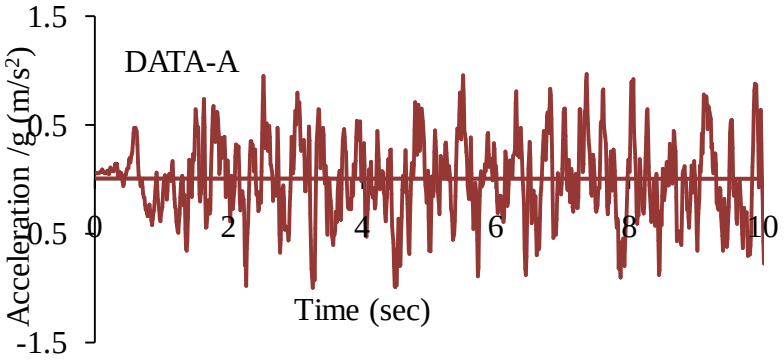

Fig C.2: Artificially generated Spectral consistent earthquake motion

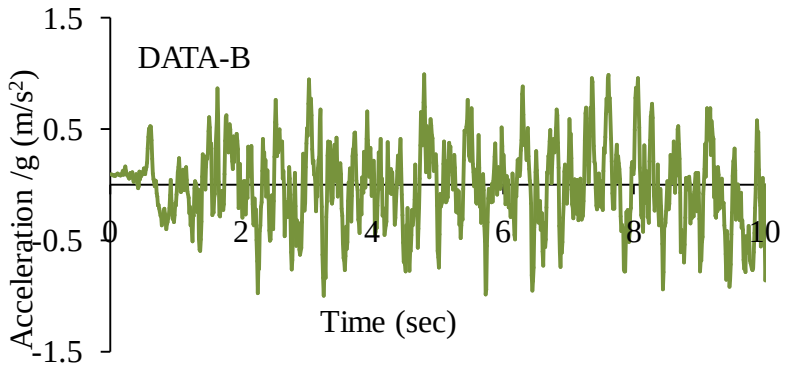

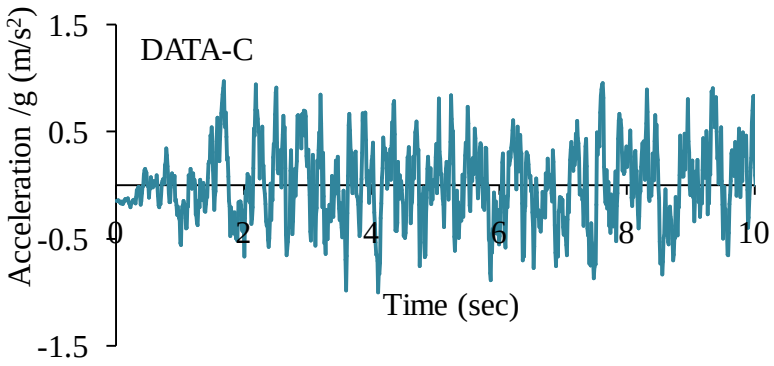

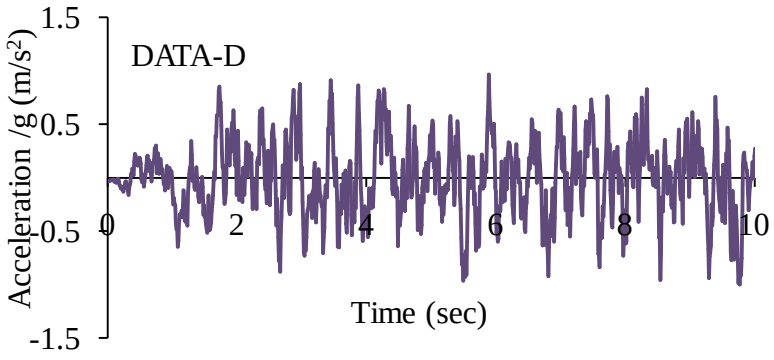

Fig C.2(contd.): Artificially generated Spectral consistent earthquake motion

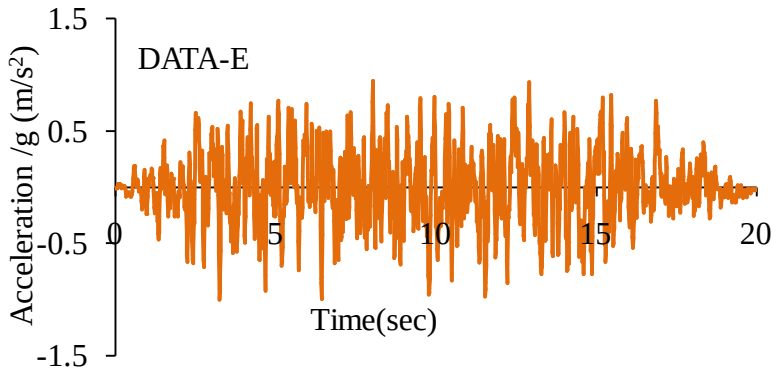

Fig C.2(contd.): Artificially generated Spectral consistent earthquake motion

C.2. ADDITIONAL RESULTS FROM TIME HISTORY ANALYSIS

Roof displacement and roof rotation response of the three building variant with respect to time as obtained from the nonlinear dynamic analysis for all 15 ground motion records (ten naturaland five generated) are presented inFigs. C.3-C.30

C.2.1. Roof Displacement Responseduring Nonlinear Dynamic Analysis

Figs. C.3-C.16 presents roof displacement response with time. Each figures presents results for symmetric building (SYM), asymmetric building designed without code provisions (ASYM1) and asymmetric building designed with Indian Standard IS 1893:2002 (Part1) provisions (ASYM2).

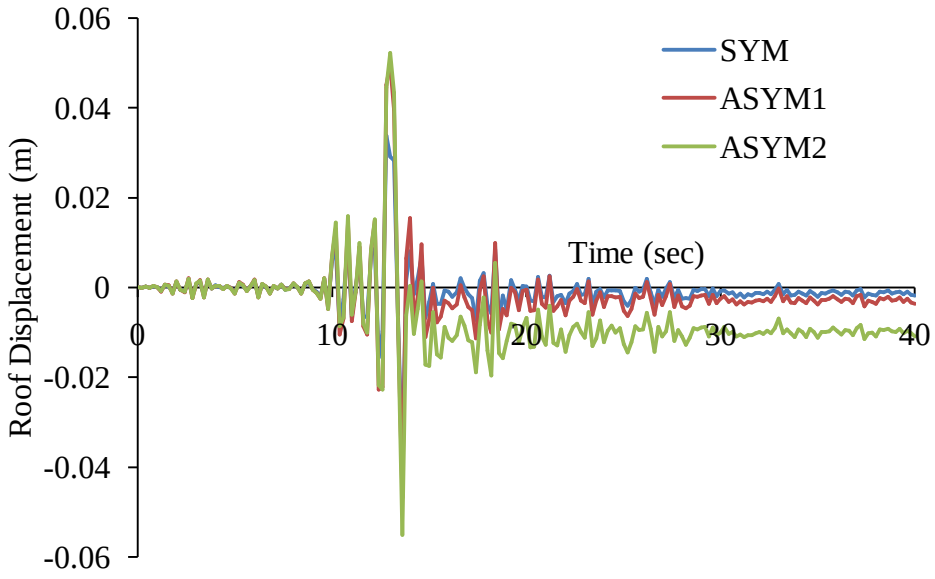

Fig. C.3: Roof Displacement -versus-time data for Loma Prieta – Oakland (1989)

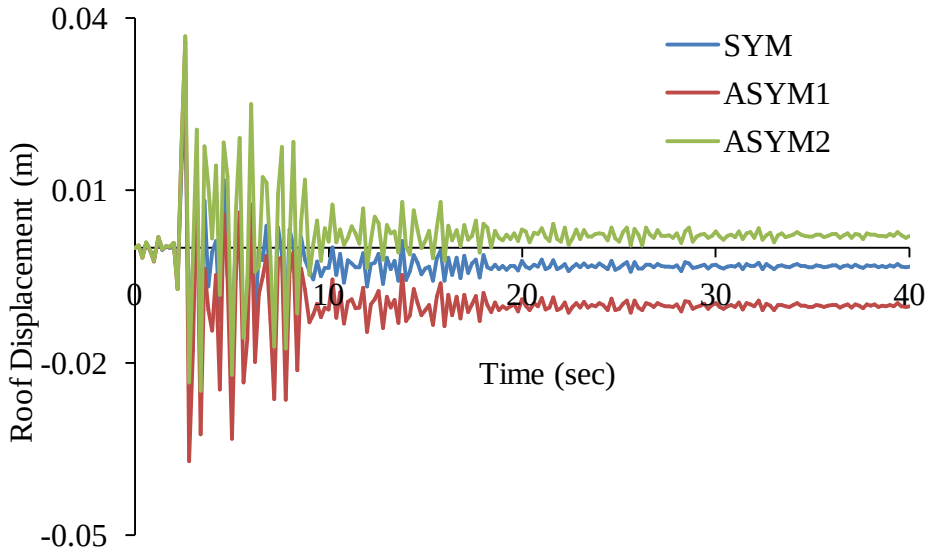

Fig. C.4: Roof Displacement -versus-time displacement data for Loma Prieta – Corralitos

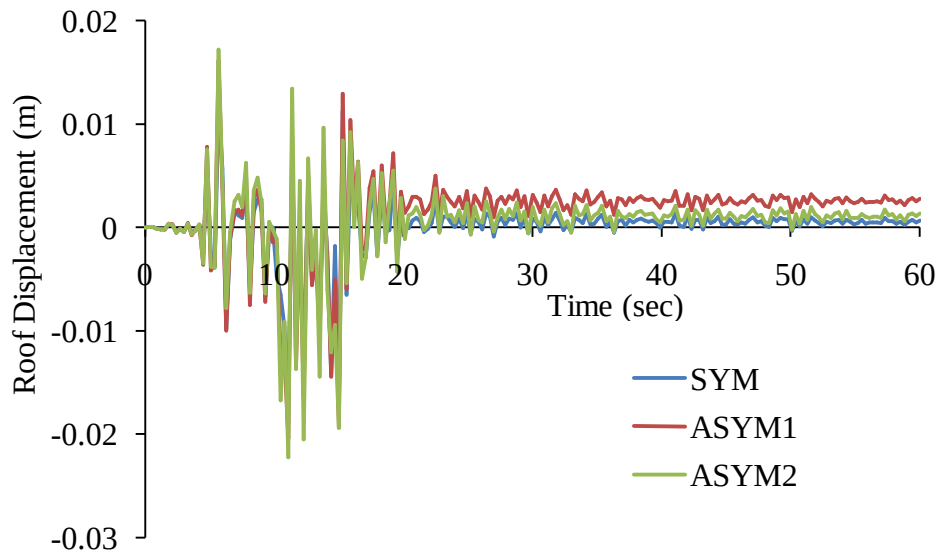

Fig. C.5: Roof Displacement -versus-time data for Northridge – Santa Monica (1994)

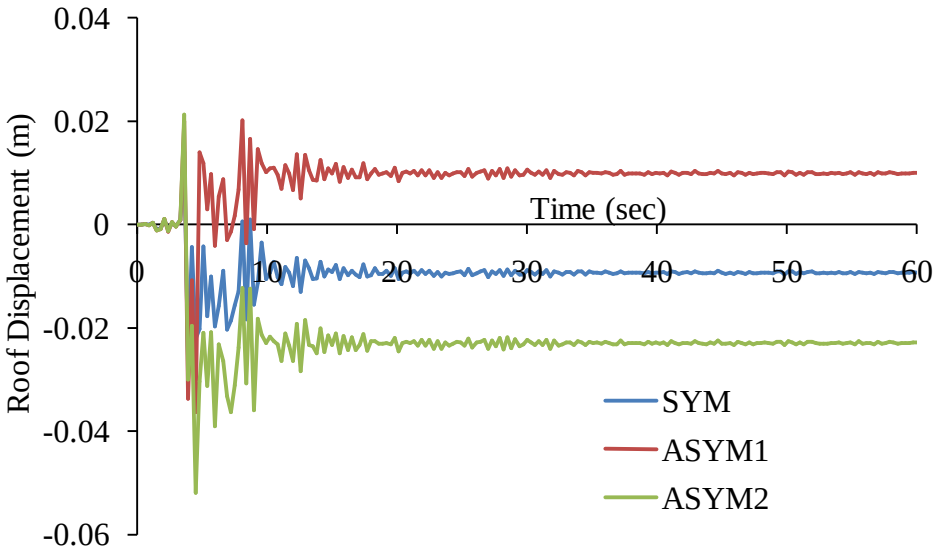

Fig. C.6: Roof Displacement -versus-time data for Northridge – Sylmar (1994)

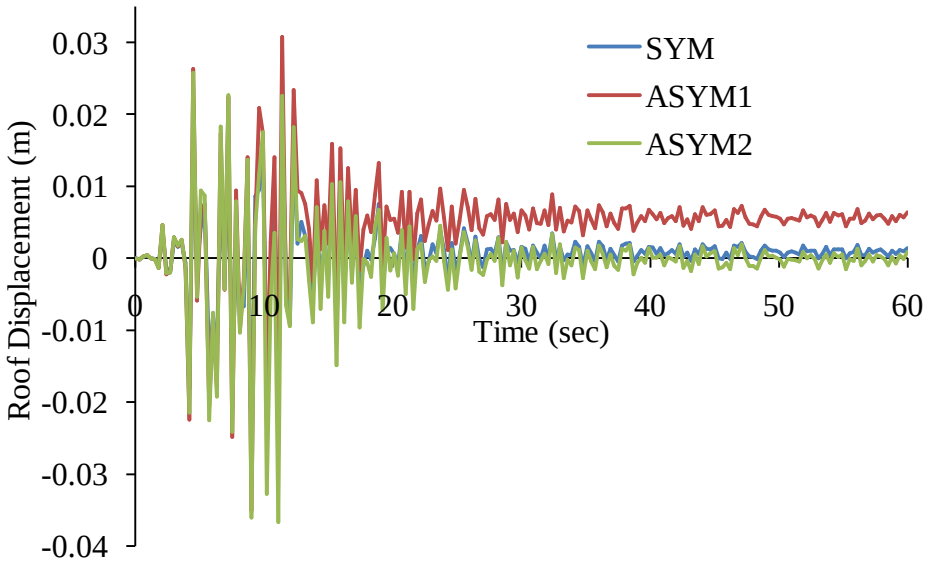

Fig. C.7: Roof Displacement -versus-time data for Northridge Century City

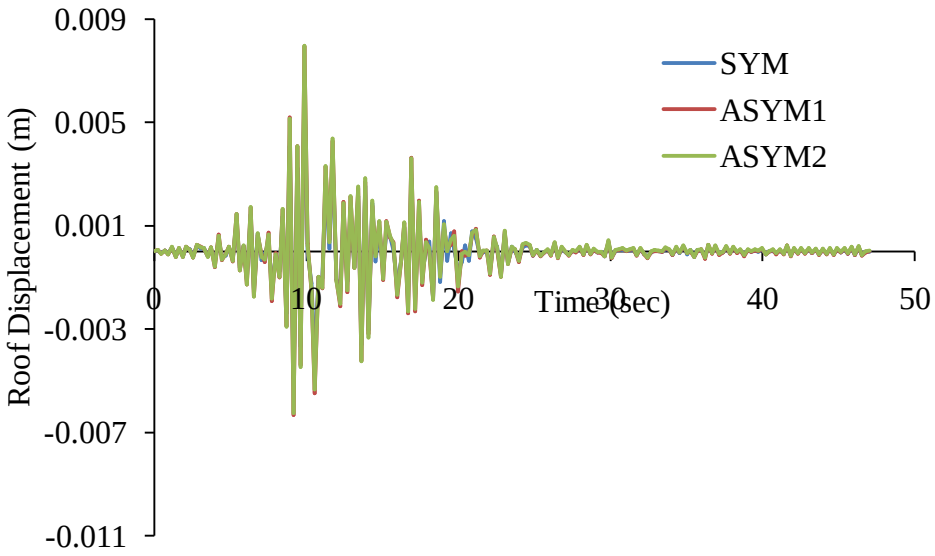

Fig. C.8: Roof Displacement -versus-time data for Landers – Lucerne Valley (1992)

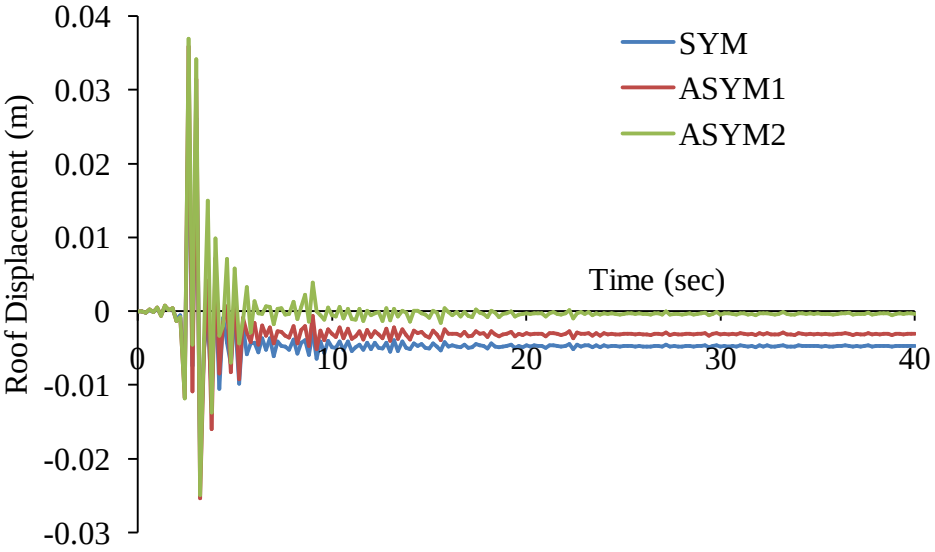

Fig. C.9: Roof Displacement -versus-time data for Sierra Madre – Altadena (1991)

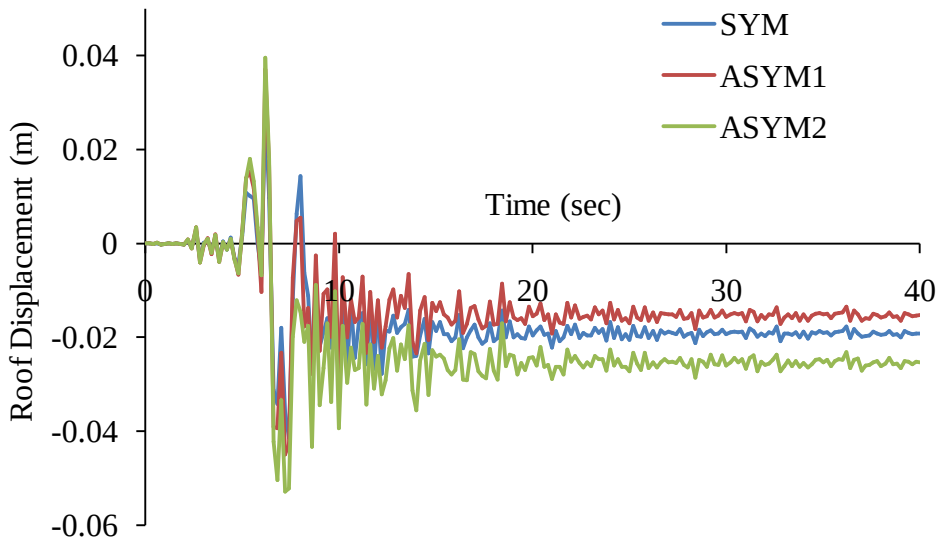

Fig. C.10: Roof Displacement -versus-time data for Imperial Valley Eq. (1979)

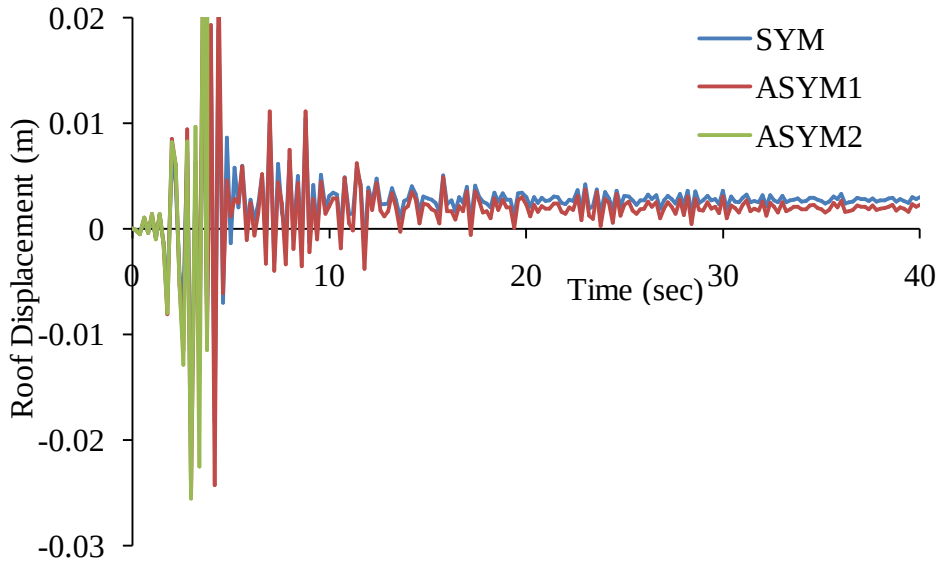

Fig. C.11: Roof Displacement -versus-time data for Morgan Hill – Gilroy4 (1984)

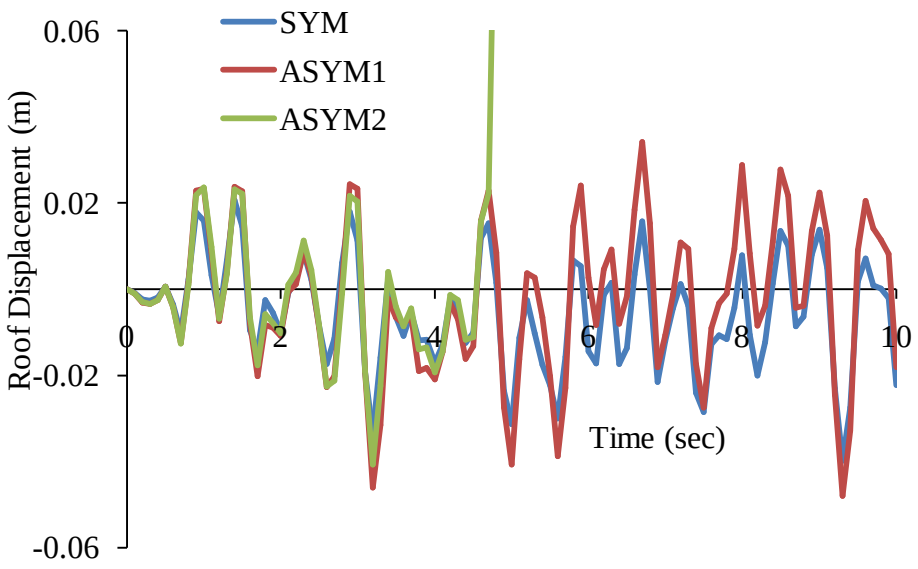

Fig. C.12: Roof Displacement -versus-time data for Data-A

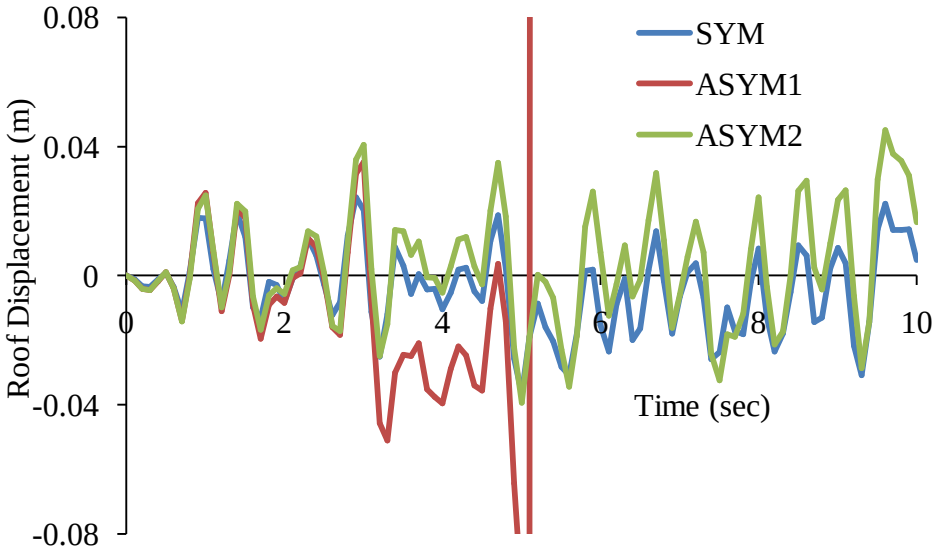

Fig. C.13: Roof Displacement -versus-time data for Data-B

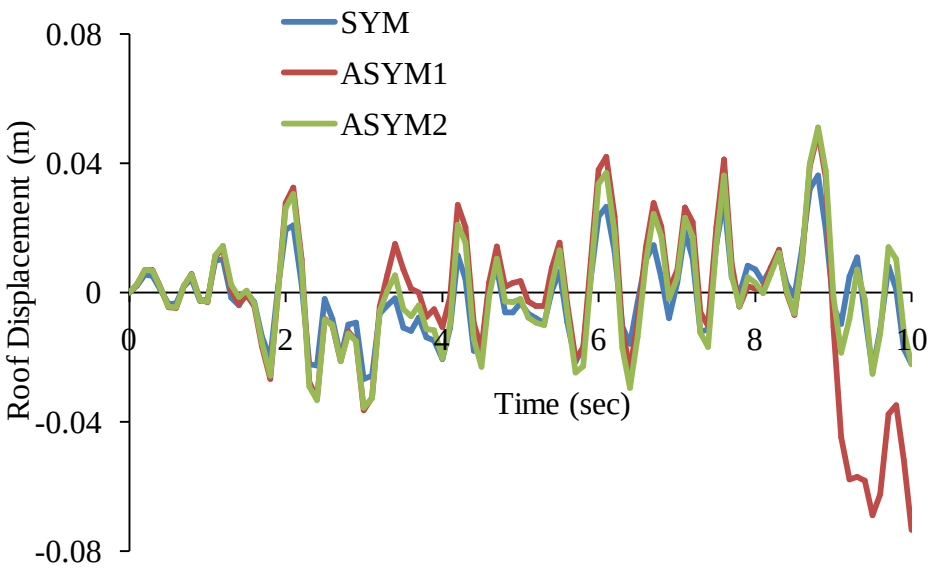

Fig. C.14: Roof Displacement -versus-time data for Data-C

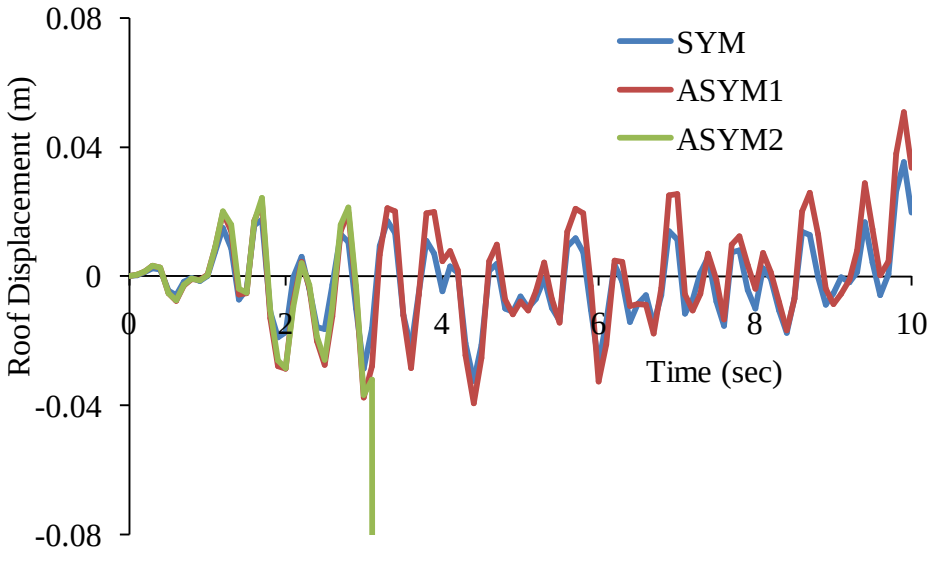

Fig. C.15: Roof Displacement -versus-time data for Data-D

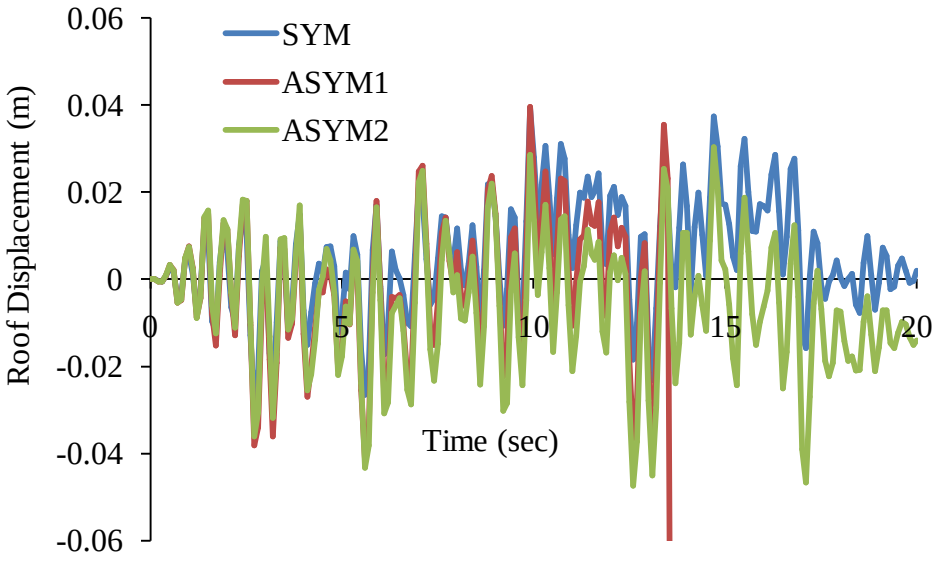

Fig. C.16: Roof Displacement -versus-time data for Data-E

C.2.2. Roof Rotation Responseduring Nonlinear Dynamic Analysis

The graphical representation of roof rotation versus time shows that there is no rotation in symmetric building (SYM). However the other two asymmetric building variants (ASYM1 & ASYM2) exists roof rotation due there eccentricity results torsion.

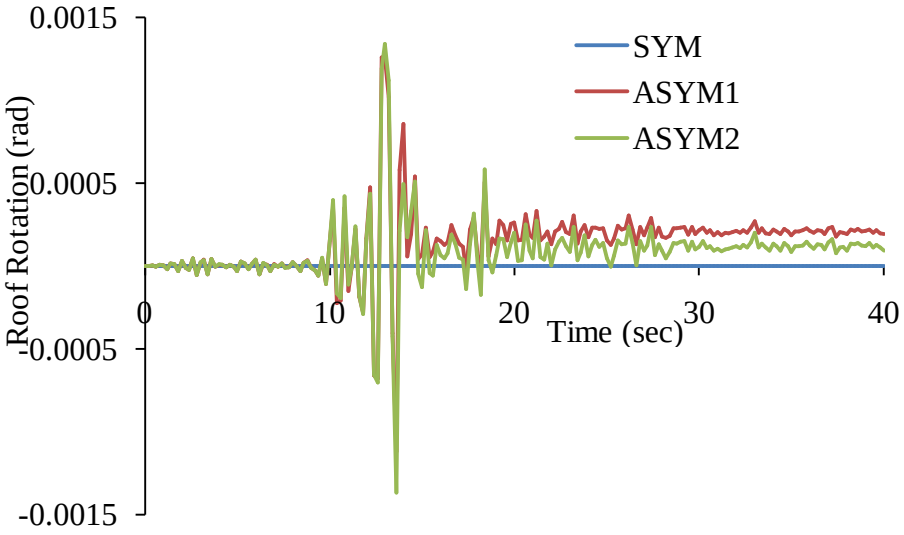

Fig. C.17: Roof Rotation -versus-time data for Loma Prieta – Oakland (1989)

Figs. C.17-C.30 presents roof rotation response of three buildings for ten natural records and five generated ground motion.

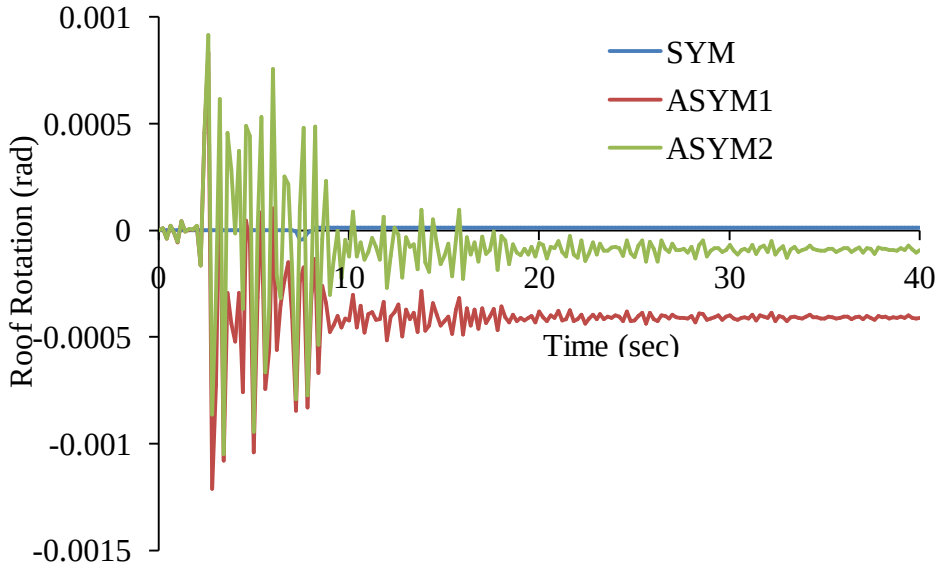

Fig. C.18: Roof Rotation -versus-time displacement data for Loma Prieta – Corralitos

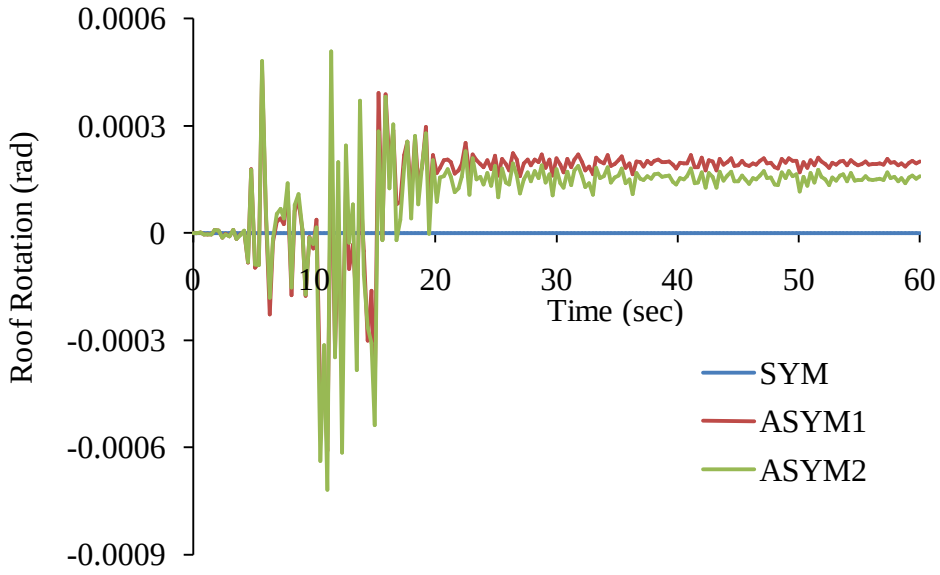

Fig. C.19: Roof Rotation -versus-time data for Northridge – Santa Monica (1994)

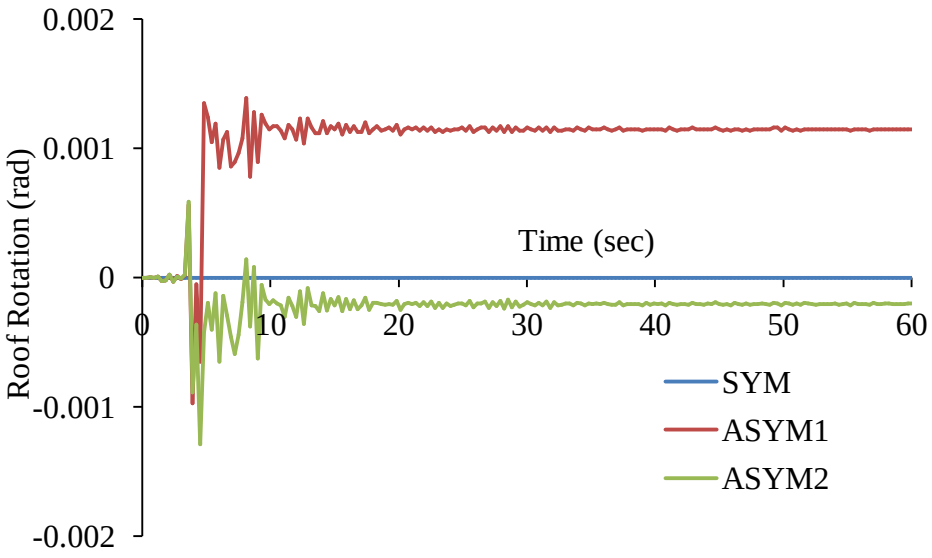

Fig. C.20: Roof Rotation -versus-time data for Northridge – Sylmar (1994)

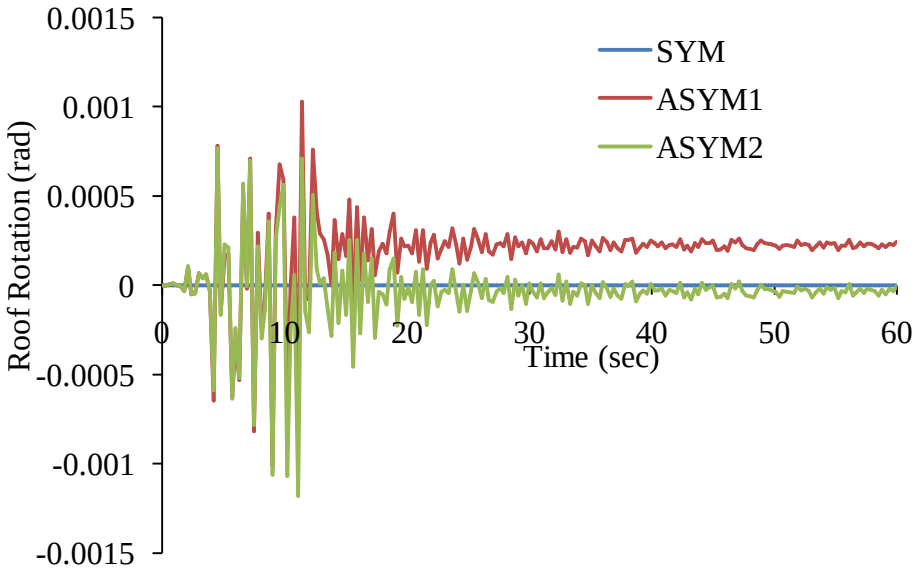

Fig. C.21: Roof Rotation -versus-time data for Northridge Century City

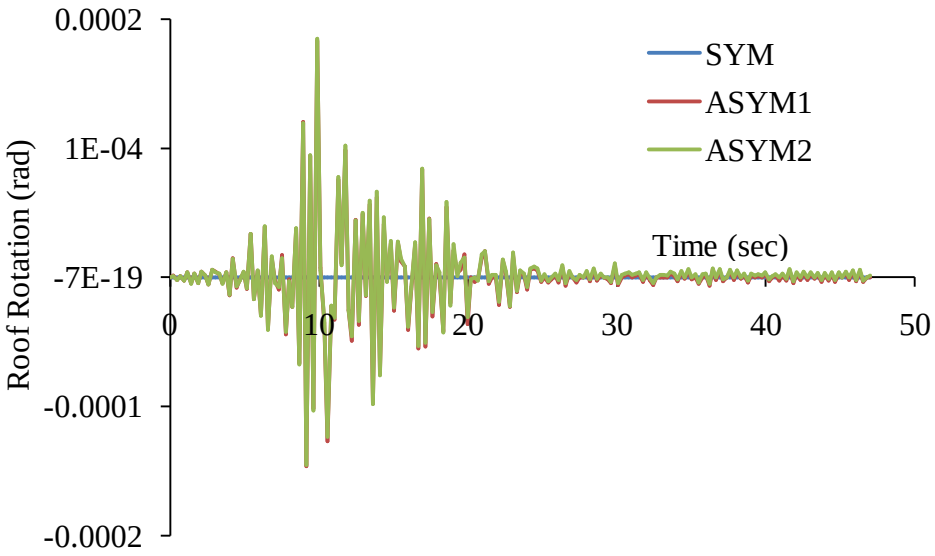

Fig. C.22: Roof Rotation -versus-time data for Landers – Lucerne Valley (1992)

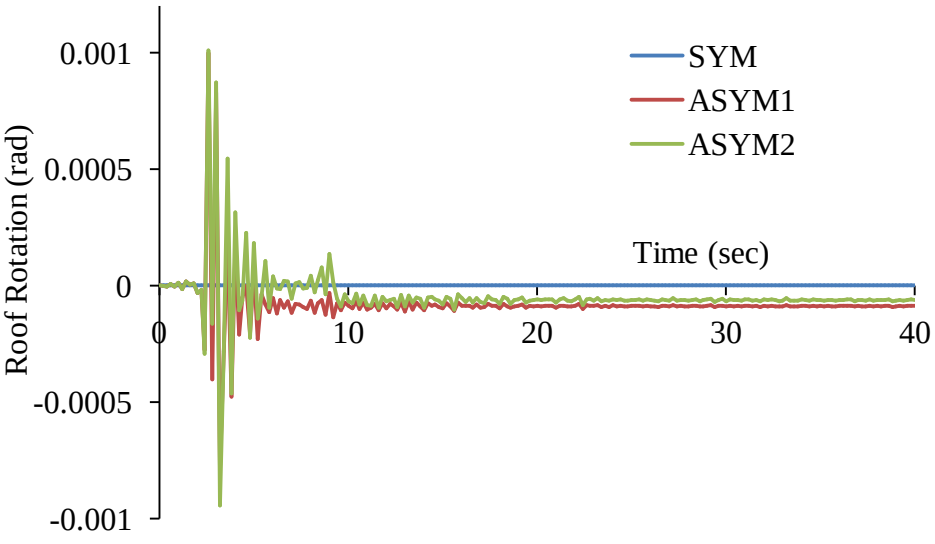

Fig. C.23: Roof Rotation -versus-time data for Sierra Madre – Altadena (1991)

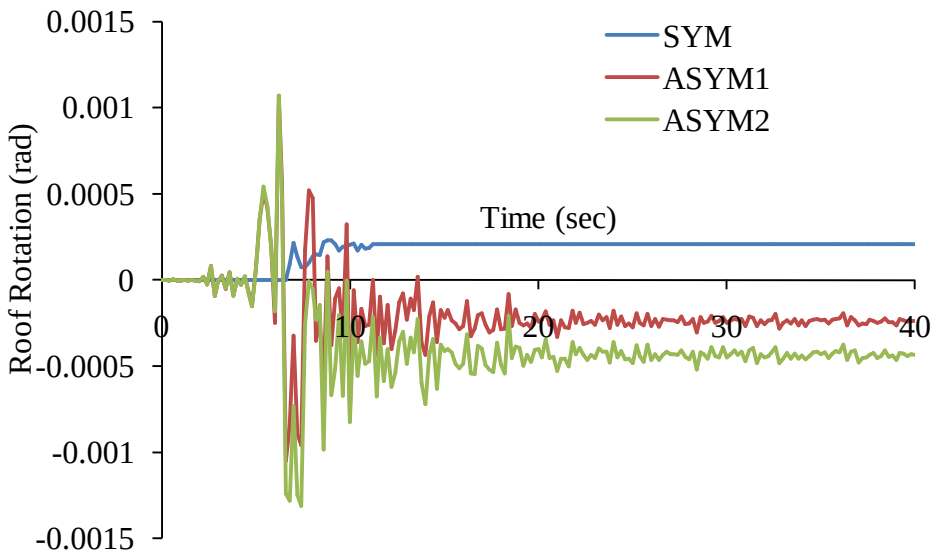

Fig. C.24: Roof Rotation -versus-time data for Imperial Valley Eq. (1979)

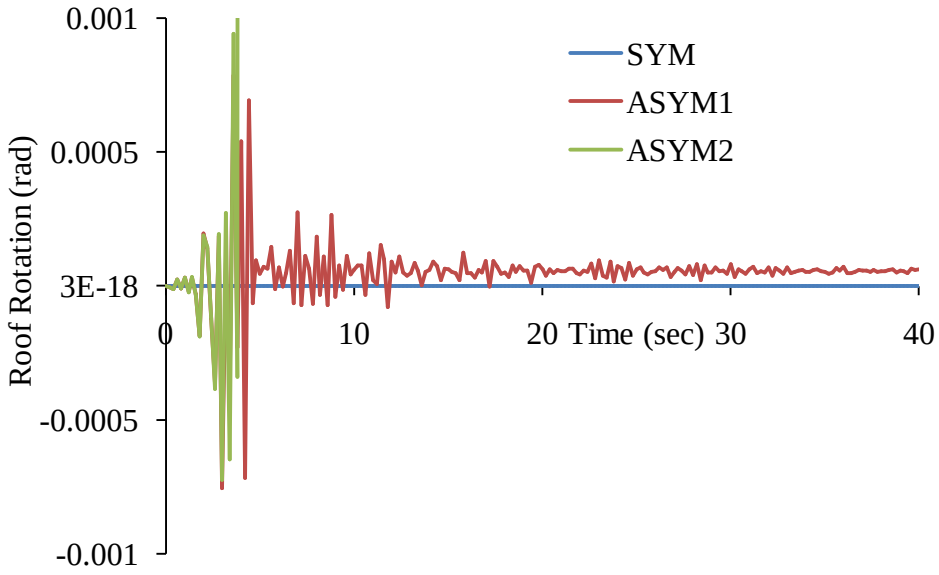

Fig. C.25: Roof Rotation -versus-time data for Morgan Hill – Gilroy4 (1984)

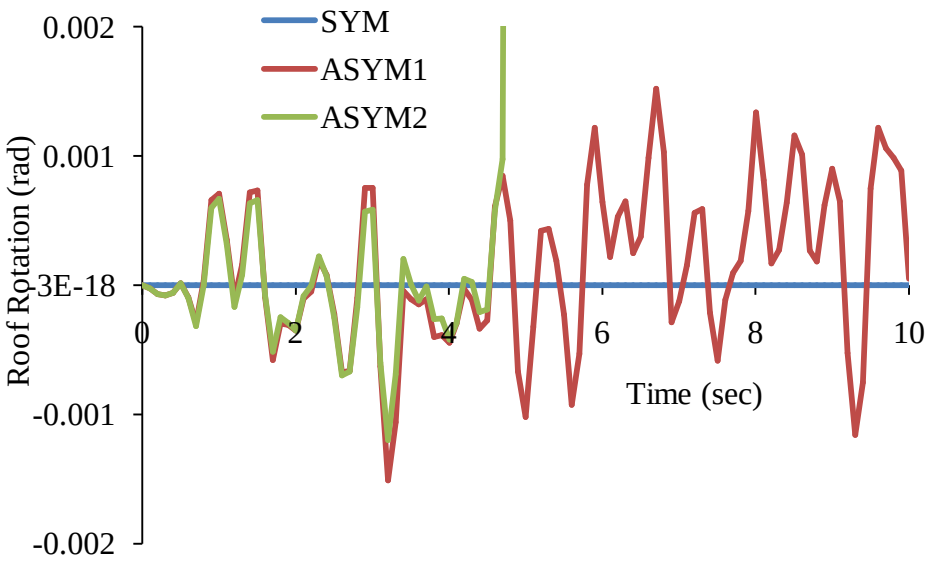

Fig. C.26: Roof Rotation -versus-time data for Data-A

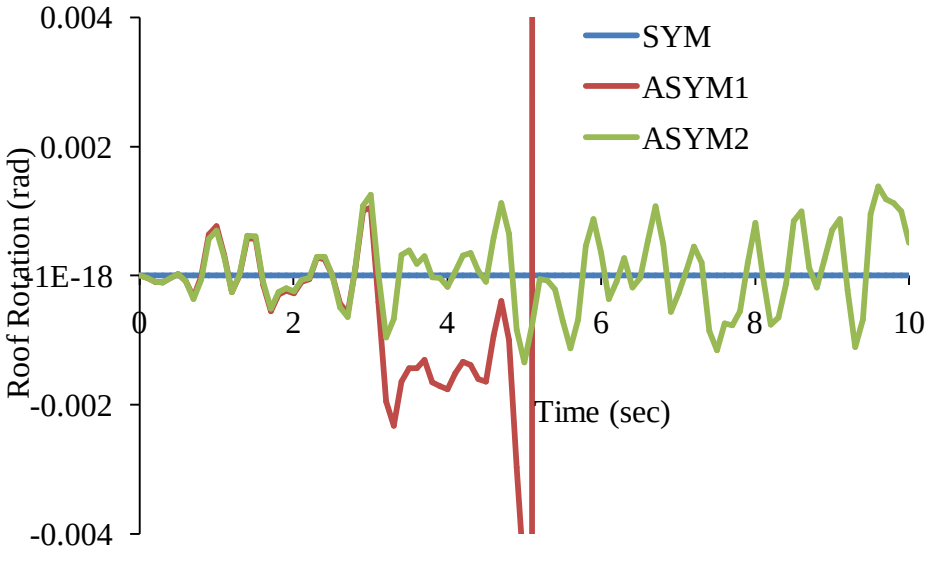

Fig. C.27: Roof Rotation -versus-time data for Data-B

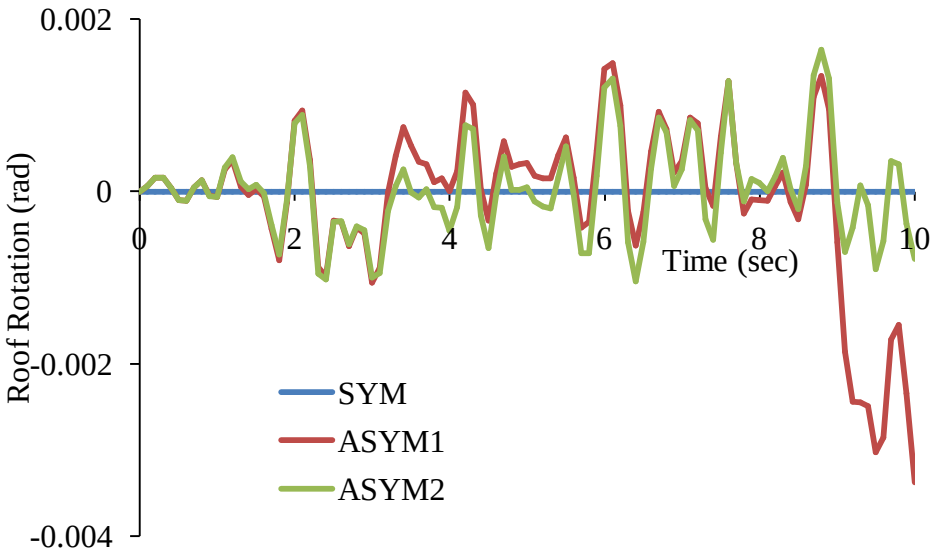

Fig. C.28: Roof Rotation -versus-time data for Data-C

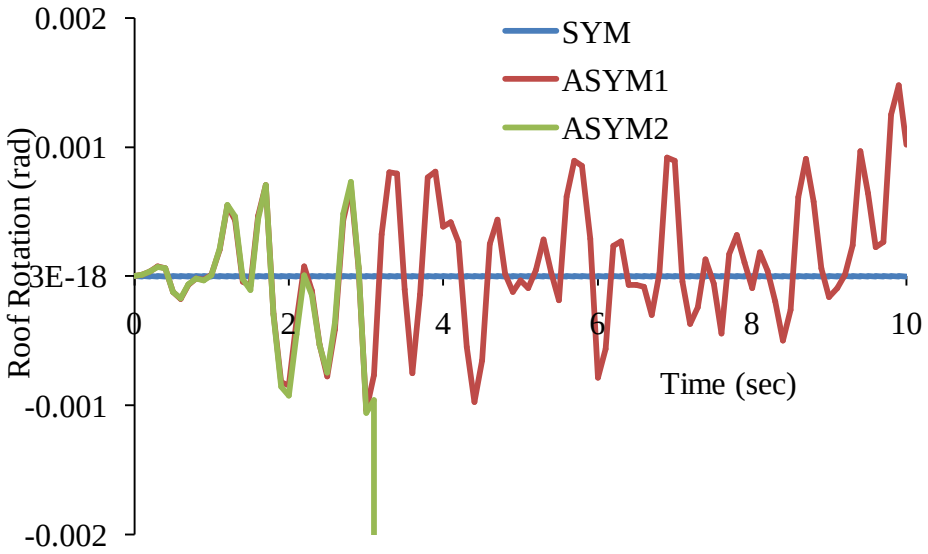

Fig. C.29: Roof Rotation -versus-time data for Data-D

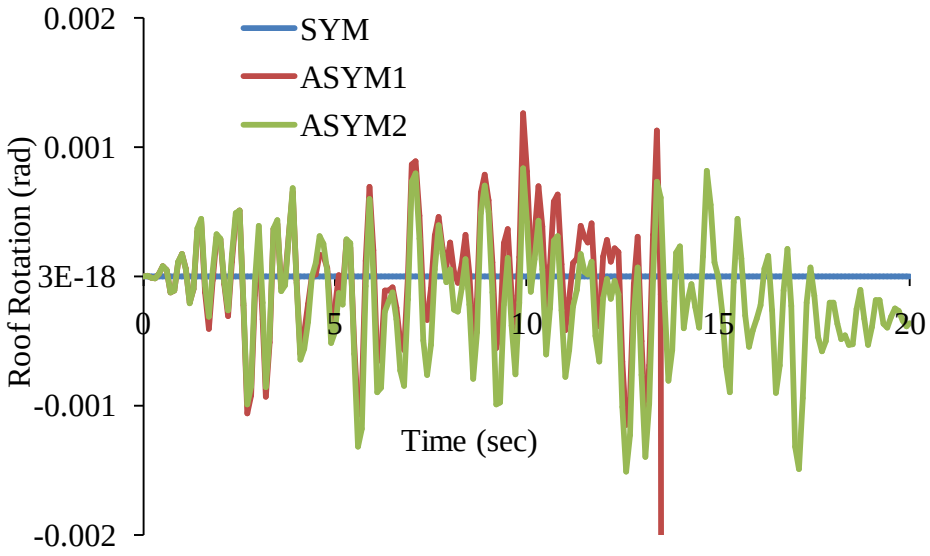

Fig. C.30: Roof Rotation -versus-time data for Data-E

ANNEXURE D

SPECTRAL IDENTICAL DATA

The spectral identical data used for nonlinear dynamic analysis is generated using commercial software called SIMQKE 2000. The steps involved in the generation are explained below.

D.1. INPUT WINDOW

The spectral consistent data is generated using commercial software called SIMQKE 2000 which is used for generating artificial ground motion compactable with user defined target response spectrum or spectrum density function. In this case the target response spectrum selected is the design spectrum given in IS 1893 Part-1: 2002 for 5% damping. As noted in SIMQKE User's Manual, the program can be used in three modes.

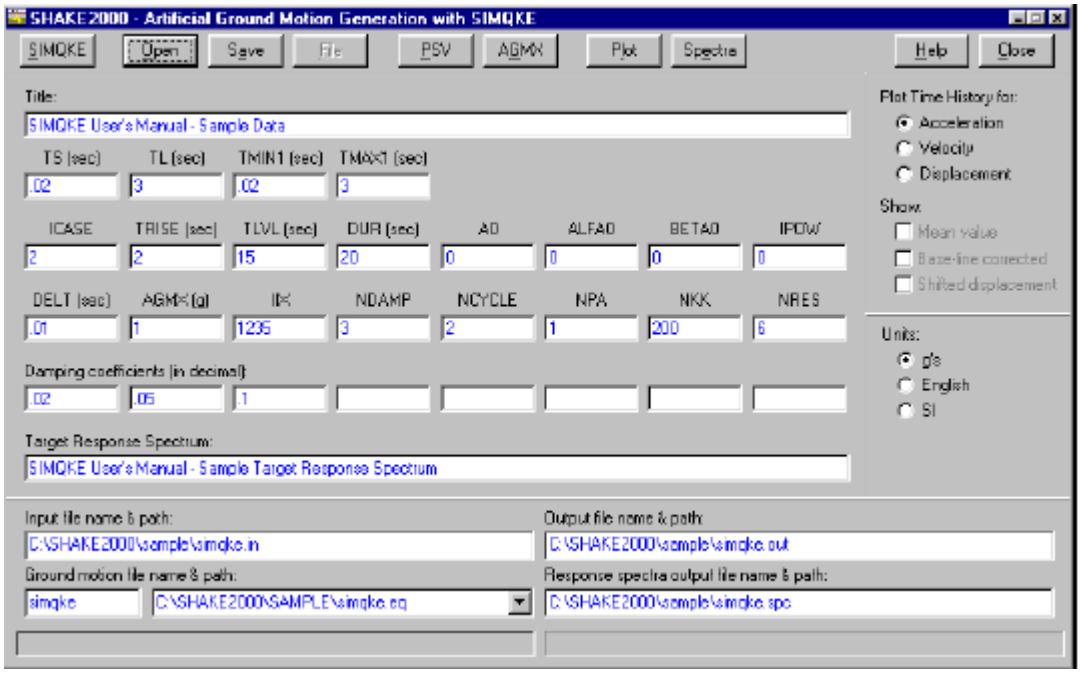

Fig. D.1: Input Window in SIMQKE commercial software

In the first mode the target response spectrum is specified; in mode two, the earthquake is specified in terms of the spectral density function; and, in the third mode, the earthquake is specified in terms of the spectral density function and changes to it. In this version of SHAKE 2000, only mode one is supported. The input window in this software is shown in the Fig. D.1.

To enter the value place the cursor on the respective text box for the parameter and type in the data. To delete a value, place the cursor in the corresponding box and use the delete key. Then press Tab key to move cursor to another cell.

Further information required for each parameter is given below;

Line 1;

- Title: Enter a description for the ground motion to be generated up to 80 characters long.

Line 2;

- TS: Smallest period (seconds) of desired response spectrum.
- TL: Largest period (seconds) of desired response spectrum.
- TMIN 1: Smallest period used to determine the range of frequencies to be represented in the simulation. Generally it is equal to TS.
- TMAX 1: Largest period used to determine the range of frequencies to be represented in the simulation. Generally it is equal to TL.
- YMIN: An estimated smallest velocity response spectral value. It is mainly used to determine the minimum ordinate on a plot of the spectrum.

Line 3;

- ICASE: If ICASE=1, no intensity envelope is used

  =2, trapezoidal intensity envelope is used.

  =3, exponential intensity envelope is used.

  =4, compound intensity envelope is used.
- TRISE: Earthquake rise time (sec) of intensity envelope (when ICASE= 1, 3; TRISE =0)
- TLVL: Earthquake level time (sec) of intensity envelope (when ICASE= 1,3; TLVL=0)
- DUR: Desired duration of accelerogram
- AO: Parameter of intensity function (specifies when ICASE= 3, 4).
- ALFAO: Parameter of intensity function (specifies when ICASE= 3, 4).
- BETAO: Parameter of intensity function (specifies when ICASE= 3, 4).
- IPOW: Parameter of compound intensity function (specifies when ICASE= 3).

Line 4;

- DELT: Discretization interval (sec), standard input is 0.01sec.
- AGMX: Desired maximum ground acceleration in “g”.
- IIX: An arbitrary odd integer, which acts as a seed for the random phase angle generator.
- NDAMP: Number of damping values for which Sv(w) is desired.
- NCYCLE: Number of cycles to smoothen a response spectrum. If NCYCLE=1, no cycling is made.

- NPA: Number of artificial earthquake desired from one target response spectrum (with one spectral density function).
- NKK: Total number of periods at equal intervals on a logarithmic scale. 0< NKK <300 (generally NKK is on the order of 200and 300).
- NGWK: Set NGWK=0 for option1.
- IPCH: If IPCH=0, no punched output is obtained. If IPCH=1, punched output is obtained

Line 5;

- AMOR (I): Damping coefficients in decimal parts of critical damping. The first damping entered will be the one for which cycling, if desired, will be done.

Line 6 to Line (5+NRES);

- Target Response Spectrum: These data are entered in the Target Response Spectrum form.

The attenuation relationship provided with SHAKE 2000 is used to enter the data for response spectrum, some useful relationship and other parameters are available in the text box below the target response spectrum label upon returning from the spectra values form. Direct typing mode also available for entering the spectrum values from different sources. After entering all values need for analysis click on SAVE button to save the data file to text file. Then the input file name and path are available on the text box. The software is providing *simqke.in* as default name to the input file. Three other files also created in it. The first one is the name of output file for the SIMQKE analysis. The analysis results are saved in this file. The text box will show all the files generated after the analysis where more than one motion generated. The input file contains the

names and paths of these files. The data stored in an input file can be retrieved with open command button.

The analysis is executed by clicking the SIMQKE button and a doc file will open and automatically the analysis will start. After the analysis finished the automatically file will close and if any error is there a pop up window will be displayed. If no error occurred in the analysis user can directly plot the ground motions generated by clicking on PLOT command button. The response spectrum is plotting for the generated artificial earthquake data is done by clicking the Spectra command button.

The Target Response Spectrum values are entered in the Target Spectrum form which is obtainedon clicking the PSV command button. The values for TS, TL, TMIN1 and TMAX1 may automatically update to reflect the range of periods entered in target values form.Appropriately this can be modified to any value. The desired maximum ground acceleration can be estimated using attenuation relationships included with SHAKE 2000. This can be done by clicking on the AGMX command button to display the attenuation relationships included with SHAKE 2000. From this use can select a relation and click on ok to come back to original form. Then the value will be displayed on the text box.

D.2. PLOT TIME HISTORY

The time history of acceleration, velocity or displacement plot for the ground motion generated is plotted using the plot command. The velocities and displacement time history is generated in step by step double integration from acceleration time history. The calculations are based on assuming that the acceleration varies linearly during the time step. The time history is displayed on clicking the respective button to select it and click plot to get the graph. The ground motion

file is formed by 7 header lines and the data are stored in 8 columns of 10 figures each with 6 decimal figures i.e. with a format of (8F10.6). The time history generated is shown in the Fig. D.2. In this study five spectral consistent data is generated using this software.

D.3. ANALYSIS OF GENERATED GROUND MOTION

The ground motion generated is possible for visual analysis and a mean value option is enabled for the velocity and displacement time histories. An arithmetic mean value is doing by this option and it will compute and display a horizontal line on the graph.

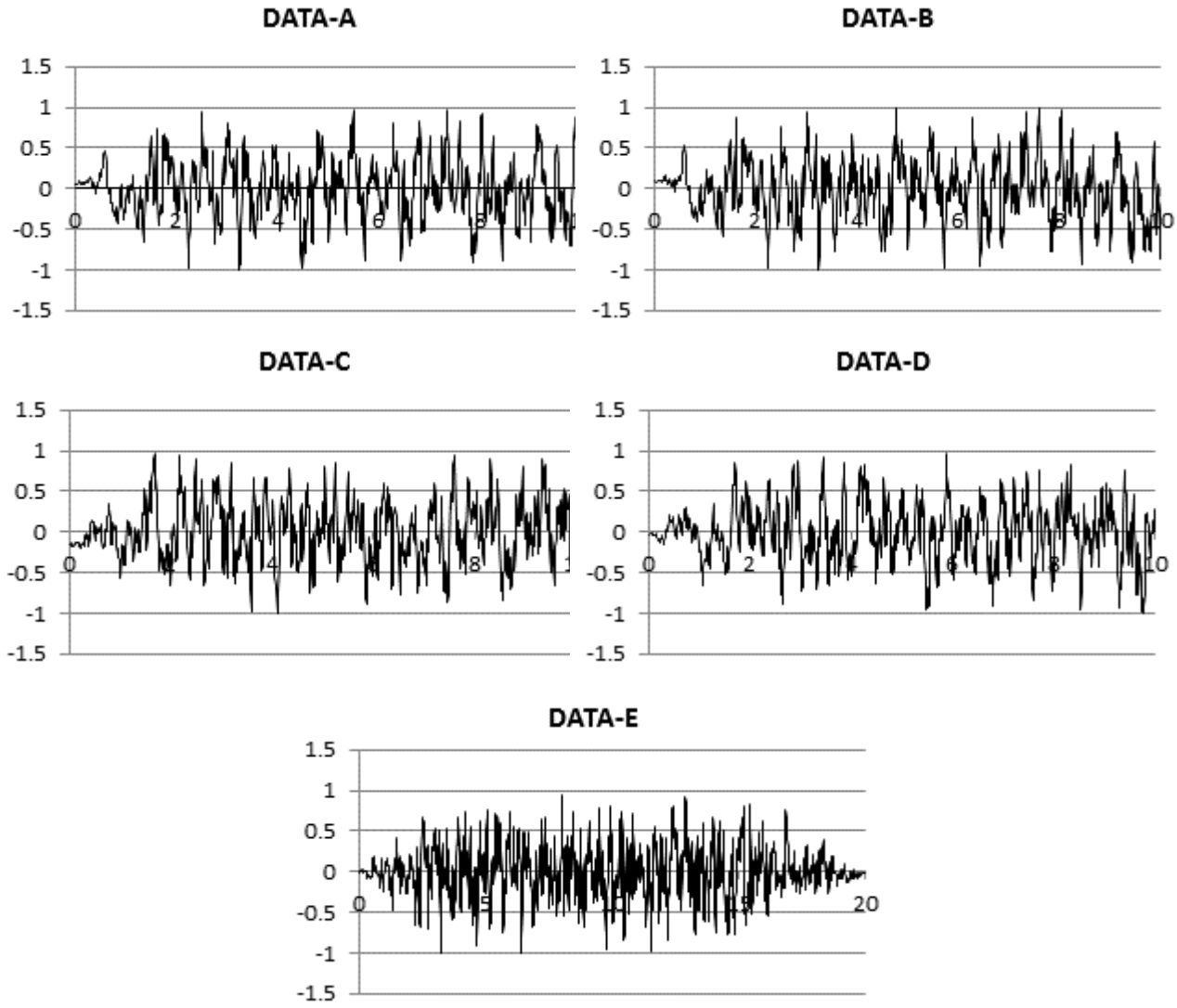

Fig. D.2: Spectral consistent time history ground motion generated

The corrected velocity or displacement time histories can be doing by BASE-Line corrected option. After selecting the Base line corrected and velocity options the corrected velocity-time histories is displayed. The mean value of the corrected-displacement time history is computed and then deducted from this time history to obtain a final displacement time history, identified as shifted displacement time history. The displacement time history obtained by shifting the baseline of the corrected displacement time history is displayed after selecting displacement and shifted displacement option.

D.4. TARGET RESPONSE SPECTRUM

The Target Response Spectrum is the one defined by user and that can be plotted together with other spectrum. For plotting this period and pseudo velocity spectra value or spectra value is need to enter the window shown in the Fig.D.3. This value is filling in the text box shown is alternatively going on. The spectra can be plotted by clicking the AASHTO, Attenuation, NEHRP, or UBC command button. For example if attenuation relation is using then click on attenuation button and select one relation and click plot command button. Click on the ok command button to return to original window form.

The period and spectra values are available in the data cells of the form. Also some description regarding the response spectrum is available in the text box given below the Target Response Spectrum label. This can be modified manually by placing the cursor in it and the desire information is able to type there. The period and PSV values entering time a delete and add button is enabled which is used to create a new set of value. These values will be exactly same as the previous values and the editing can be done by using modifying button.

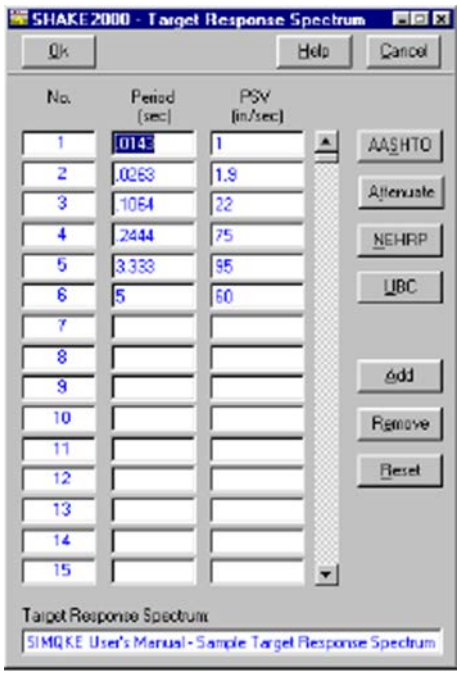

Fig.D.3: Window in SIMQKE software where Target Response Spectrum data is entering

At the end where the entry of pair of values finished then click ok to return back to Artificial Ground Motion Generator form of SIMQKE 2000.

REFERENCES

1. **ACI 318,** (2005). Building code requirement for reinforced concrete and commentary, ACI 318-05/ACI 318R-05, *American Concrete Institute*.

2. **ATC 40,** (1996). Seismic Evaluation and Retrofit of Concrete Buildings, *Applied Technology Council*,USA,1.

3. **BS 8110 Part 1 and 2,** (1997). Structural Use of Concrete, Code of Practice for Design and Construction, *British Standards Institute*.

4. **Chandler, A. M.,** (1986). Building Damage in Mexico City Earthquake, *Nature*, 320(6062), 497-501.

5. **Chandler, A.M.,Duan, X.N. and Rutenberg, A.,** (1996). Seismic torsional response: assumptions, controversies and research progress. *European Earthquake Engineering*, 10 (1), 37-51.

6. **Chandler, A. M. and Hutchinson, G. L.,** (1992). Effect of Structural Period and Ground Motion Parameters on the Earthquake Response of Asymmetric Buildings, *Engineering Structures*,14(6), 354-360.

7. **Chopra, A. K. and Goel, R. K.,** (1991). Evaluation of Torsional Provisions in Seismic Codes, Journal of Structural Engineering, ASCE, 117(12), 3762-3782.

8. **Chugh**, **R.,**(2004). Studies on RC Beams, Columns and Joints for Earthquake Resistant Design, M.Tech. Project Report, *Indian Institute of Technology Madras*, Chennai, India.

9. **Combined Strong-Motion Data**, (Sept. 25, 2011).*The Center for Engineering Strong Motion Data*, http://www.strongmotioncenter.or/.

10. **Correnza, J. C., Hutchinson, G. L. and Chandler, A. M.,** (1994), Effect of Transverse Load-resisting Elements on Inelastic Earthquake Response of Eccentric-plan Buildings, *Earthquake Engineering and Structural Dynamics*, 23 (1), 75-89.

11. **De La Llera, J. C. and Chopra, A. K.,** (1994). Accidental Torsion in Buildings due to Stiffness Uncertainty, *Earthquake Engineering and Structural Dynamics*, 23(2), 117-136.

12. **De Stefano, M., Faella, G. and Ramasco, R.,** (1993). Inelastic Response and Design Criteria of Plan-wise Asymmetric Systems, *Earthquake Engineering and Structural Dynamics*, 22(3), 245-259.

13. **Duan, X. N. and Chandler, A. M.,** (1993), Inelastic Seismic Response of Code-designed Multistorey Frame Buildings with Regular Asymmetry, *Earthquake Engineering and Structural Dynamics*, 22 (5), 431-445.

14. **Duan, X. N. and Chandler, A. M.,** (1997). An Optimized Procedure for Seismic Design of Torsionally Unbalanced Structures, *Earthquake Engineering and Structural Dynamics*, 26(7), 737-757.

15. **Dutta, S. C.,** (2001). Effect of Strength Deterioration on Inelastic Seismic Torsional Behaviour of Asymmetric RC Buildings,*Building and Environment*, 36(0), 1109-1118.

16. **Eurocode 8,** (2003). Design of Structures for Earthquake Resistance, Part-1: General Rules, *Seismic Actions and Rules for Buildings*, European Committee for Standardization (CEN), Brussels.

17. **Farzad, Noeim. and Marshall, Lew.,** (1995). On the use of Design Spectrum Compatible Time Histories, *Earthquake Specra*, 11(1), 111-127.

18. **FEMA 356,** (2000).Prestandard and Commentary for the seismic Rehabitation of buildings, *American Society of Civil Engineers*, USA.

19. **FEMA 450,** (2003). NEHRP Recommended Provisions for Seismic Regulations for New Buildings and Other Structures (Part 1: Provisions), *Building Seismic Safety Council* (BSSC), Washington D.C., USA.

20. **Gasparini, Dario and Vanmarcke, Erike.,** (1976). SIMQKE,*A Program for artificial Motion Generation User's Manual and Documentation*, Department of Civil Engineering, Massachusette Institute of Technology.

21. **Goel, R. K.,** (1997). Seismic Response of Asymmetric Systems: Energy-based Approach, *Journal of Structural Engineering, ASCE*,123(11), 1444-1453.

22. **Goel, R. K.,**(2001). Performance of building during the January 26, 2001 Bhuj earthquake. *EERI Special Earthquake Report in Earthquake in Gujarat*, India.

23. **Goel, R. K. and Chopra, A. K.,** (1994). Dual-level Approach for Seismic Design of Asymmetric-plan Buildings, *Journal of Structural Engineering, ASCE*,120(1), 161-179.

24. **Gupta, B. and Kunnath, S.K.,**(2000). Adaptive spectra-based pushover procedure for seismic evaluation of structures,*Earthquake Spectra*, 16(2), 367-391.

25. **Hart, G.C.,DiJulio, R.M. and Lew, M.,** (1975).Torsional response of high-rise buildings, *Journal Structure Engineering*. *ASCE*, 101 (ST2), 397-416.

26. **Housner, G. W. and Outinen, H.,** (1958). The Effect of Torsional Oscillations on Earthquake Stresses, *Bulletin of Seismological Society of America*, 48(0), 221-229.

27. **Humar, J. H. and Kumar**, **P.,** (2004). Review of code provisions to account for earthquake induced torsion, *CDROM Proceeding of 13th World Conference on Earthquake Engineering*, Vancouver, B. C., Canada.

28. **IBC-2003,** (2003). International building code, *International Conference of Building Officials* (ICBO). USA.

29. **Irvine, H. M. and Kountouris, G. E.,** (1980). Peak Ductility Demands in Simple Torsionally Unbalanced Building Models Subjected to Earthquake Excitation, *Proceedings of 7th World Conference on Earthquake Engineering*, Istanbul, 4(0), 117-120.

30. **IS: 13920,**(1993). Indian Standard Code of Practice for Ductile Detailing of Reinforced Concrete Structure Subjected to Seismic Forces. *Bureau of Indian Standards*, New Delhi

31. **IS 1893 Part 1,**(2002).Indian Standard Criteria for Earthquake Resistant Design of Structures. *Bureau of Indian Standards*, New Delhi.

32. **IS: 456 (Fourth Revision),**(2000).Indian standard code for practice for plain reinforced concrete for general building construction. *Bureau of Indian Standards*, New Delhi.

33. **IS 875 Part 1, 2, 3 and 4,**(1987). Indian Standard Code of practice for Design loads for buildings and structures. *Bureau of Indian Standards*, New Delhi.

34. **Kan, C. L. and Chopra, A. K.,** (1981a). Simple Model for Earthquake Response Studies of Torsionally Coupled Buildings, *Journal of Engineering Mechanics Division, ASCE*, 107(EM5), 935-951.

35. **Kan, C. L. and Chopra, A. K.,** (1981b). Torsional Coupling and Earthquake Responses of Simple Elastic and Inelastic Systems, *Journal of Structural Division, ASCE*, 107(ST8), 1569-1588.

36. **Kilar, V.,** (2001).Seismic response of asymmetric frame building designed according to euro codes. *Proceeding of the first international structural engineering and construction conference*, Honolulu, Hawaii, 681-686.

37. **Kramer, Steven.,**(2000). Seismic Hazard Analysis for Construction Facilities, *Short Course at the University of Washington*, Department of Civil and Environmental Engineering, Professional Engineering Practice Liaison Program, May 19-20, 2000.

38. **Mander, J.B., Priestley, M.J.N. and Park, R.,**(1988). Theoretical Stress-Strain Model for Confined Concrete, *Journal of Structural Engineering*, ASCE, 114(8), 1804-1823.

39. **Mwafy, A.M. and Elnashai, S.A.,**(2000). Static Pushover verse dynamic-to-collapse analysis of RC buildings, Engineering Seismology and Earthquake Engineering Section, Imperial College of Science, Technology and Medicine. Report No. 00/1.

40. **NBCC,** (1995). National Building Code of Canada, Associate Committee on the National Building Code; *National Research Council of Canada*, Quebec.

41. **NZS-4203,**(1992). New Zealand Standard: General Structural Design and Design Loadings for Buildings, *Standards Assoc. of New Zealand*, Wellington New Zealand.

42. **Pam, H.J., and Ho, J.C.M.,** (2001). Flexural Strength Enhancement of Confined Reinforcement Concrete Columns, *Structures and Buildings Journal*, 146(4), 363-370.

43. **Panagiotakos, T.B. and Fardis, M.N.,** (2001). Deformation of Reinforced Concrete Members at Yielding Ultimate, *ACI Structural Journal*, 98(2), 135-148.

44. **Park, R.; and Paulay, T.,** (1975). Reinforced Concrete structures, *John Wiley & Sons*, New York.

45. **Paulay, T and Priestley, M.J.N.,** (1992). Seismic design of reinforced concrete and masonry buildings, *John Wiley & Sons*, New York

46. **PCM 3274,** (2003).Primi Element in Materia di CriteriGenerali per la ClassificationeSismicadelTerritorioNazionale e di Normative Tecniche per le Costruzioni in ZonaSismica (in Italian), Roma, Italy.

47. **Pillai, S.U and Devdas, M.,** (2009).Reinforced Concrete Design, Tata McGraw Hill Publishing Company Limited, New Delhi.

48. **Pradip, Sarkar.,** (Dec. 2008). Seismic Evaluation of Reinforced concrete stepped building frames, *A thesis for the award of the degree of doctor of philosophy*, IIT Madras, Chennai.

49. **Prithwish, Kumar. Das., (2003).** Effect of Coupled Lateral-Torsional Vibration on Inelastic Seismic Behaviour of R/C Buildings with Uni-directional and Bi-directional Asymmetry, *A Thesis Submitted to Bengal Engineering College (Deemed University) for the Award of the Degree of Doctor of Philosophy*. Department of Applied Mechanics, Bengal Engineering College (Deemed University), Howrah-711103, West Bengal, India.

50. **Riddell, R. and Santa-Maria, H.,** (1999). Inelastic Response of One-storey Asymmetric-plan Systems Subjected to Bi-directional Earthquake Motions, *Earthquake Engineering and Structural Dynamics*, 28(3), 273-285.

51. **Robin, Davis.P.,** (2009). Earthquake Resistant Design Open Ground Storey RC Framed buildings, *A thesis for the award of the degree of doctor of philosophy*, IIT Madras, Chennai.

52. **Rosenblueth, E., and Meli, R.,** (1986). The 1985 Earthquake: Causes and Effects in Mexico City, *Concrete International*,8(5), 23-34.

53. **Rutenberg, A.,** (1992). Nonlinear Response of Asymmetric Building Structures and Seismic Codes: A State of the Art Review, *European Earthquake Engineering*,6(2), 3-19.

54. **Sadek, A. W., Sobaih, M. E. and Esmail, H. S.,** (1992). Approximate Seismic Analysis of Inelastic Asymmetric Structures, *Engineering Structures*, 14(1), 49-62.

55. **SAP 2000 (Version 14.0),**(2010).Integrated Software for Structural Analysis and Design. *Computers & Structures, Inc.*, Berkeley, California.

56. **Tjhin, T., Aschheim, M. and Hernandez-Montes, E.,** (2005). Estimates of peak roof displacement using "Equivalent" single degree of freedom system. ASCE Journal of Structural Engineering. 131(13), 517-522.

57. **Tso, W. K. and Smith, R. S. H.,** (1999). Re-evaluation of Seismic Torsional Provisions, *Earthquake Engineering and Structural Dynamics*, 28(8), 899-917.

58. **Tso, W. K. and Ying, H.,** (1990). Additional Seismic Inelastic Deformation Caused by Structural Asymmetry, *Earthquake Engineering and Structural Dynamics*, 19(2), 243-258.

59. **Tso, W. K. and Ying, H.,** (1992). Lateral Strength Distribution Specification to Limit Additional Inelastic Deformation of Torsionally Unbalanced Structures, *Engineering Structures*, 14(4), 263-277.

60. **Tso, W. K. and Zhu, T. J.,** (1992). Design of Torsionally Unbalanced Structural Systems Based on Code Provisions I: Ductility Demand, *Earthquake Engineering and Structural Dynamics*, 21(7), 609-627.

61. **Vanmarcke, E.H., Cornell, C.A.,Gasparini, D.A. and Hou, S.,**(1990). SIMQKE-I; Stimulation of Earthquake Ground Motions, *Department of Civil Engineering*, Massachusetts Institute of Technology.